

UCSF

UC San Francisco Electronic Theses and Dissertations

Title

Localization and sorting of nucleoside transporters in the kidney

Permalink

<https://escholarship.org/uc/item/65x5s653>

Author

Mangravite, Lara,

Publication Date

2002

Peer reviewed|Thesis/dissertation

Localization and Sorting of Nucleoside Transporters

In the Kidney

by

Lara Mangravite

DISSERTATION

Submitted in partial satisfaction of the requirements for the degree of

DOCTOR OF PHILOSOPHY

in

Pharmaceutical Chemistry

in the

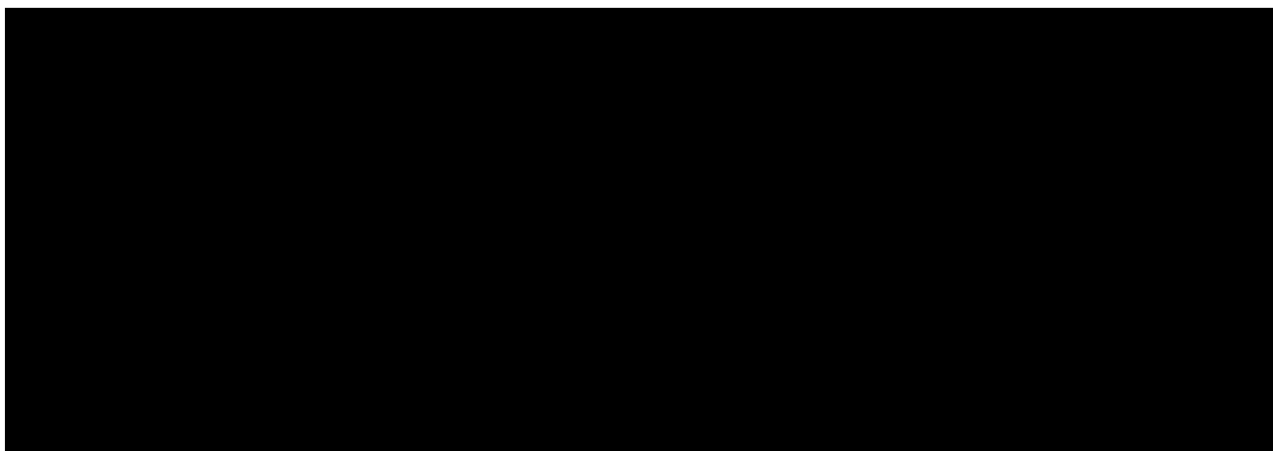
GRADUATE DIVISIONS

of the

UNIVERSITY OF CALIFORNIA SAN FRANCISCO

and

UNIVERSITY OF CALIFORNIA BERKELEY



Date

University Librarian

Degree Conferred:

ACKNOWLEDGEMENTS

Graduate school is not an easy time. While there is a peaceful simplicity in the single-minded quest for knowledge, there is a lot of failure involved in experimental biology. Any body of work professing successes and novel findings stands atop a pile of dead end discoveries and late night failures. That is the nature of the beast. There have been a lot of bright spots in my graduate career, but I have hit many frustrating walls. I could not have possibly dragged myself through those difficult times without the loyalty and support of a small army of friends and colleagues.

First and foremost, I want to thank Kathy. She has taught me that there is a lot more to science than graceful pipetting and successful experiments. From her, I have learned the art of presenting science in a manner which sounds interesting (and exciting to fund), an essential survival tool for any fledgling scientist. I've also learned to manage my time and choose my battles wisely--the "life is too short" mentality. Most importantly, I have learned to seek scientific collaborations. We are all experts in tiny little circles. It is only when those circles come together that science becomes relevant in a broader scheme.

I would also like to thank Deanna Kroetz and Les Benet, my thesis committee, both of whom have offered me valuable advice and helpful hints along the way. Deanna, in particular, has always taken time out of her busy schedule to listen to my needs and try to point me in the right direction. In addition, Josh Lipshutz and Keith Mostov, my collaborators in my first year of experiments, taught me much about the value of good advice and well thought out scientific questions.

While the above people taught me the theory of science, it was the people in the trenches with me whom taught me the nuts and bolts of scientific technique. To Dr. Karin Gerstin--my nucleoside guru and good friend, Dr. Mark Dresser--the transporter god, Dr. Maya Leabman, and Carlo Bello. There have also been a posse of "new recruits" who actually look to me for advice and respect my scientific opinion. More importantly, they offer their friendship--the Friday afternoon round table: Jenn Gray (and Jamie), Ryan Owen, Chesi Ho, and Tom Urban. How can science not be fun when you get to do it with people like this?

I have made a large number of friends in my years here in San Francisco--some inside the walls of this university and many outside. I am constantly amazed at how friendly people are in this city. I have made friends walking down the street, standing in elevators, and dancing in clubs. The support of every one of them has helped me through. To list them would take pages so I will stick to those that greatly affected this project. Thanks go to the scientific crew: Carolyn Cummins--who took one look at me during first year orientation and invited me home for a swim, Mieke Van Zante--who understands me in astonishing ways, Dan Adamson--who taught me that love is worth moving to Texas, Anson Nomura--for silent and unconditional support, and Mike Oakley--who reminded me every day that life is a process and the ultimate goal is to enjoy it. Without him, I would of finished graduate school in half the time and been twice as miserable. Thanks also go to the non-scientists: to Rachel Schutt, Tamsen Mitchell and all my other roommates whom have listened to many end of day frustrations, to Laura Vitale for bringing a piece of family back into my life, and to Tricia Sykes who is a constant reminder that good things happen when you follow your heart.

I was asked at the age of twelve, by my Uncle Carl, whether I wanted to go to college. I looked up from my Christmas presents and said, "I would like to get a Ph.D." My greatest happiness in life comes when I am learning new things and that is what I have focused on thus far. I have had the luxury to do that because my parents--all of them--have stood behind me every step of the way. They don't always understand where I am going, but they believe in me enough to help me get there in any way that they can. That means the world. Thank you.

Lara Mangravite

December, 2002



Lara Mangravite
Department of Biopharmaceutical Sciences
University of California
San Francisco, California 94143-0446

Telephone: (415) 514-0301
FAX: (415) 502-4322
email: lmmang@itsa.ucsf.edu

APS Permissions Office
9650 Rockville Pike
Bethesda MD 20814
(301) 571-5742

August 23, 2002

To Whom It May Concern:

I am writing to obtain permission to reprint the enclosed article as part of my Ph.D. dissertation at the University of California, San Francisco. The article is entitled, "Localization of GFP-tagged concentrative nucleoside transporters in a renal polarized epithelial cell line" (Am J Physiol Renal Physiol 280: F879-885, 2001.).

If possible, I would like the letter of authorization faxed to me at 415-502-4322.

Thank you very much for your assistance.

Sincerely,

Lara Mangravite
Lara Mangravite

THE AMERICAN PHYSIOLOGICAL SOCIETY
9650 Rockville Pike - Bethesda, MD 20814-3991

Permission is granted for use of the material specified above provided the publication is credited as the source.

8-1-02 M. Reich/RR
Date Pub Mgr & Exec Editor

Tue, 10 Dec 2002 10:14:22 -0800 (PST)
Lara Michelle Mangravite <lmmang@itsa.ucsf.edu>
lmmang@itsa.ucsf.edu
Subject: RE: Reprint Permission (fwd)

----- Forwarded message -----
Tue, 29 Oct 2002 08:18:00 -0500
Georgia Prince <Georgia.Prince@wkap.com>
'lmmang@itsa.ucsf.edu' <lmmang@itsa.ucsf.edu>
Subject: RE: Reprint Permission

October 29, 2002

Ms. Mangravite:

PERMISSION GRANTED provided the material has appeared in our work without
reference to another source; you obtain the consent of the author*; you credit
the original publication; and reproduction is confined to the purpose for
which permission is hereby given.

Georgia Prince
Manager, Rights and Permissions
Wiley Academic/Plenum Publishers
350 Spring Street, New York, NY 10013
(212) 620-8023 Fax: (212) 463-0742

Author requesting use of own material.

Original Message-----
Lara Michelle Mangravite [mailto:lmmang@itsa.ucsf.edu]
Monday, October 28, 2002 6:06 PM
Kathleen Lyons
Subject: Reprint Permission

Lyons-

writing to obtain permission to reprint in my Ph.D. dissertation an
article I have written
which has recently been accepted for publication in Pharmaceutical
Research.
Manuscript #02-0237, "Sorting of Rat SPNT in Renal Epithelium is
Independent of N-Glycosylation"). I would be very grateful if you could
send me a letter of
authorization at 415-502-4322 or send it to the below address. If you are
the appropriate person to contact regarding this matter, would you be
able to redirect me?

Thank you very much for your assistance.

Sincerely,
Lara Mangravite
Department of Biopharmaceutical Sciences
University of California, San Francisco
Parnassus Ave, Box 0446
San Francisco, CA 94143-0446

ABSTRACT

Localization and Sorting of Nucleoside Transporters in the Kidney

Lara Mangravite

Nucleosides and nucleoside analogs are administered therapeutically for the treatment of neoplasms, viral infections and cardiac arrhythmias. Renal handling of nucleosides and nucleoside analogs is compound dependent: some undergo net reabsorption whereas others undergo net secretion. These processes depend upon interactions of compounds with transporter proteins and the arrangement of these transporters on the plasma membrane of the renal tubule.

To date, there are five functionally characterized nucleoside-specific transporters: three concentrative nucleoside transporters (CNT, SLC28)--CNT1, SPNT, and CNT3-- and two equilibrative nucleoside transporters (ENT, SLC29)--ENT1 and ENT2.

In order to interpret the role that these transporters may play in renal handling of nucleosides and nucleoside analogs, it is essential to understand the subcellular localization of each within renal epithelium. To this aim, we tagged each transporter with green fluorescence protein (GFP) and stably expressed in MDCK, a renal epithelial cell line. Using immunofluorescence techniques and functional assays, we explored the subcellular localization of each protein.

The CNTs all localized predominantly to the apical membrane where they are predicted to govern the first step in reabsorptive flux of nucleosides. The purine selective concentrative nucleoside transporter, SPNT, was partially expressed on the basolateral

membrane. Using mutagenesis studies, we determined that trafficking of SPNT to the plasma membrane was independent of N-linked glycosylation.

ENT1 and ENT2 localized predominantly to the basolateral membrane where they are predicted to govern the second step in nucleoside reabsorption. ENT1 was found in small amounts on the apical membrane. Both ENT1 and ENT2 sequences contained a basolateral targeting motif within their carboxy-terminal tail. Removal of these domains did not affect basolateral targeting for either protein but steady-state surface expression of ENT2 was altered.

The results of this research support the hypothesis that the five known nucleoside transporters mediate reabsorptive flux within the kidney. The concentrative transporters mediate the first step in reabsorption, passage from the kidney to the cell, whereas the equilibrative transporters mediate movement from the cell to the pericellular spaces. Equilibrative nucleoside transporters may also participate in the secretory flux of nucleoside analogs, working in concert with other active transporters at the apical membrane.

Nathleen M. Giacomin
Dec. 10, 2002

TABLE OF CONTENTS

Acknowledgements	iii
Abstract	viii
List of Tables	xv
List of Figures	xvi
Chapter 1.	
Introduction to Renal Nucleoside Transport	
Renal Excretion	1
Carrier-Mediated Transport in Renal Excretion	4
Nucleosides	9
Nucleoside Transport Within the Kidney	15
Nucleoside Transporter Proteins	18
Concentrative Nucleoside Transporters	19
CNT1	21
SPNT	28
CNT3	30
Equilibrative Nucleoside Transporters	32
ENT1	34
ENT2	37
Renal Subcellular Localization of Nucleoside Transporters	38
Molecular Determinants of Subcellular Localization	39

Summary of Chapters	42
References	44
Chapter 2.	
Localization of Concentrative Nucleoside Transporters, SPNT and CNT1, in Renal Epithelial Cells	
Introduction	58
Materials and Methods	60
Materials	60
Plasmid construction	61
Cell culture	61
Uptake measurements	62
Inhibition studies	62
Localization uptake studies	63
Data analysis	63
Confocal microscopy	64
Transient transfection of LLC-PK ₁	64
Results	64
Stable expression of SPNT-GFP and CNT1-GFP in epithelial cells	64
Localization of SPNT-GFP and CNT1-GFP in polarized MDCK cells	69
Discussion	71
References	74

Chapter 3.

Sorting of SPNT in Renal Epithelium is Independent of N-Glycosylation

Introduction	80
Materials and Methods	81
Materials	81
Site-directed mutagenesis	81
Construction of stably transfected MDCK	81
Western blot	82
Confocal microscopy	82
Functional localization and statistical analysis	82
Results	83
SPNT but not CNT1 localization is sensitive to tunicamycin	83
Stable transfections of deglycosylated SPNT mutants in MDCK	84
Deglycosylation does not affect localization of SPNT mutants	84
Discussion	87
References	92

Chapter 4.

Localization and Sorting of Human Equilibrative Nucleoside Transporters, hENT1 and hENT2, in Renal Epithelial Cells

Introduction	95
Materials and Methods	97
Materials	97

Plasmid construction	98
Site-directed mutagenesis	98
Stable transfection of MDCK	99
Transient transfection of LLC-PK ₁	99
Confocal microscopy	99
Functional uptake in MDCK	100
Immunoblot analysis	100
Expression and functional analysis in <i>Xenopus laevis</i> oocytes	101
Statistical and data analysis	101
Results	102
Localization of hENT1 and hENT2 in polarized renal epithelial cells	102
Basolateral targeting is independent of the carboxy-terminal tail of both hENT1 and hENT2	107
Identification of a hENT2 variant	112
Discussion	120
References	124
Chapter 5.	
Localization of CNT3, a Broadly Selective Concentrative Nucleoside Transporter, in Renal Epithelial Cells	
Introduction	132
Materials and Methods	133
Materials	133

Cloning of CNT3 and plasmid construction	134
Stable transfection of MDCK	134
Confocal microscopy	135
Functional localization of MDCK	135
Functional kinetic analysis in MDCK	135
Immunoblot analysis	136
Statistics and data analysis	136
Results	137
Preparation of a GFP-tagged CNT3 stably transfected cell line in MDCK	137
Localization of CNT3 in MDCK	139
Kinetic analysis and drug interactions of CNT3	139
Discussion	144
References	147
Chapter 6.	
Conclusions and Future Studies	
Localization of nucleoside transporters within renal epithelial cells	150
Renal handling of nucleoside analogs	154
Trafficking of nucleoside transporters within the kidney	157
Cellular regulation of nucleoside transporters	163
Summary	165
References	170

LIST OF TABLES

Chapter 1.

Table 1. Renal handling of clinically administered nucleoside analogs	14
Table 2. Nucleoside transport functions characterized from whole tissue	16
Table 3. Cloned nucleoside transporters expressed in kidney	20
Table 4. Substrate specificity of the rat and human orthologs of cloned nucleoside transporters	22
Table 5. Apparent Michaelis-Menten kinetic constant (K_m , substrate concentration at half-maximal velocity, in μM , of naturally occurring nucleosides and the nucleobase, hypoxanthine	25

Chapter 4.

Table 1. Apparent K_m and V_{max} of Adenosine	103
--	-----

Chapter 6.

Table 1. Known interactions between nucleoside analogs and nucleoside transporters	155
Table 2. Known interactions between nucleoside or nucleotide analogs and secretory transporters in the kidney	156
Table 3. Effects of sorting signals on targeting and steady state expression of NTs	160

LIST OF FIGURES

Chapter 1.

Figure 1. Mechanisms of renal elimination	2
Figure 2. Transporters involved in renal elimination	5
Figure 3. Chemical structure of endogenous nucleosides	10
Figure 4. Chemical structures of several clinically relevant nucleoside analogs	12
Figure 5. Secondary structure of hCNT1	26
Figure 6. Sequence alignments of CNTs in region responsible for substrate selectivity	33
Figure 7. Secondary structure of hENT1	35
Figure 8. Trafficking pathways and targeting motifs	40

Chapter 2.

Figure 1. Localization of SPNT-GFP and CNT1-GFP in MDCK and LLC-PK ₁ cells	65
Figure 2. Uptake of ³ H-uridine, ³ H-inosine, and ³ H-thymidine in transfected MDCK cells	67
Figure 3. Inhibition of ³ H-uridine uptake by unlabeled uridine in transfected MDCK cells	68
Figure 4. Functional localization of SPNT-GFP and CNT1-GFP in MDCK cells	70

Chapter 3.

Figure 1. Multiple alignments of predicted extracellular C-terminal tail of CNTs	85
Figure 2. Western blot analysis of SPNT glycosylation mutants	86
Figure 3. Localization of SPNT glycosylation mutants in MDCK	88
Figure 4. Functional localization of SPNT glycosylation mutants	90

Chapter 4.

Figure 1. Immunofluorescent localization of wild type ENT1 and ENT2 in MDCK	104
Figure 2. Functional localization of GFP-tagged wild type hENT1 and hENT2 in MDCK	106
Figure 3. Expression and localization of mutagenized ENT1 and ENT2 in MDCK	108
Figure 4. Immunoblot analysis of hENT1 and hENT2 protein in MDCK	111
Figure 5. Localization of hENT2 wt and mutants in LLC-PK ₁	113
Figure 6. Effect of mutations on hENT1- and hENT2- mediated uptake of adenosine and thymidine in oocytes	114
Figure 7. Sequence analysis of hENT2 and hENT2A	116
Figure 8. Protein sequences of hENT2 and hENT2A	117
Figure 9. Function and localization of the slice variant, hENT2A	118

Chapter 5.

Figure 1. Immunoblot of CNT3-GFP positive MDCK cells	138
--	-----

Figure 2. Michaelis-Menten analysis of inosine transport by CNT3-GFP in MDCK	140
Figure 3. Localization of CNT3-GFP to apical membrane of MDCK	141
Figure 4. Functional localization of CNT3-GFP to apical membrane	142
Figure 5. Interaction of CNT3-GFP with clinically relevant nucleoside analogs	143
 Chapter 6.	
Figure 1. Model of nucleoside transporters within renal epithelium	151
Figure 2. Renal transporters known to interact with nucleoside analogs	158
Figure 3. Actin and microtubules are important for steady-state expression of CNT1 and SPNT	162
Figure 4. Sequence alignment of N-terminal tails of ENTs	164
Figure 5. PKC-mediated internalization of CNT1	166

CHAPTER 1

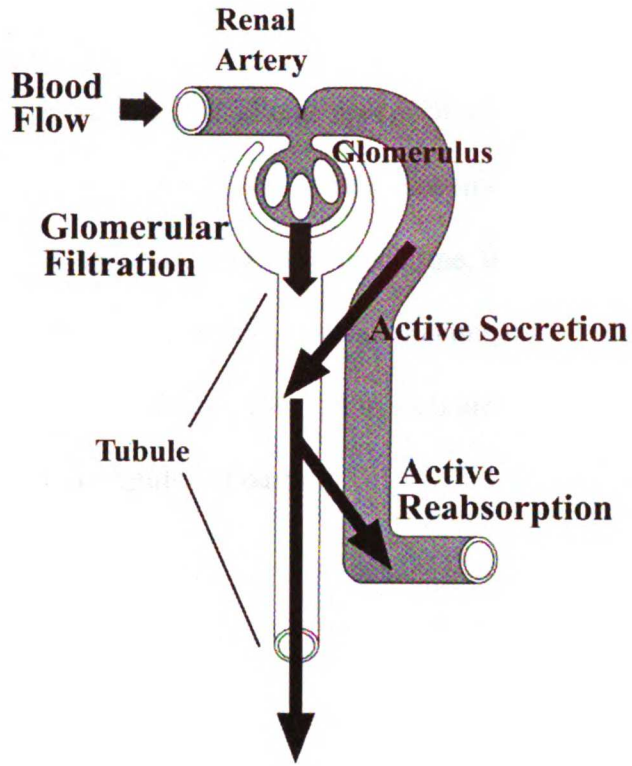
INTRODUCTION TO RENAL NUCLEOSIDE TRANSPORT

Renal Excretion

Renal function is essential for maintaining homeostasis within the body. The kidneys are responsible for regulating the composition of interstitial fluids by excreting waste and metabolites, salvaging nutrients and essential compounds, and regulating levels of water and ions. Renal excretion is the major pathway for elimination of many therapeutically administered drugs and their metabolites. Thus, the kidneys play a major role in determining the pharmacokinetic properties of many therapeutic agents. Identifying the mechanisms of renal excretion is essential to understanding these parameters.

Renal excretion of a drug involves three distinct processes: glomerular filtration, reabsorption, and secretion (Figure 1A). Plasma is passively filtered through the glomeruli. Water and small solutes (e.g., urea, glucose, sodium, and nucleosides) pass through the glomeruli and enter the tubule lumen whereas larger particles, including anionic molecules and proteins, are retained in the blood stream (3). As filtrate flows through the lumen, its composition is closely monitored by the epithelium that lines the tubules. Tubule epithelial cells are polarized, having two distinct membranes: an apical membrane, which is in contact with the tubule lumen and a basolateral membrane, which is in contact with the interstitium (Figure 1B). These two membranes differ in lipid and protein content and are separated by tight junctions. Tight junctions not only separate the

A.



B.

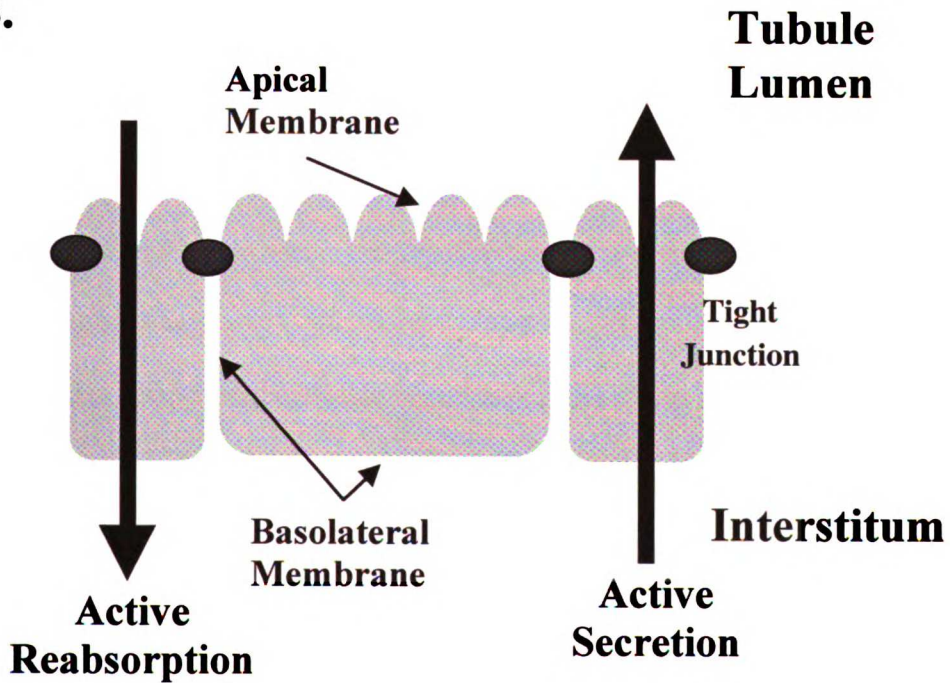


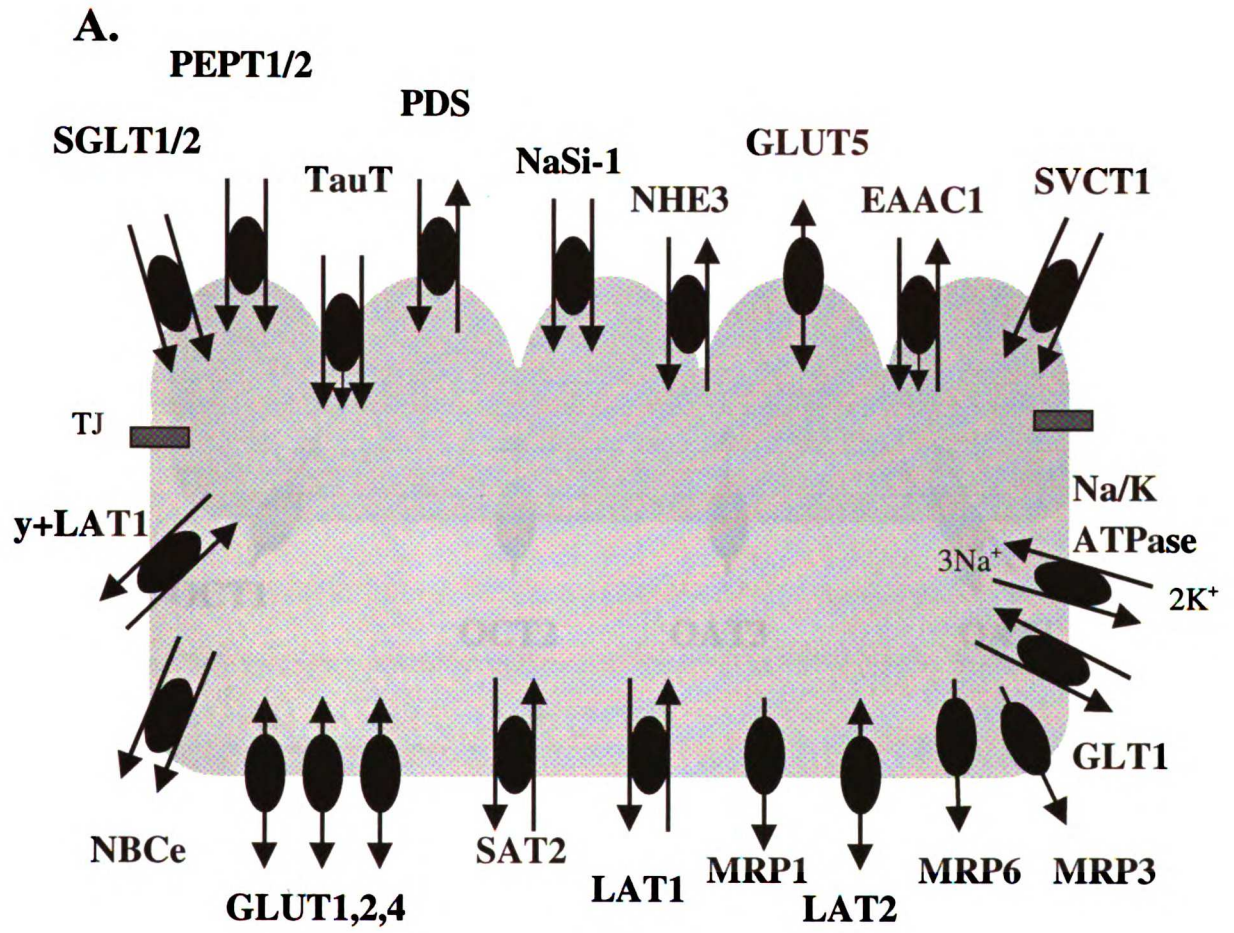
Figure 1. Mechanisms of renal elimination. (A.) Renal elimination involves three processes: 1., glomerular filtration, 2., secretion, and 3., reabsorption through the tubule wall and into or out of the renal vein. (B.) Renal epithelial cells line the tubule lumen, providing a barrier between filtrate and blood. The plasma membrane is divided into two distinct membranes by tight junctions: the apical membrane, which is in contact with the tubule filtrate, and the basolateral membrane, which is in contact with the blood. While there is some paracellular flux of solutes, most solutes that are secreted or reabsorbed must be transported through the epithelial barrier.

two poles of the cell but also connect neighboring cells, sealing them into an impermeable barrier. By this means, the renal epithelium provides a barrier between the internal system of the body and the tubule lumen. While there is some opportunity for paracellular movement of solute, most movement requires transcellular transport.

Essential nutrients and ions are reabsorbed from the filtrate through the luminal epithelium and returned to the circulation (Figure 1B) (3). This reabsorptive process salvages essential nutrients that cannot be synthesized *de novo*, and recycles complex molecules, which require large amounts of energy to synthesize (3). In addition, waste products and foreign solutes can be actively secreted, passing into the filtrate through the epithelium (Figure 1B). This secretory process concentrates unwanted compounds in the filtrate for excretion.

Carrier-Mediated Transport in Renal Excretion

Renal transepithelial flux of solutes in both the reabsorptive and secretory direction is mediated predominantly by transporter proteins (Figure 2). Transporters are poly-membrane spanning proteins that form a pore in the cellular membrane through which specific substrates pass. The substrate specificity of a transporter may be restricted as with glucose transporters, which only transport glucose, or much broader as with P-glycoprotein, which transports a large range of bulky hydrophobic molecules (1). Typically, transepithelial transport is mediated by two distinct transporter proteins localized to opposite membranes, allowing for passage of solute in one side of the cell and out of the other. Understanding the mechanisms by which transporters recognize and translocate substrates is a topic of much current research.



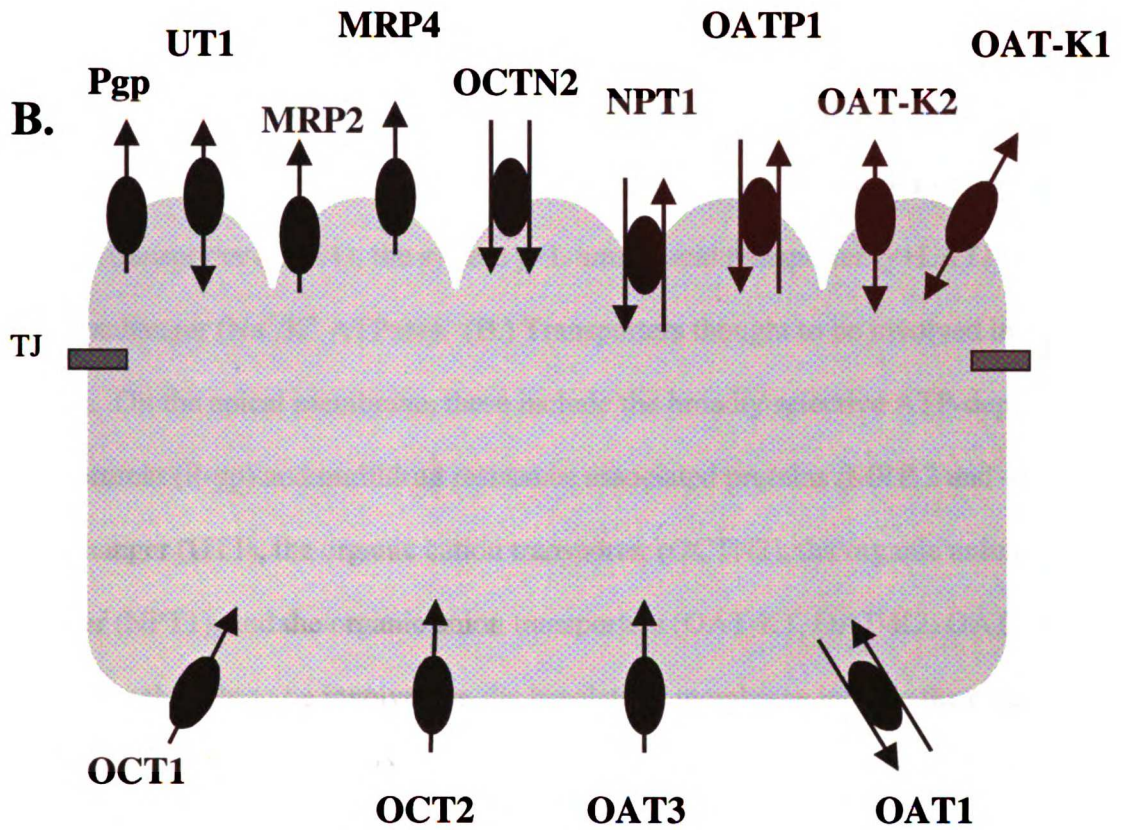


Figure 2. Transporters involved in renal elimination. Only those transporters for which subcellular localization is known are shown. (A.) Transporters thought to be involved in active reabsorption. On the apical membrane, these include the sodium-dependent glucose transporters (SGLT1, SGLT2), the taurine/ Na^+ / Cl^- transporter (TauT), the sodium-dependent peptide transporters (PEPT1, PEPT2), the glucose exchanger (GLUT 5), pendrin (PDS, which can act as a Cl^- /format, Cl^- /hydroxyl or Cl^- /bicarbonate exchanger), the sodium sulfate cotransporter (NaSi-1), the Na^+ / H^+ exchanger (NHE3), the

glutamate transporter (EAAC1), and the sodium-dependent vitamin C transporter (SVCT1). Transporters thought to be involved on the basolateral membrane include the Na⁺/bicarbonate transporter (NBC), the glucose exchangers (GLUT 1,2, and 4), the sodium-dependent sulfate transporter (SAT), the L-type amino acid transporters (LAT 1 and 2), multidrug resistance associated proteins (MRP 1, 3 and 6), the sodium-dependent glutamate transporter (GLT1), the system y⁺L amino acid transporter (y⁺LAT1) and the Na⁺/K⁺ exchanger (Na⁺/K⁺ ATPase). (B.) Transporters thought to be involved in active secretion. On the apical membrane, these include the broadly selective ATP-dependent P-glycoprotein (P-gp) and multidrug resistance associated proteins (MRP 2 and 4), the urea exchanger (UT1), the organic cation transporter (OCTN2), the organic anion/Cl⁻ exchanger (NPT1), and the organic anion transporters (OAT-K1, OAT-K2, OAT-P1). Transporters thought to be involved on the basolateral membrane include the organic cation transporters (OCT1 and OCT2), and the organic anion transporters (OAT1 and OAT3). Also thought to be involved in active secretion but not fully characterized or localized are the organic anion transporters (OAT2, OAT4, OATP3, OAT-PD, and OAT-PE) and the organic cation transporters (OCT3 and OCTN1).

Several classes of transporter proteins are present in the renal epithelium.

Facilitated transporters such as GLUT1 (a glucose transporter) mediate movement of a substrate down its electrochemical gradient. Movement can be either into or out of cells. Ion-coupled transporters couple uphill movement of substrate to the downhill transport of an ion (often Na^+ in higher eukaryotes but also H^+ , Cl^- , K^+ or OH^-) (65). Transport of both substrate and ion can be in the same direction as in the case of SGLT, a glucose/sodium symporter, or opposing directions as in the case of OCTN1, an organic cation/proton antiporter (50). Some transporters couple substrate movement to multiple ionic gradients as in the case of EAAT, which couples the transport of glutamate to that of two Na^+ ions, one OH^- and one K^+ (90). While these transporters are theoretically capable of acting in either direction, ionic gradients across cellular membranes are closely monitored and maintained at stable levels, forcing unidirectional movement via these transporters.

Ionic gradients are maintained by primary active transporters (1). These transporters couple uphill movement of substrate to energy consumption--usually via ATP hydrolysis. For example, Na^+/K^+ -ATPase activates extracellular movement of three Na^+ ions and intracellular movement of two K^+ ions upon hydrolysis of a single ATP molecule, thus maintaining both ionic gradients (1). The actions of this P-type ATPase are essential to kidney function, as many of the transporters that mediate active processes within the kidney are Na^+ or K^+ dependent. In fact, the compound effect of Na^+ -coupled transporters (which are generally on the apical membrane) and Na^+/K^+ -ATPase (which is confined to the basolateral membrane) provides a major pathway for transepithelial sodium reabsorption within the kidney (3).

Transporters involved in reabsorption tend to have narrow substrate specificity allowing only a small range of essential compounds to re-enter the circulation (Figure 2A). Most solutes that are reabsorbed (glucose, amino acids) tend to be small hydrophilic compounds that are not capable of passively diffusing across cellular membranes on their own. Typically, reabsorbed solutes are moved across the apical membrane against their concentration gradient and then pass through the basolateral membrane via facilitative diffusion. In general, transporters involved in active secretion interact with a much wider range of substrates, transporting a variety of compounds with similar chemical characteristics. Substrates are extracted from the interstitium and deposited in the tubule filtrate (Figure 2B).

Nucleosides

Nucleosides are small molecules consisting of a ribose or deoxyribose ring conjugated on the 1' carbon to a purine or pyrimidine nucleobase (Figure 3). Naturally occurring nucleosides are hydrophilic molecules and, as such, are impermeable to cellular membranes. They require carrier-mediated transport to pass into or out of cells. Two families of transport proteins selective for nucleosides have been identified to date. These proteins are differentially expressed in all cell types and allow for movement of nucleosides throughout the cellular environment.

The major physiologic role of nucleosides is as precursor to nucleotides, the essential building blocks of nucleic acids--both DNA and RNA (1). Thus, any cell undergoing cell division or transcription is in need of nucleosides. Nucleotides are high energy compounds, containing one or more phosphate bonds, and, as such, also serve as

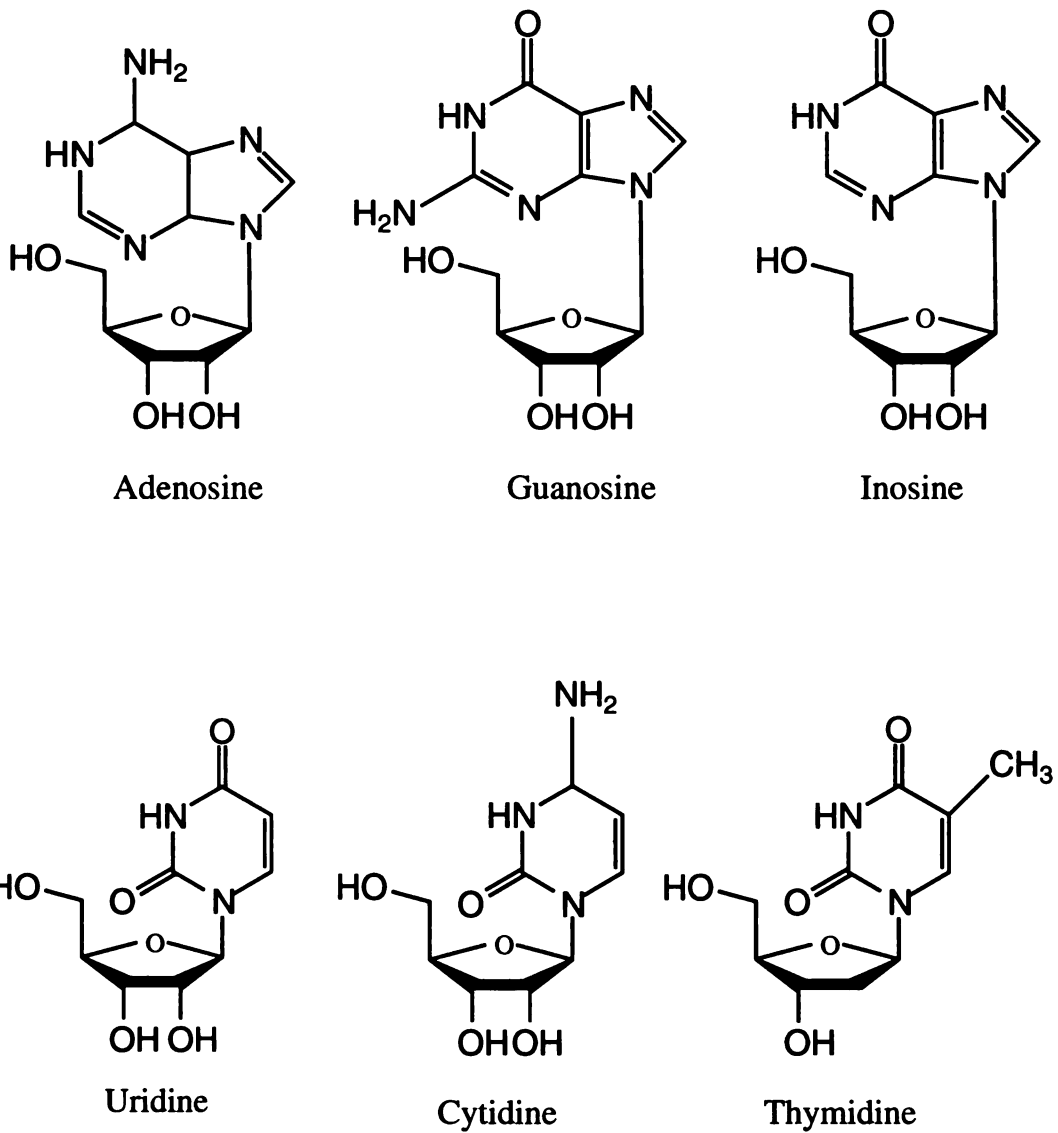


Figure 3. Chemical structure of endogenous nucleosides. Adenosine, guanosine, and inosine have a purine base linked to a ribose ring. Uridine, cytidine, and thymidine have a pyrimidine base linked to a ribose or 2'-deoxyribose ring.

physiologic energy-storing molecules (1). ATP hydrolysis is the primary source of energy used in many essential cellular processes. In addition, there are several purinoceptor systems that are stimulated by ATP or adenosine. As the natural metabolic product of ATP hydrolysis, adenosine serves as an indicator of local energy stores, and signaling modulates essential physiologic functions such as heart rate, sleep patterns, and bronchoconstriction accordingly (86). Adenosine signaling is also involved in maintaining homeostasis within the kidney where it regulates glomerular filtration rate (GFR), urine flow, solute excretion, and renin release (70).

While most types of cells are capable of biosynthesizing nucleosides *de novo* from components of the citric acid (TCA) cycle, this process is very energy consuming (96). Salvage and reuse of nucleosides provides a mechanism to minimize energy use and is preferred over *de novo* synthesis (34). In addition, several cell types such as enterocytes, leukocytes, and erythrocytes are not capable of *de novo* synthesis and rely on salvage as their only source of nucleosides (24). To this purpose, nucleosides are synthesized in the liver and circulated in the blood stream in low micromolar concentrations for use by these cells (34, 52).

There has been an increase, in recent years, of nucleoside analogs approved for therapeutic use, predominantly for the treatment of neoplasms and viral infections (Figure 4). Nucleoside analogs used as cancer chemotherapy such as cytosine- β -arabinofuranoside (ara-C) and gemcitabine enter cells via transporter proteins and are tri-phosphorylated to their active nucleotide counterparts. In this form, they can be incorporated into DNA strands where they cause both chain termination and DNA fragmentation, resulting in an inability for the cell to replicate and eventual programmed

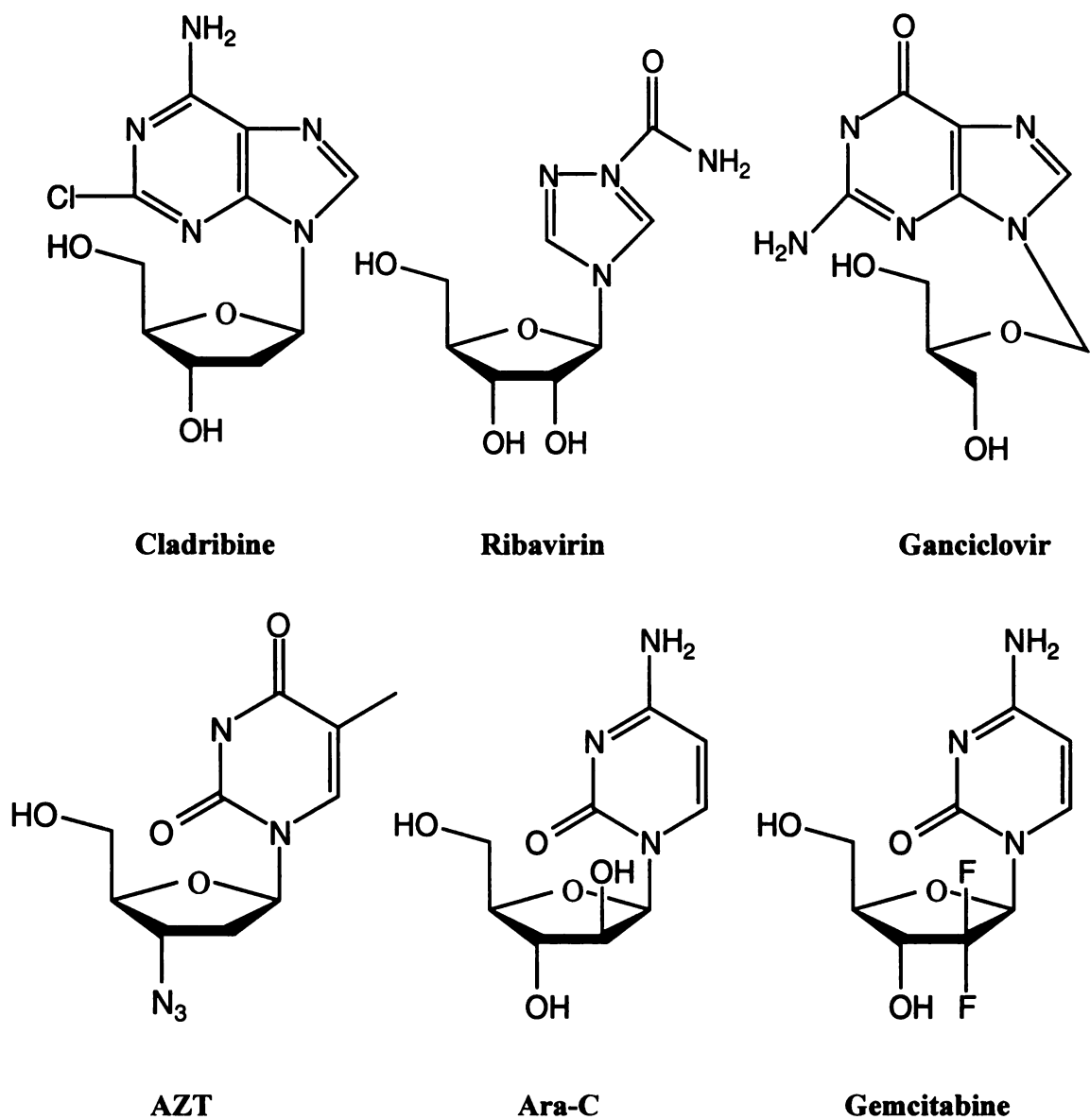


Figure 4. Chemical structures of several clinically relevant nucleoside analogs.

Cladribine is an adenosine analog, ribavirin and ganciclovir are guanosine analogs, azido-deoxythymidine (AZT) is a thymidine analog, cytosine- β -arabinofuranoside (ara-C) and gemcitabine are cytosine analogs.

cell death (23). Nucleoside analogs used in retroviral treatments such as zidovudine (AZT) or ganciclovir act similarly, causing DNA chain termination and interfering with reverse transcriptase (79). Because DNA chain elongation is a process required by all cell types, this class of compound often results in serious side effects. Toxicities appear to be most prevalent in tissues with high cellular metabolism such as pancreas and liver (79). They are also seen in tissues where nucleoside analogs become concentrated. For example, the primary side effect of ribavirin therapy is severe anemia. Ribavirin is a guanosine analog which becomes sequestered in red blood cells as the active phosphorylated form at concentrations forty times those seen in plasma, causing cell death (20).

Transmembrane transport is the first step in nucleoside analog treatment. While some nucleoside analogs such as AZT are able to diffuse across membranes at concentrations high enough to be efficacious, many nucleoside analogs require carrier-mediated transport in order to achieve therapeutic effect (48). In addition, transmembrane transport of nucleoside analogs is essential for renal elimination of these compounds. Most nucleoside analogs are excreted, in part, unchanged in urine. Clinical studies indicate that many undergo active renal secretion, though there is large interpatient variability in renal clearance data (Table 1). Several of these agents cause nephrotoxicity and eventual renal failure, suggesting that they may be concentrating in renal tubule epithelium (79).

Several nucleoside transport systems have been identified in the kidney. As an essential nutrient, one would expect nucleosides to be actively reabsorbed through the renal epithelium for reuse by the body as in the manner of glucose or amino acids. In

Table 1. Renal handling of clinically administered nucleoside analogs (30).

Therapeutic Compound	Common Indications	Fraction Unbound (f_u , %)	Renal Clearance (ml/min)	Fraction Excreted (f_e , %)
Gemcitabine	Pancreatic & non-small cell lung cancer	~100	264±135	<10
Mercaptopurine	ALL, ANL, CGL	81	169±154	22±12
Cytarabine (ara-C)	ALL, ANL, Meningial Leukemia, non-Hodgkin's Lymphoma	87	100±103	11±8
5-Fluorouracil (5FU)	Gastrointestinal & Breast Cancers	88 to 92	112±49	<10
Didanosine (ddI)	HIV-1, HIV-2, HTLV	> 95	403±277	36±9
Abacavir (ABC)	HIV-1	~100	89.6±19.5	75±10
Ganciclovir	CMV, HSV	~99	235±191	73±31
Stavudine (d4T)	HIV-1, HIV-2	~100	246±97	43.1±5.6
Acyclovir	HSV, CMV, Epstein Barr Syndrome	85 ± 4	3.37*GFR ¹	75±10
Zidovudine (AZT)	HIV-1, HIV-2, HTLV	>75	327±166	18±5
Lamivudine (3TC)	Hepatitis B, HIV-1, HIV-2	>64	144 to 339	49 to 85
Zalcitabine (ddC)	HIV-1, HIV-2	>96	186±103	65±17
Ribavirin	Hepatitis C	~100	122±52	35±8

Values given are mean ± standard deviation. In the case of 5FU f_u , and lamivudine Cl_r

and f_e , values are given as a range. Abbreviations: ALL, acute lymphocytic leukemia;

ANL, acute nonlymphocytic leukemia; HIV, human immunodeficiency syndrome; CMV,

cytomegalus virus; HSV, herpes simplex virus; HTLV, human T-cell lymphotropic

virus; AML, acute myelogenous leukemia; CGL, chronic granulocytic leukemia.

¹ GFR, glomerular filtration rate, is typically 120 ml/min for a healthy, young adult.

fact, there is clinical evidence for reabsorption of adenosine and the guanosine analog, ribavirin, within the proximal tubule (53). However, there is also significant clinical evidence for secretion of deoxyadenosine and many other nucleoside analogs (Table 1) (53). That is Cl_R exceeds $f_u \cdot GFR$. Thus, while the presence of nucleoside transporters within the kidney is well established, the role these proteins are playing in renal clearance of nucleosides and nucleoside analogs has not yet been determined. The purpose of this body of work was to examine the subcellular localization and trafficking patterns of the nucleoside transporters expressed in the kidney as a means to better understand their contribution to renal clearance of nucleosides and nucleoside analogs. This chapter will serve to introduce renal nucleoside transport systems, the six known nucleoside specific transporters and to discuss their role in renal handling of nucleosides and nucleoside analogs.

Nucleoside Transport Within the Kidney

Before the advent of molecular cloning, study of nucleoside transport function was carried out in whole tissue preparations. Several distinct types of transport were identified in this manner, differing in sodium-dependence, substrate selectivity, and sensitivity to the inhibitor, nitrobenzylthioinosine (NBMPR) (Table 2) (83). Six subtypes of sodium-dependent, concentrative nucleoside transport were observed (N1 - N6). N1-N4 are insensitive to NBMPR and differ in substrate selectivity: N1 is purine selective, N2 is pyrimidine selective, N3 is broadly selective and N4 transports pyrimidines and guanosine. Interestingly, all four systems are permeable to adenosine and uridine. N5 and N6 are both sensitive to NBMPR and transport adenosine analogs and guanosine,

Table 2. Nucleoside transport functions characterized from whole tissue.

Transport System	Na⁺-dependence	NBMPR Sensitive	Substrate Selectivity	Functional Renal Expression
<i>Concentrative Transport</i>				
N1	+	-	purines, uridine	yes
N2	+	-	pyrimidines, adenosine	yes
N3	+	-	purines, pyrimidines	N/D
N4	+	-	pyrimidines, guanosine, adenosine	yes
N5	+	+	adenosine analogs (Formycin B, 2CdA)	no
N6	+	+	guanosine	no
<i>Facilitative Diffusion</i>				
es	-	+	purines, pyrimidines	yes
ei	-	-	purines, pyrimidines	no

N/D: not determined. Abbreviations: 2CdA, 2-choro 2' deoxyadenosine (Cladribine).

respectively. Two subtypes of sodium-independent, equilibrative transport activities were observed, one that is sensitive to NBMPR (termed *es* for equilibrative, sensitive) and one that is insensitive (termed *ei* for equilibrative, insensitive).

Initial examinations of nucleoside transport systems within the kidney were carried out in membrane vesicle preparations from whole tissue in an attempt to identify the systems present on each membrane. For these studies, the apical or brush border membrane vesicles (BBM) were separated from the basolateral membrane vesicles (BLM) based on unique surface properties (31). While these processes serve to selectively concentrate either BBM or BLM for further analysis, there is always some residual cross-contamination of membranes--from the opposite membrane as well as from internal organelles (31). For this reason, identification of a transport system on one membrane or the other is not definitive proof of actual subcellular localization.

Initial examination of nucleoside interactions with vesicles prepared from rat renal brush border membranes identified, for the first time, the existence of a sodium-coupled transport system for adenosine (39, 41). Further studies observed active transport of a wide range of nucleosides--both purines and pyrimidines (38-40). All of these initial vesicle studies used either adenosine or uridine as a model substrate (16, 40). Because these nucleosides are universal substrates of transport systems N1-N4, it was difficult to determine which system was responsible for the observed transport. The first study to clearly identify the presence of distinct nucleoside transport systems was carried out by Williams *et al.* in bovine BBM (88, 89). Using guanosine and thymidine as substrates, these investigators clearly identified the presence of both system N1 and system N2 in the BBM (88, 89).

Equilibrative transport of nucleosides in renal vesicles has been limited to observation of system *es* and remains controversial. *Es* transport has been identified selectively on the BBM, selectively on the BLM, or on both membranes, depending on the study (6, 11, 66, 87). *Ei*-type transport was never observed. We now know that the *ei* system has a much lower affinity for most nucleosides than does *es* and, so, these studies do not exclude the possibility that *ei* activity may also be present in the kidney.

The first studies examining nucleoside transport activity in human renal vesicles were carried out in this laboratory (27). These studies indicated existence in BBM of both sodium-dependent and sodium-independent transport. Further characterization of concentrative transport identified only one system, termed N4. This system was permeable to pyrimidines, like the N2 system, but also transported guanosine (27, 28). The sodium-independent system was not characterized.

The advent of expression cloning techniques allowed for molecular characterization of these transporter systems. Initially, sodium-dependent systems were examined via heterologous expression of isolated renal poly-A mRNA in *Xenopus laevis* oocytes (19). Studies using both human and rat mRNA indicated the expression of a single sodium-dependent system--the pyrimidine-preferring system N2 (19). While these studies give us an idea of the nature of nucleoside transport activities in the kidney, they do not provide information about the molecular identities of the transporters.

Nucleoside Transporter Proteins

With the advent of cloning techniques, it is possible to identify and characterize the proteins responsible for nucleoside transport. To date, two families of mammalian

nucleoside transporters have been identified, both of which have three known members: the concentrative nucleoside transporters (CNT or SLC28) and the equilibrative nucleoside transporters (ENT or SLC29). All transporters cloned thus far appear to be expressed to some degree in the kidney and so a brief description of all six transporters follows (Table 3).

Concentrative Nucleoside Transporters

Three members of the mammalian concentrative nucleoside transporter family (CNT) have been cloned and functionally characterized to date: CNT1, CNT2 or SPNT (Sodium-dependent Purine-selective Nucleoside Transporter), and CNT3 (61, 62, 84). CNT1 is pyrimidine preferring (system N2), SPNT is purine preferring (system N1) and CNT3 is broadly selective (system N3). Proteins correlating to systems N4, N5 and N6 have not been identified and may reflect the properties of multiple transporters present in tissue preparations.

All three of the cloned nucleoside transporters appear to be expressed in the kidney to some degree. mRNA transcripts have been identified from kidney homogenate in all cases, though SPNT and CNT3 appear to be expressed at significantly lower levels than CNT1 (59, 61, 84). The physiological relevance of high levels of pyrimidine-specific nucleoside transport in kidney remains unclear. Protein levels of these transporters in kidney have not been quantified to date. However, protein levels of hepatic SPNT and CNT1 have been quantified (14). Interestingly, protein and mRNA levels did not correlate—SPNT mRNA levels were higher than CNT1 in liver but more CNT1 protein appeared to be expressed than SPNT (14). A similar phenomena may

Table 3. Cloned nucleoside transporters expressed in kidney.

Clone	Type Transport	Kidney Expression	
		mRNA	Protein
Concentrative Nucleoside Transporters (CNTs)			
CNT1	N1	high	yes
SPNT/CNT2	N2	low	yes
CNT3	N3	low	N/D
Equilibrative Nucleoside Transporters (ENTs)			
ENT1	es	high	N/D
ENT2	ei	low	N/D
ENT3	N/D	low	N/D

N/D: not determined

prove true in the kidney. With this in mind, we have chosen to examine the role of all three CNTs in the renal transport of nucleosides. We will first discuss the molecular characteristics of each individual transporter, and then briefly discuss important advances in understanding the mechanisms of action and physiologic relevance of the CNT family.

CNT1

CNT1 was the first member of this family to be isolated and heterologously expressed in oocytes (19). The rat cDNA (2.4 kb) encoding CNT1 was identified by Huang *et al.* via expression cloning techniques (32). CNT1 mRNA causes sodium-dependent nucleoside influx when injected in oocytes and is predicted to encode a 648 amino acid protein (~71 kDa) (32). CNT1 preferentially transports pyrimidine nucleosides (thymidine, cytidine, and uridine) and some pyrimidine analogs but not the purine nucleosides, guanosine or inosine, or their analogs (Tables 4 and 5). Interestingly, CNT1 does transport adenosine albeit at low capacity (32). It does not interact with either nucleobases (uracil, hypoxanthine) or nucleotides (UMP, UDP, UTP). Northern blot analysis indicates that CNT1 is expressed in abundance in jejunum and kidney. Sequence analysis and topology studies suggest that CNT1 has 13 transmembrane domains (TMDs) with a cytoplasmic N-terminal tail and an extracellular C-terminal tail (Figure 5) (29, 32). All known CNTs are thought to have a similar secondary structure. The rCNT1 sequence contains three putative glycosylation sites, two of which are known to be glycosylated (N605 and N643), and four putative protein kinase C phosphorylation (PKC) sites (29, 32). Both of these glycosylated sites reside in the predicted C-terminal tail.

The human ortholog, hCNT1, was cloned by hybridization from a kidney cDNA

Table 4. Substrate specificity of the rat (R) and human (H) orthologs of cloned nucleoside transporters.

Substrate	CNT						ENT				Reference
	1		2		3		1		2		
	R	H	R	H	M	H	R	H	R	H	

Naturally Occurring Compounds

Adenosine	[Dark Grey]										(4, 25, 32, 61, 62, 85, 93)
Uridine	[Dark Grey]										(4, 25, 32, 61, 84, 85, 93)
Cytidine	[Dark Grey]	[Dark Grey]	[Light Grey]	[Light Grey]	[Dark Grey]	[Dark Grey]	[Dark Grey]	[Dark Grey]	[Dark Grey]	[Dark Grey]	(17, 25, 45, 61, 81, 84, 85, 93)
Thymidine	[Dark Grey]	[Dark Grey]	[Light Grey]	[Light Grey]	[Dark Grey]	[Dark Grey]	[Dark Grey]	[Dark Grey]	[Dark Grey]	[Dark Grey]	(17, 32, 42, 61, 62, 76, 81, 84, 85, 92, 93)
Inosine	[Light Grey]	[Light Grey]	[Dark Grey]	[Dark Grey]	[Dark Grey]	[Dark Grey]	[Dark Grey]	[Dark Grey]	[Dark Grey]	[Dark Grey]	(25, 44, 61, 67, 81, 84, 85, 93)
Guanosine	[Light Grey]	[Light Grey]	[Dark Grey]	[Dark Grey]	[Dark Grey]	[Dark Grey]	[Dark Grey]	[Dark Grey]	[Dark Grey]	[Dark Grey]	(13, 25, 61-63, 85, 93)
Formycin B	[Light Grey]	[Light Grey]	[Dark Grey]	[Dark Grey]	[White]	[Dark Grey]	[White]	[White]	[White]	[White]	(4, 10, 45, 61, 84)
Hypoxanthine	[Light Grey]	[Light Grey]	[Light Grey]	[Light Grey]	[Light Grey]	[Light Grey]	[Light Grey]	[Light Grey]	[Light Grey]	[Dark Grey]	(61, 85, 94)
Uracil	[White]	[White]	[Light Grey]	[Light Grey]	[Light Grey]	[Light Grey]	[Light Grey]	[Light Grey]	[Light Grey]	[Dark Grey]	(10, 61, 63, 85, 93, 94)
Cytosine	[White]	[White]	[White]	[White]	[White]	[White]	[White]	[White]	[Light Grey]	[Dark Grey]	(94)
Adenine	[White]	[White]	[Light Grey]	[Light Grey]	[White]	[White]	[White]	[Light Grey]	[Dark Grey]	[Light Grey]	(10, 17, 46, 94)
Guanine	[White]	[White]	[White]	[White]	[White]	[White]	[White]	[White]	[Dark Grey]	[Dark Grey]	(94)
Thymine	[White]	[White]	[White]	[White]	[White]	[White]	[White]	[White]	[Dark Grey]	[Dark Grey]	(94)
UMP	[White]	[White]	[White]	[White]	[White]	[White]	[White]	[Dark Grey]	[White]	[White]	(46)
AMP	[White]	[Dark Grey]	[Light Grey]	[White]	[White]	[White]	[White]	[White]	[White]	[White]	(17)
ADP	[White]	[Dark Grey]	[Dark Grey]	[White]	[White]	[White]	[White]	[White]	[White]	[White]	(17)
ATP	[White]	[Dark Grey]	[Dark Grey]	[White]	[White]	[White]	[White]	[White]	[White]	[White]	(17)

Traditional Inhibitors

NBMPR	[Light Grey]	[Light Grey]	[Light Grey]	[White]	[White]	[Light Grey]	[Dark Grey]	[Dark Grey]	[Dark Grey]	[Dark Grey]	(4, 13, 25, 26, 61, 62, 93)
dilazep	[Light Grey]	[Light Grey]	[Light Grey]	[White]	[White]	[Light Grey]	[Light Grey]	[Dark Grey]	[Dark Grey]	[Dark Grey]	(13, 21, 25, 26, 61, 62, 93)
dipyridamole	[Light Grey]	[Light Grey]	[Light Grey]	[White]	[White]	[Light Grey]	[Light Grey]	[Dark Grey]	[Dark Grey]	[Dark Grey]	(4, 10, 25, 60, 77, 93)

Antiviral agents

AZT, Zidovudine	[Dark Grey]	[Dark Grey]	[Light Grey]	[Light Grey]	[White]	[Dark Grey]	[Dark Grey]	[Dark Grey]	[Dark Grey]	[Dark Grey]	(32, 46, 60, 62, 63, 67, 85)
Zalcitabine, ddC	[Dark Grey]	[Dark Grey]	[Light Grey]	[Light Grey]	[White]	[Dark Grey]	[Dark Grey]	[Dark Grey]	[Dark Grey]	[Dark Grey]	(32, 46, 60, 62, 63, 67)

Table 5. Apparent Michaelis-Menten kinetic constant (K_m , substrate concentration at half-maximal velocity), in μM , of naturally occurring nucleosides and the nucleobase, hypoxanthine.

	CNT1	SPNT	CNT3	ENT1	ENT2
Adenosine	N/D	8.3±2.7	15.1±1.8	50±1	140±40
Uridine	45±8	80±10	21.6±5.4	480±260	270±50
Cytidine	34±7	---	15.4±2.7	680±130	5210±570
Thymidine	16.3±3.3	---	21.2±6.3	240±060	620±90
Guanosine	---	N/D	43.0±6.6	140±20	2700±1640
Inosine	---	4.5±10	52.5±12.6	200±50	50±10
Hypoxanthine	---	---	---	---	700±100
References	(63, 84, 94)	(44, 45, 62, 94)	(61, 94)	(85, 94)	(85, 94)

N/D, not determined; ---, not a substrate. All values from primary literature.

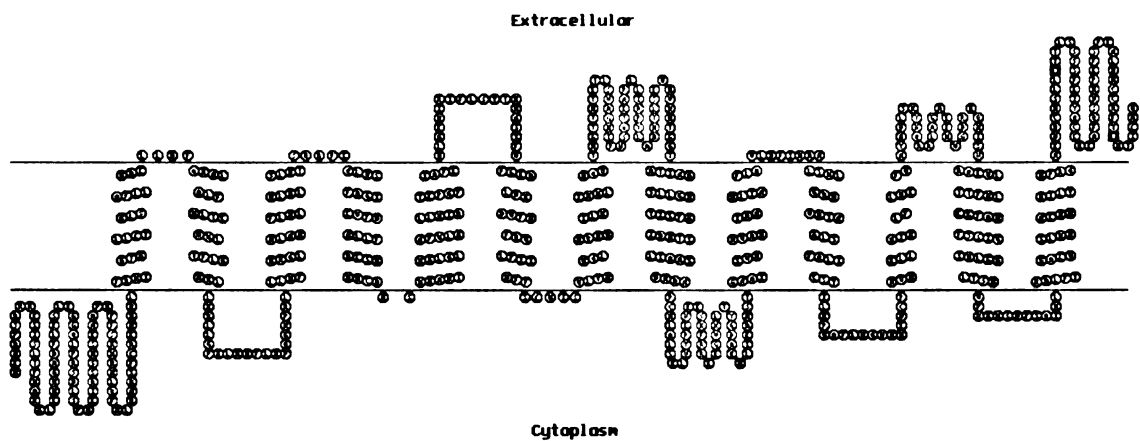


Figure 5. Secondary structure of hCNT1. All members of the CNT family are predicted to have 13 transmembrane spanning domains with a cytosolic N-terminal tail and an extracellular C-terminal tail. All N-linked glycosylation sites in each CNT are located within this C-terminal tail. hCNT1 contains two glycosylation sites, at N605 and N643 (indicated by black squares).

library in 1997 (62). hCNT1 encodes a protein of 650 amino acids (72 kDa), is 83% identical to rCNT1, and has a very similar secondary structure and substrate selectivity to its rat ortholog (see Table 4). That is, hCNT1 prefers pyrimidine nucleosides but also transports adenosine as a high-affinity, low-capacity substrate. hCNT1 has two putative glycosylation sites in the C-terminal extracellular tail, at positions N606 and N654. Treatment with endoglycosidase F, a deglycosylation agent, indicates that at least one of these sites is glycosylated (29). hCNT1 is encoded by 17 exons located on chromosome 15q25-26 (62). An ortholog of CNT1 has also been cloned from pig kidney (54).

Identification of the molecular structure of rat and human CNT1 has allowed for extensive analysis of both the mechanism of transport and the substrate selectivity of these proteins. Transport is sodium-dependent, with a likely coupling ratio of 1:1 (sodium: nucleoside). Transport also appears to be sensitive to membrane potential for both orthologs as some transport remains in the absence of sodium (12, 45, 49). A wide variety of nucleoside analogs pass through the kidney and may be affected by the presence of this system within renal epithelia. Both rat and human CNT1 have been expressed in multiple heterologous expression systems (oocytes, mammalian cells, and yeast) and examined for interaction with a variety of substrates. Standard assays in these systems involved determination of the uptake of radiolabeled nucleosides or nucleoside analogs and, often, the inhibition of uptake by unlabeled compounds. While this methodology provides a rapid way to test for interactions of compounds with transporters, it requires the use of radiolabeled substrate in order to determine definitively whether a substance is acting as a substrate or an inhibitor, a difficult and costly task. The advent of electrophysiological techniques has allowed for a much broader

understanding of the substrate specificity of CNT1. Dresser *et al.* used this technique to examine the specificity of rCNT1 and elegantly examined the structural basis for substrate interaction (12). They found that pyrimidine analogs modified at the 3-, 4-, or 5- positions on the base continued to be transported by rCNT1 but modification at the 6- position negated substrate\transporter interactions. 5'-Hydroxylation of the ribose was not essential for transport. A summary of the substrates and inhibitors known to interact with rat and human CNT1, and the other clones discussed below, is provided in Table 4.

SPNT

The transcript encoding the purine-preferring (N1-type) transporter was cloned from rat liver in 1995 (4). This 2.9 kb transcript contains an open reading frame (ORF) encoding a protein 659 amino acids (~72 kDa) in length that is 64% identical to rCNT1. Sequence analysis indicates these two proteins have similar secondary structure. The rSPNT amino acid sequence contains five putative N-linked glycosylation sites (three of them in the extracellular C-terminal tail) and six putative PKC sites. Initial Northern blot analysis did not identify SPNT transcript in kidney tissue but further analysis via RNA dot blot indicates that low levels of mRNA are expressed (4, 59). Low levels of SPNT protein have also been detected in rat kidney homogenate (75). Large amounts of rSPNT have been identified in the intestine and liver (4, 59). This protein preferentially transports purine nucleosides—adenosine, guanosine, inosine—and purine nucleoside analogs over pyrimidine nucleosides although it also transports uridine (Table 4). A transcript identical to SPNT was also cloned from rat blood brain barrier (42). Interestingly, this clone appears to transport small but significant amounts of thymidine

(42). SPNT-dependent nucleoside transport appears to be mechanistically very similar to CNT1-mediated transport. The ratio of sodium to nucleoside transport via SPNT is 1:1

(43). In addition, there is some residual nucleoside transport in the absence of sodium, as was observed for both rat and human CNT1, suggesting that the protein may transport other ions (17).

The human ortholog of SPNT, termed hSPNT1, was originally cloned in this laboratory from kidney using homology cloning strategies (84). This cDNA, which is 81% identical to rSPNT and 72% identical to hCNT1, contains an ORF predicted to encode a protein of 658 amino acids (72 kDa) and causes sodium-dependent nucleoside transport when heterologously expressed (63). The protein is predicted to have a similar secondary structure to the other cloned CNTs, and contains six putative N-linked glycosylation sites (only the four in the C-terminal tail are predicted to be extracellular) and six putative PKC sites. hSPNT1 appears to be transcribed from 17 exons on chromosome 15q15 (63). Rabbit and mouse orthologs have also been cloned (18, 57). hSPNT1 has a wider tissue distribution than hCNT1 and is most abundant in the GI tract where it appears to be responsible for the absorption of ribavirin (58, 59). Significant amounts of hSPNT1 mRNA transcript were also detected in kidney, liver, skeletal muscle, lymph nodes and mammary gland (59).

There are some significant species differences in substrate selectivity for nucleosides and nucleoside analogs between rat and human SPNT (Table 4). Both selectively transport purinergic nucleosides but rat SPNT prefers adenosine to inosine whereas human SPNT prefers inosine to adenosine (17). hSPNT1 appears more selective than rSPNT which can interact with 5'-AMP and several ribose-modified nucleoside

analogs that are not transported by the human ortholog (17). Neither ortholog interacts with 5'-uridine analogs, indicating that renal elimination of these analogs will not be dependent on SPNT expression (17).

CNT3

hCNT3 and mCNT3 were identified in the EST database and simultaneously cloned from human mammary gland, human myeloid HL-60 cells, and mouse liver (61). hCNT3 encodes a 691 amino acid protein (77 kDa) containing four N-linked glycosylation sites, all within the C-terminal tail. mRNA is transcribed from 18 exons on chromosome 9q22.2. The sequence of the rat ortholog of CNT3 has been identified and placed in the database (Genebank accession number NM_080908) but no functional information is available.

The amino acid sequence of hCNT3 is 48% identical to hCNT1 and 47% identical to hSPNT1. These three proteins are predicted to have very similar secondary structures; however their sequences are different enough to place the CNT3 proteins into their own subfamily within the CNT family structure. Mechanistically, hCNT3 differs from CNT1 and SPNT in two major ways. First, the sodium: nucleoside coupling ratio for hCNT3 is 2:1, as opposed to 1:1 for the other CNTs. In a physiological situation, this means that hCNT3 concentrates nucleosides intracellularly at a rate 100 times that of hCNT1 or hSPNT1. Thus, hCNT3-mediated transport of nucleosides or analogs may be important even in tissues such as kidney where lower levels of transporter are expressed. Secondly, hCNT3 is broadly selective for nucleoside substrates, transporting both purine and pyrimidine nucleosides. Therefore, it interacts with a much broader range of therapeutic

nucleoside analogs and is expected to play a large role in absorption, distribution, and elimination of these drugs. CNT3 transport characteristics (broad specificity and 2:1 coupling ratio) corresponds to the N3 transport system, which was originally described by Wu and Giacomini from rabbit choroid plexus studies (91).

The molecular determinants of substrate selectivity and translocation for all three cloned CNTs appear to be related. Removal of the N-terminus of hCNT3, containing the intracellular tail and first three TMDs, results in a truncated protein that is still functional, indicating that translocation is independent of this portion of the protein (29).

Examination of the conserved differences between these proteins in the remaining amino acid sequence has provided insight in determining which regions are responsible for substrate selectivity. This was originally examined via a series of chimeric studies in this laboratory, using rat CNT1 and SPNT (80-82). Using CNT1 as template, the sequence surrounding TMD 8 was replaced with the corresponding sequence from SPNT, resulting in a broadly selective nucleoside transporter (80, 82). Further studies determined that replacement of a single pair of residues in CNT1 (S318G/Q319M) with SPNT sequence also caused broad substrate selectivity, implicating these residues in substrate binding and possibly in the translocation pathway of these proteins (82). Similar studies repeated and expanded upon this using the human clones (hCNT1 and hCNT2). From these, we see that alteration of these two residues (S319G/Q320M in human CNT2) confers the ability to transport purines to an otherwise pyrimidine-selective transporter (44). In addition, mutations of conserved differences in a nearby region (S353T and L354V) selectively reduce pyrimidine transport, indicating that purine-selection and pyrimidine-selection

may occur at different positions within these proteins (44). Examination of residues at these positions in the broadly selective hCNT3 and its orthologs supports the importance of these four residues and the area surrounding TMDs 7-8 in determination of substrate selectivity (Figure 6).

While much work has been done examining the molecular determinants responsible for transporter function, few studies have examined the physiologic role of these transporters. The construction of transporter specific antibodies has facilitated such studies and extensive work in this vein has been carried out by the Pastor-Anglada laboratory, focusing on CNT expression in hepatocytes and macrophages (56). Both SPNT and CNT1 protein are present in rat hepatocytes, where they appear to have differential subcellular localization and regulatory patterns (56). SPNT is confined to sinusoidal (basolateral) membranes while CNT1 localizes to caveolin-enriched fractions, early endosomes, and canalicular (apical) membranes (56). Differential expression indicates that these proteins may have different functional roles within a cell. In addition, there is increasing evidence that these transporters are differentially regulated, creating a model of nucleoside transport that is closely governed by cellular needs and actions. This may be relevant in the kidney as a primary role of this organ is to monitor the composition of extracellular fluids throughout the body.

Equilibrative Nucleoside Transporters

Three members of the mammalian equilibrative nucleoside transporter (ENT, SLC29) family have been cloned to date: ENT1, ENT2, and ENT3 (25, 26).

ENT1

	311		TMD 8	371
hCNT1	SVAGNIFV	TEAPLLIRPYLADMTLSEVHVMTGGYATIAG	ILGAYISFGIDATSLIAA	
rCNT1	SVAGNIFV	TEAPLLIRPYLADMTLSEVHVMTGGYATIAG	ILGAYISFGIDAASLIAA	
hSPNT1	AVAGNIFV	TEAPLLIRPYLGDMTLSEIHAVMTGGFATISG	ILGAFIAFGVDASSLISA	
rSPNT	AVAGNIFV	TEAPLLIRPYLADMTLSEIHAVMTGGFATIAG	VLGAFISFGIDASSLISA	
hCNT3	VASGNIFV	TESPLLVRPYLPYITKSELHAIMTAGFSTIAG	ILGAYISFGVPSHLLTA	
rCNT3	VAAGNIFV	TESPLLVPYLPYITKSELHTIMTAGFATIAG	ILGAYISFGVSSTHLLTA	

Figure 6. Sequence alignments of CNTs in the region responsible for substrate specificity. Residues proven to be important for purine and pyrimidine specificity are highlighted. Predicted TMD 8 is overscored. Alignment is between residues 311 and 371 relative to the hCNT1 sequence.

exhibits equilibrative nucleoside transport, which is sensitive to inhibition by nanomolar concentrations of NBMPR (system *es*). Nucleoside transport by ENT2 is insensitive to inhibition by similar concentrations of NBMPR (system *ei*). Both ENT1 and ENT2 are transcribed in the kidney (59). Protein levels have not been determined.

The hENT3 sequence (accession number AF326987) has only recently been identified within the Genbank database by its homology to members of the ENT family. While examination of the EST database indicates that ENT3 is expressed in kidney, this protein does not localize to the plasma membrane in renal epithelial cells (unpublished observation). This intracellular localization has made functional characterization impossible thus far (33). For this reason, discussion of ENTs in this study will focus on ENT1 and ENT2.

ENT1

In 1997, a transcript encoding ENT1 was cloned from human placenta (25). The 2.1 kb transcript, which has been assigned to chromosome 6p21, is encoded by 12 exons, and contains an ORF predicted to encode a protein 456 residues (50 kDa) in length (8, 25). Topology studies and sequence analysis indicates that this protein has 11 TMDs, with an internal eleven residue N-terminal tail, an external four-residue C-terminal tail, and two large loops: an extracellular, glycosylated loop between TMDs 1-2 and a cytoplasmic loop between TMDs 6-7 (Figure 7) (71).

ENT1 is broadly selective, transporting both pyrimidine and purine nucleosides and their analogs but is impermeable to nucleobases or nucleotide monophosphates (Table 4) (46, 94). Pharmacological analysis indicates that ENT1 substrate binding is not

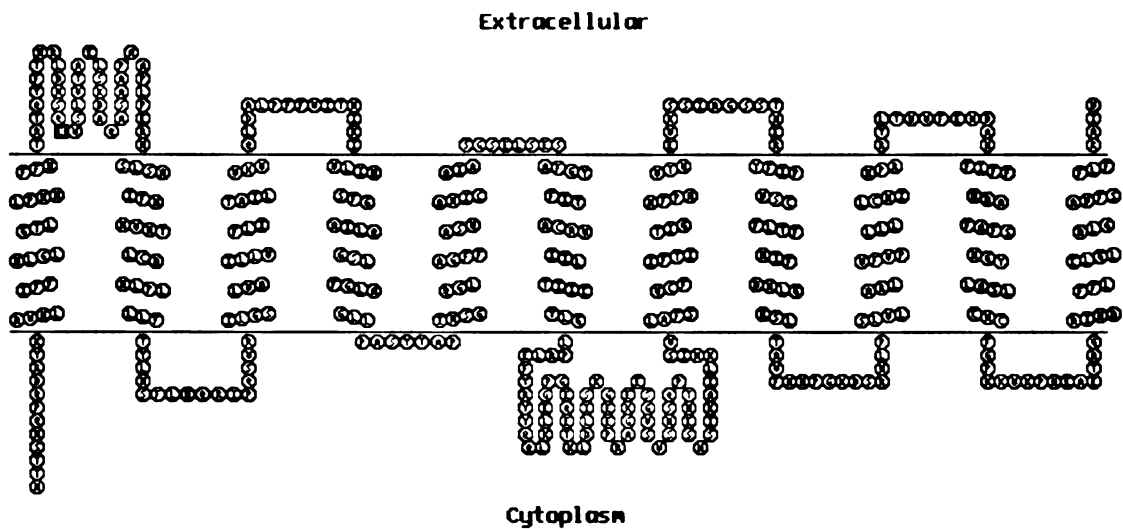


Figure 7. Secondary structure of hENT1. All members of the ENT family are predicted to contain 11 TMDs with a very short cytoplasmic N-terminal tail and extracellular C-terminal tail. These proteins have two predicted large loops--an extracellular loop between TMD 1-2 that is glycosylated and a cytosolic loop between TMD 6-7. hENT1 has one glycosylation site at position N48 (shown as a black square).

affected by base modifications but is sensitive to dehydroxylation at the 2', 3' or 5' positions of the ribose ring (46). Transport is inhibited by nanomolar concentrations of NBMPR (IC₅₀ is 3.7 nM for uridine inhibition) (25). NBMPR is not itself a substrate. In addition, transport is competitively inhibited by several coronary vasodilators: dilazep, draflazine, and dipyridamole. These compounds are structurally distinct from nucleosides but appear to bind to the same region of the transporter (71).

A number of studies have focused on mapping the substrate-binding region of hENT1. Mutagenesis studies indicate that TMDs 3-6 of hENT1 are responsible for interacting with both the vasodilators and NBMPR, suggesting that this region of the transporter is also responsible for substrate binding (71, 72). In addition, deglycosylation at position 48 and mutagenesis of residue 33, both within the first extracellular loop, decrease affinity of hENT1 for NBMPR (76, 78). Further mutagenesis studies demonstrate that the conserved glycine at residue 179 in TMD 5 is important for both NBMPR binding and nucleoside transport, linking the two functions to the same region of the transporter (69).

Transcripts of hENT1 are expressed within the kidney and are expected to be responsible for the *es*-type transport seen in membrane vesicle preparations from whole kidney tissue (59). Recent studies have shown that hENT1 transport can be regulated by several of the signaling pathways that are present in renal epithelium including protein kinase C (PKC) and purinoreceptor activity, indicating that renal nucleoside transport may be a dynamic phenomena (7, 55).

The rat ortholog of ENT1, which was cloned from jejunum, contains 457 residues and is 78% identical to hENT1 with a similar predicted secondary structure (93). rENT1

has similar substrate selectivity to hENT1, is equally as sensitive to inhibition by NMBPR (IC_{50} is 4.6 nM for uridine inhibition) but is insensitive to inhibition by any of the coronary vasodilators (73, 93). A mouse ortholog has also been cloned which is expressed in kidney (5, 35).

ENT2

ENT2 was initially cloned from rat jejunum. This 1.4 kb transcript encodes a protein of 456-residues that is 49% identical to rENT1 and has the same predicted secondary structure (93). A 1.4 kb transcript encoding a 456-residue protein (~50 kDa), termed hENT2, was simultaneously cloned in two separate laboratories from human placenta and the HeLa cell line (10, 26). hENT2 is encoded by 12 exons on chromosome 11q13. Both ENT2 proteins have a lower affinity for all nucleosides than ENT1 with the exception of inosine (85). Both the human and rat orthologs of ENT2 are poor transporters of guanosine and cytidine (85). ENT2 transport is partially inhibited by NBMPR at micromolar concentrations whereas ENT1 transport was entirely inhibited at nanomolar concentrations (93). Recent studies indicate that ENT2 binds and translocates nucleobases via the same pathway as nucleosides (94). The region of the protein responsible for nucleobase transport appears to lie within TMDs 5 and 6 (94).

mRNA expression profiling indicates that in the kidney hENT2 is far less abundant than hENT1 (59). Thus, hENT2-mediated transport of nucleosides within the kidney is likely to take a secondary role to hENT1-mediated transport, which has a higher expression level and a higher affinity for most nucleosides. However, hENT2 has a high affinity for inosine and hypoxanthine, two primary metabolites of adenosine. This may

be important for termination of actions generated by adenosine-mediated pathways within the kidney.

Renal Subcellular Localization of Nucleoside Transporters

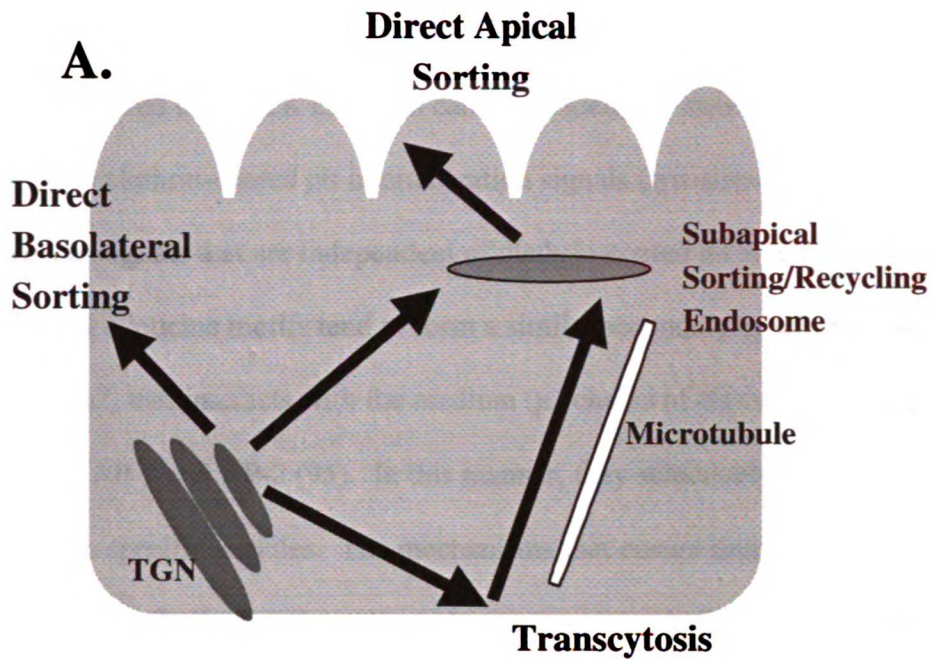
Presence of nucleoside transporters in the kidney likely plays a role in renal disposition of nucleosides and nucleoside analogs. Clinical studies indicate that some nucleosides and nucleoside analogs are actively reabsorbed whereas others are actively secreted (Table 1) suggesting that several transporters are involved in their disposition within the kidney. The chemical modifications of the analogs likely affect their relative affinity for various reabsorptive and secretory transporters, resulting in net reabsorption of some nucleoside analogs and net secretion of others (37). The presence of sodium-dependent nucleoside transport activity on the apical membrane of renal tissue preparations suggests that nucleoside transporters are localized to enhance renal reabsorption of the naturally occurring nucleosides. Identification and functional characterization of the molecules responsible for nucleoside-specific transport--the CNTs and ENTs--enables us to look at the individual role each transporter may have in these renal processes.

To determine the role of nucleoside transporters in the renal disposition of nucleosides, it is critical to determine the subcellular localization of these proteins, particularly of the concentrative nucleoside transporters. CNTs mediate unidirectional transport of nucleosides selectively into cells. Thus, presence on the basolateral membrane will imply that the transporters function to scavenge nucleosides from the

blood stream whereas presence on the apical membrane will imply that they function to salvage nucleosides from the tubule filtrate. In order to construct a model explaining the role of these proteins in renal distribution, we have chosen to examine the subcellular localization of all cloned nucleoside transporters known to be expressed in the kidney. To accomplish this, we have fluorescently tagged each transporter with green fluorescent protein (GFP) and stably expressed it in MDCK, a renal epithelial cell line. Presence of GFP did not alter the function of any of these transporters. Using this system, subcellular localization can be determined directly via immunofluorescence and functionally via membrane-specific nucleoside transport.

Molecular Determinants of Subcellular Localization

Plasma membrane proteins in polarized cells are targeted specifically to either the apical or basolateral membrane (or both) based on molecular signals within their own amino acid sequence. These proteins are formed in the endoplasmic reticulum and sorted into trafficking vesicles within the trans-golgi network. These vesicles travel throughout the cell, guided by the cytoskeleton, via a series of endosomes and selectively dock with either the apical or basolateral membrane (Figure 8A) (95). While most proteins are sent directly to the membrane on which they reside, some proteins are initially sent to the basolateral membrane and then selectively shuttled or transcytosed to the apical membrane. This indirect pathway is the major mechanism for trafficking newly synthesized apical proteins within hepatocytes and happens to a lesser degree in all other cell types.



B.

<u>Common Basolateral Targeting Motifs</u>	<u>Common Apical Targeting Motifs</u>
YXXØ or NPXY	GPI-Anchor
LL or II	TMD Domain
R/HXXV	Glycans

Figure 8. Trafficking pathways and targeting motifs. (A.) Newly synthesized membrane proteins are sorted in the trans-golgi network (TGN) and trafficked to either the basolateral or apical membranes. Some apical proteins are initially sent to the basolateral membrane and then transcytosed to their final destination. (B.) Several common basolateral and apical targeting motifs are shown. Y, tyrosine; X, any amino acid; Ø, bulky hydrophobic amino acid; N, asparagine; P, proline; L, leucine; I, isoleucine; R, arginine, H, histidine; V, valine.

The molecular determinants for basolateral sorting of plasma membrane proteins are well characterized and tend to rely on specific, short amino acid sequences, or targeting motifs, within the terminal tails of the protein (Figure 8B). These motifs are best characterized in MDCK cells and can be divided into two categories: signals that overlap with clathrin-coated pit internalization signals (tyrosine-based or dileucine motifs), and signals that are independent of clathrin-coated pit internalization (2). The tyrosine and dileucine motifs tend to form a similar secondary structure, known as a “tight β -turn”, that interacts with the medium (μ) chains of clathrin adaptor protein complexes, AP-1 and AP-2 (95). In this manner, they selectively concentrate basolateral proteins into specific vesicles. The mechanisms that ensure that these vesicles traffic to and dock with only the basolateral membrane are currently the topic of intense research (2). The cytoskeleton, docking machinery, and GTPases used to energize these actions are all implicated (2).

In contrast, apical sorting sequences are more complex and poorly understood (Figure 8B). For soluble proteins, linkage to a glycosylphosphatidylinositol (GPI)-anchor ensures apical trafficking (2). For some membrane-spanning proteins, the signal appears to be incorporated into the TMD itself (36). For others, apical sorting is mediated by lectins or N-glycans (2). A common theme for apical sorting has yet to emerge.

At the time this body of work began, it was known that MDCK and LLC-PK₁ cells, both renal epithelial cell lines, sorted proteins differently. Some proteins that localized to the basolateral membrane in MDCK appeared on the apical membrane in LLC-PK₁ (64). It became evident that LLC-PK₁ cells were missing a key element of the adaptor protein complexes, the μ 1B chain, which selectively interacts with tyrosine-based

basolateral targeting motifs (15). Thus, all basolateral proteins that rely on a tyrosine-based motif were missorted to the apical membrane in LLC-PK₁ cells. For this reason, all of the studies in this dissertation that identify partial or full basolateral targeting of a nucleoside transporter in MDCK also examine targeting patterns in LLC-PK₁.

Summary of Chapters

The goal of my dissertation research was to examine the subcellular localization of the known cloned nucleoside transporters in order to understand the role that these proteins play in renal disposition of nucleosides and nucleoside analogs. In addition, we sought to examine the targeting motifs responsible for trafficking of several of the transporters.

Transporter expression is often highly regulated. Understanding the molecular determinants for steady-state localization of nucleoside transporters will aid in accessing the mechanisms that govern transporter expression.

In **Chapter 2** of this dissertation, localization of two concentrative nucleoside transporters, SPNT and CNT1, within renal epithelial cells is determined. We find that both transporters localize predominantly to the apical membrane in both MDCK and LLC-PK₁ however significant amounts of SPNT (approximately 20%) are also present on the basolateral membrane.

Chapter 3 examines the role of glycosylation as a targeting motif in the trafficking of CNT1 and SPNT. Because steady-state expression of SPNT differs from CNT1, we hypothesized that these two proteins would have different targeting motifs. Preliminary studies indicated that SPNT but not CNT1 localization was affected by

deglycosylation. However, removal of all unique glycosylation sites from SPNT did not affect steady-state expression of this protein within MDCK.

In **Chapter 4**, the localization and targeting of the cloned equilibrative nucleoside transporters, ENT1 and ENT2, are studied. Both transporters localize predominantly to the basolateral membrane in MDCK and LLC-PK₁ cells. ENT1 is also expressed in small amounts on the apical membrane. The amino acid sequence for both transporters contained a putative targeting motif in the carboxy terminal tail: a R/HXXV motif on ENT1 and a dileucine repeat on ENT2. We examined the influence of these motifs on steady-state localization of these transporters using mutagenesis studies. Neither motif was required for membrane targeting of these proteins but the dileucine motif appeared to play a role in surface expression of ENT2.

Chapter 5 examines localization of the newly cloned concentrative nucleoside transporter, CNT3. CNT3 is entirely confined to the apical membrane of MDCK. It interacts with several clinically relevant nucleoside analogs (ribavirin, cladribine, and gemcitabine) and may play a role in renal handling of these molecules.

Chapter 6 summarizes these results and builds a model of renal nucleoside handling based on the findings of this dissertation. Some preliminary work that expands on these findings is also presented.

References

1. Alberts, B., D. Bray, J. Lewis, M. Raff, K. Roberts, and J. D. Watson. *Molecular Biology of the Cell*. New York: Garland, 1994.
2. Aroeti, B., H. Okhrimenko, V. Reich, and E. Orzech. Polarized trafficking of plasma membrane proteins: emerging roles for coats, SNAREs, GTPases and their link to the cytoskeleton. *Biochim Biophys Acta* 1376: 57-90, 1998.
3. Berne, R. M., and M. N. Levy. *Physiology*. New York: Mosby, 1998.
4. Che, M., D. F. Ortiz, and I. M. Arias. Primary structure and functional expression of a cDNA encoding the bile canalicular, purine-specific Na(+)-nucleoside cotransporter. *J Biol Chem* 270: 13596-9, 1995.
5. Choi, D. S., M. Handa, H. Young, A. S. Gordon, I. Diamond, and R. O. Messing. Genomic organization and expression of the mouse equilibrative, nitrobenzylthioinosine-sensitive nucleoside transporter 1 (ENT1) gene. *Biochem Biophys Res Commun* 277: 200-8, 2000.
6. Ciruela, F., J. Blanco, E. I. Canela, C. Lluís, R. Franco, and J. Mallol. Solubilization and molecular characterization of the nitrobenzylthioinosine binding sites from pig kidney brush-border membranes. *Biochim Biophys Acta* 1191: 94-102, 1994.
7. Coe, I., Y. Zhang, T. McKenzie, and Z. Naydenova. PKC regulation of the human equilibrative nucleoside transporter, hENT1. *FEBS Lett* 517: 201-5, 2002.
8. Coe, I. R., M. Griffiths, J. D. Young, S. A. Baldwin, and C. E. Cass. Assignment of the human equilibrative nucleoside transporter (hENT1) to 6p21.1-p21.2. *Genomics* 45: 459-60, 1997.

9. Crawford, C. R., C. E. Cass, J. D. Young, and J. A. Belt. Stable expression of a recombinant sodium-dependent, pyrimidine-selective nucleoside transporter (CNT1) in a transport-deficient mouse leukemia cell line. *Biochem Cell Biol* 76: 843-51, 1998.
10. Crawford, C. R., D. H. Patel, C. Naeve, and J. A. Belt. Cloning of the human equilibrative, nitrobenzylmercaptapurine riboside (NBMPR)-insensitive nucleoside transporter ei by functional expression in a transport-deficient cell line. *J Biol Chem* 273: 5288-93, 1998.
11. Doherty, A. J., and S. M. Jarvis. Na(+)-dependent and -independent uridine uptake in an established renal epithelial cell line, OK, from the opossum kidney. *Biochim Biophys Acta* 1147: 214-22, 1993.
12. Dresser, M. J., K. M. Gerstin, A. T. Gray, D. D. Loo, and K. M. Giacomini. Electrophysiological analysis of the substrate selectivity of a sodium-coupled nucleoside transporter (rCNT1) expressed in *Xenopus laevis* oocytes. *Drug Metab Dispos* 28: 1135-40, 2000.
13. Fang, X., F. E. Parkinson, D. A. Mowles, J. D. Young, and C. E. Cass. Functional characterization of a recombinant sodium-dependent nucleoside transporter with selectivity for pyrimidine nucleosides (cNT1rat) by transient expression in cultured mammalian cells. *Biochem J* 317 (Pt 2): 457-65, 1996.
14. Felipe, A., R. Valdes, B. Santo, J. Lloberas, J. Casado, and M. Pastor-Anglada. Na⁺-dependent nucleoside transport in liver: two different isoforms from the same gene family are expressed in liver cells. *Biochem J* 330: 997-1001, 1998.

15. Folsch, H., H. Ohno, J. S. Bonifacino, and I. Mellman. A novel clathrin adaptor complex mediates basolateral targeting in polarized epithelial cells. *Cell* 99: 189-98, 1999.
16. Franco, R., J. J. Centelles, and R. K. Kinne. Further characterization of adenosine transport in renal brush-border membranes. *Biochim Biophys Acta* 1024: 241-8, 1990.
17. Gerstin, K. M., M. J. Dresser, and K. M. Giacomini. Specificity of human and rat orthologs of the concentrative nucleoside transporter, SPNT. *Am J Physiol Renal Physiol* 283: F344-9, 2002.
18. Gerstin, K. M., M. J. Dresser, J. Wang, and K. M. Giacomini. Molecular cloning of a Na⁺-dependent nucleoside transporter from rabbit intestine. *Pharm Res* 17: 906-10, 2000.
19. Giacomini, K. M., D. Markovich, A. Werner, J. Biber, X. Wu, and H. Murer. Expression of a renal Na(+)-nucleoside cotransport system (N2) in *Xenopus laevis* oocytes. *Pflugers Arch* 427: 381-3, 1994.
20. Glue, P., S. Schenker, S. Gupta, R. P. Clement, D. Zambas, and M. Salfi. The single dose pharmacokinetics of ribavirin in subjects with chronic liver disease. *Br J Clin Pharmacol* 49: 417-21, 2000.
21. Gourdeau, H., M. L. Clarke, F. Ouellet, D. Mowles, M. Selner, A. Richard, N. Lee, J. R. Mackay, J. D. Young, J. Jolivet, R. G. Lafreniere, and C. E. Cass. Mechanisms of uptake and resistance to troxacitabine, a novel deoxycytidine nucleoside analogue, in human leukemic and solid tumor cell lines. *Cancer Res* 61: 7217-24, 2001.
22. Graham, K. A., J. Leithoff, I. R. Coe, D. Mowles, J. R. Mackey, J. D. Young, and C. E. Cass. Differential transport of cytosine-containing nucleosides by recombinant

human concentrative nucleoside transporter protein hCNT1. *Nucleosides Nucleotides Nucleic Acids* 19: 415-34, 2000.

23. Grant, S. Ara-C: cellular and molecular pharmacology. *Adv Cancer Res* 72: 197-233, 1998.

24. Griffith, D. A., and S. M. Jarvis. Nucleoside and nucleobase transport systems of mammalian cells. *Biochim Biophys Acta* 1286: 153-81, 1996.

25. Griffiths, M., N. Beaumont, S. Y. Yao, M. Sundaram, C. E. Boumah, A. Davies, F. Y. Kwong, I. Coe, C. E. Cass, J. D. Young, and S. A. Baldwin. Cloning of a human nucleoside transporter implicated in the cellular uptake of adenosine and chemotherapeutic drugs. *Nat Med* 3: 89-93, 1997.

26. Griffiths, M., S. Y. Yao, F. Abidi, S. E. Phillips, C. E. Cass, J. D. Young, and S. A. Baldwin. Molecular cloning and characterization of a nitrobenzylthioinosine-insensitive (ei) equilibrative nucleoside transporter from human placenta. *Biochem J* 328: 739-43, 1997.

27. Gutierrez, M. M., C. M. Brett, R. J. Ott, A. C. Hui, and K. M. Giacomini. Nucleoside transport in brush border membrane vesicles from human kidney. *Biochim Biophys Acta* 1105: 1-9, 1992.

28. Gutierrez, M. M., and K. M. Giacomini. Expression of a human renal sodium nucleoside cotransporter in *Xenopus laevis* oocytes. *Biochem Pharmacol* 48: 2251-3, 1994.

29. Hamilton, S. R., S. Y. Yao, J. C. Ingram, D. A. Hadden, M. W. Ritzel, M. P. Gallagher, P. J. Henderson, C. E. Cass, J. D. Young, and S. A. Baldwin. Sub-cellular

- Distribution and Membrane Topology of the Mammalian Concentrative Na⁺-Nucleoside Co-Transporter rCNT1. *J Biol Chem* 25: 25, 2001.
30. Hardman, J. G., L. E. Limbird, and A. G. Gilman. *Goodman and Gilman's The Pharmacological Basis of Therapeutics*. New York: McGraw Hill, 2001.
31. Hoyer, U. Tracer studies with isolated membrane vesicles. *Methods Enzymol* 172: 313-31, 1989.
32. Huang, Q. Q., S. Y. Yao, M. W. Ritzel, A. R. Paterson, C. E. Cass, and J. D. Young. Cloning and functional expression of a complementary DNA encoding a mammalian nucleoside transport protein. *J Biol Chem* 269: 17757-60, 1994.
33. Hyde, R. J., C. E. Cass, J. D. Young, and S. A. Baldwin. The ENT family of eukaryote nucleoside and nucleobase transporters: recent advances in the investigation of structure/function relationships and the identification of novel isoforms. *Mol Membr Biol* 18: 53-63, 2001.
34. Karle, J. M., L. W. Anderson, D. D. Dietrick, and R. L. Cysyk. Determination of serum and plasma uridine levels in mice, rats, and humans by high-pressure liquid chromatography. *Anal Biochem* 109: 41-6, 1980.
35. Kiss, A., K. Farah, J. Kim, R. J. Garriock, T. A. Drysdale, and J. R. Hammond. Molecular cloning and functional characterization of inhibitor-sensitive (mENT1) and inhibitor-resistant (mENT2) equilibrative nucleoside transporters from mouse brain. *Biochem J* 352 Pt 2: 363-72, 2000.
36. Kundu, A., R. T. Avalos, C. M. Sanderson, and D. P. Nayak. Transmembrane domain of influenza virus neuraminidase, a type II protein, possesses an apical sorting signal in polarized MDCK cells. *J Virol* 70: 6508-15, 1996.

37. Lai, Y., A. D. Bakken, and J. D. Unadkat. Simultaneous expression of hCNT1-CFP and hENT1-YFP in Mardin-Darby canine kidney (MDCK) cells: Localization and vectorial transport studies. *J Biol Chem* 277: 3, 2002.
38. Le Hir, M., and U. C. Dubach. Concentrative transport of purine nucleosides in brush border vesicles of the rat kidney. *Eur J Clin Invest* 15: 121-7, 1985.
39. Le Hir, M., and U. C. Dubach. Sodium gradient-energized concentrative transport of adenosine in renal brush border vesicles. *Pflugers Arch* 401: 58-63, 1984.
40. Lee, C. W., C. I. Cheeseman, and S. M. Jarvis. Na⁺- and K⁺-dependent uridine transport in rat renal brush-border membrane vesicles. *Biochim Biophys Acta* 942: 139-49, 1988.
41. Lee, C. W., C. I. Cheeseman, and S. M. Jarvis. Transport characteristics of renal brush border Na⁽⁺⁾- and K⁽⁺⁾-dependent uridine carriers. *Am J Physiol* 258: F1203-10, 1990.
42. Li, J. Y., R. J. Boado, and W. M. Pardridge. Cloned blood-brain barrier adenosine transporter is identical to the rat concentrative Na⁺ nucleoside cotransporter CNT2. *J Cereb Blood Flow Metab* 21: 929-36, 2001.
43. Li, J. Y., R. J. Boado, and W. M. Pardridge. Differential kinetics of transport of 2',3'-dideoxyinosine and adenosine via concentrative Na⁺ nucleoside transporter CNT2 cloned from rat blood-brain barrier. *J Pharmacol Exp Ther* 299: 735-40, 2001.
44. Loewen, S. K., A. M. Ng, S. Y. Yao, C. E. Cass, S. A. Baldwin, and J. D. Young. Identification of amino acid residues responsible for the pyrimidine and purine nucleoside specificities of human concentrative Na⁽⁺⁾ nucleoside cotransporters hCNT1 and hCNT2. *J Biol Chem* 274: 24475-84, 1999.

45. Lostao, M. P., J. F. Mata, I. M. Larrayoz, S. M. Inzillo, F. J. Casado, and M. Pastor-Anglada. Electrogenic uptake of nucleosides and nucleoside-derived drugs by the human nucleoside transporter 1 (hCNT1) expressed in *Xenopus laevis* oocytes. *FEBS Lett* 481: 137-40, 2000.
46. Lum, P. Y., L. Y. Ngo, A. H. Bakken, and J. D. Unadkat. Human intestinal es nucleoside transporter: molecular characterization and nucleoside inhibitory profiles. *Cancer Chemother Pharmacol* 45: 273-8, 2000.
47. Mackey, J. R., L. L. Jennings, M. L. Clarke, C. L. Santos, L. Dabbagh, M. Vsianska, S. L. Koski, R. W. Coupland, S. A. Baldwin, J. D. Young, and C. E. Cass. Immunohistochemical variation of human equilibrative nucleoside transporter 1 protein in primary breast cancers. *Clin Cancer Res* 8: 100-6, 2002.
48. Mackey, J. R., R. S. Mani, M. Selner, D. Mowles, J. D. Young, J. A. Belt, C. R. Crawford, and C. E. Cass. Functional nucleoside transporters are required for gemcitabine influx and manifestation of toxicity in cancer cell lines. *Cancer Res* 58: 4349-57, 1998.
49. Mangravite, L. M., J. H. Lipschutz, K. E. Mostov, and K. M. Giacomini. Localization of GFP-tagged concentrative nucleoside transporters in a renal polarized epithelial cell line. *Am J Physiol Renal Physiol* 280: F879-85, 2001.
50. Masereeuw, R., and F. G. Russel. Mechanisms and clinical implications of renal drug excretion. *Drug Metab Rev* 33: 299-351, 2001.
51. Mata, J. F., J. M. Garcia-Manteiga, M. P. Lostao, S. Fernandez-Veledo, E. Guillen-Gomez, I. M. Larrayoz, J. Lloberas, F. J. Casado, and M. Pastor-Anglada. Role of the human concentrative nucleoside transporter (hCNT1) in the cytotoxic action of 5'-

deoxy-5-fluorouridine, an active intermediate metabolite of capecitabine, a novel oral anticancer drug. *Mol Pharmacol* 59: 1542-8, 2001.

52. Monks, A., and R. L. Csyk. Uridine regulation by the isolated rat liver: perfusion with an artificial oxygen carrier. *Am J Physiol* 242: R465-70, 1982.

53. Nelson, J. A., J. R. Kuttesch, Jr., and B. H. Herbert. Renal secretion of purine nucleosides and their analogs in mice. *Biochem Pharmacol* 32: 2323-7, 1983.

54. Pajor, A. M. Sequence of a pyrimidine-selective Na⁺/nucleoside cotransporter from pig kidney, pkCNT1. *Biochim Biophys Acta* 1415: 266-9, 1998.

55. Parodi, J., C. Flores, C. Aguayo, M. I. Rudolph, P. Casanello, and L. Sobrevia. Inhibition of nitrobenzylthioinosine-sensitive adenosine transport by elevated D-glucose involves activation of P2Y2 purinoceptors in human umbilical vein endothelial cells. *Circ Res* 90: 570-7, 2002.

56. Pastor-Anglada, M., F. J. Casado, R. Valdes, J. Mata, J. Garcia-Manteiga, M. Molina, A. Felipe, B. del Santo, J. F. Mata, B. Santo, J. Lloberas, and J. Casado. Complex regulation of nucleoside transporter expression in epithelial and immune system cells. *Mol Membr Biol* 18: 81-5, 2001.

57. Patel, D. H., C. R. Crawford, C. W. Naeve, and J. A. Belt. Cloning, genomic organization and chromosomal localization of the gene encoding the murine sodium-dependent, purine-selective, concentrative nucleoside transporter (CNT2). *Gene* 242: 51-8, 2000.

58. Patil, S. D., L. Y. Ngo, P. Glue, and J. D. Unadkat. Intestinal absorption of ribavirin is preferentially mediated by the Na⁺-nucleoside purine (N1) transporter. *Pharm Res* 15: 950-2, 1998.

59. Pennycooke, M., N. Chaudary, I. Shuralyova, Y. Zhang, and I. R. Coe. Differential expression of human nucleoside transporters in normal and tumor tissue. *Biochem Biophys Res Commun* 280: 951-9, 2001.
60. Ritzel, M. W., A. M. Ng, S. Y. Yao, K. Graham, S. K. Loewen, K. M. Smith, R. G. Ritzel, D. A. Mowles, P. Carpenter, X. Z. Chen, E. Karpinski, R. J. Hyde, S. A. Baldwin, C. E. Cass, and J. D. Young. Molecular identification and characterization of novel human and mouse concentrative Na⁺-nucleoside cotransporter proteins (hCNT3 and mCNT3) broadly selective for purine and pyrimidine nucleosides (system cib). *J Biol Chem* 276: 2914-27, 2001.
61. Ritzel, M. W., A. M. Ng, S. Y. Yao, K. Graham, S. K. Loewen, K. M. Smith, R. G. Ritzel, D. A. Mowles, P. Carpenter, X. Z. Chen, E. Karpinski, R. J. Hyde, S. A. Baldwin, C. E. Cass, and J. D. Young. Molecular identification and characterization of novel human and mouse concentrative Na⁺-nucleoside cotransporter proteins (hCNT3 and mCNT3) broadly selective for purine and pyrimidine nucleosides (system cib). *J Biol Chem* 276: 2914-27, 2000.
62. Ritzel, M. W., S. Y. Yao, M. Y. Huang, J. F. Elliott, C. E. Cass, and J. D. Young. Molecular cloning and functional expression of cDNAs encoding a human Na⁺-nucleoside cotransporter (hCNT1). *Am J Physiol* 272: C707-14, 1997.
63. Ritzel, M. W., S. Y. Yao, A. M. Ng, J. R. Mackey, C. E. Cass, and J. D. Young. Molecular cloning, functional expression and chromosomal localization of a cDNA encoding a human Na⁺/nucleoside cotransporter (hCNT2) selective for purine nucleosides and uridine. *Mol Membr Biol* 15: 203-11, 1998.

64. Roush, D. L., C. J. Gottardi, H. Y. Naim, M. G. Roth, and M. J. Caplan. Tyrosine-based membrane protein sorting signals are differentially interpreted by polarized Madin-Darby canine kidney and LLC-PK1 epithelial cells. *J Biol Chem* 273: 26862-9, 1998.
65. Sadee, W., V. Drubbisch, and G. L. Amidon. Biology of membrane transport proteins. *Pharm Res* 12: 1823-37, 1995.
66. Sayos, J., J. Blanco, F. Ciruela, E. I. Canela, J. Mallol, C. Lluís, and R. Franco. Regulation of nitrobenzylthioninosine-sensitive adenosine uptake by cultured kidney cells. *Am J Physiol* 267: F758-66, 1994.
67. Schaner, M. E., J. Wang, S. Zevin, K. M. Gerstin, and K. M. Giacomini. Transient expression of a purine-selective nucleoside transporter (SPNTint) in a human cell line (HeLa). *Pharm Res* 14: 1316-21, 1997.
68. Schaner, M. E., J. Wang, L. Zhang, S. F. Su, K. M. Gerstin, and K. M. Giacomini. Functional characterization of a human purine-selective, Na⁺-dependent nucleoside transporter (hSPNT1) in a mammalian expression system. *J Pharmacol Exp Ther* 289: 1487-91, 1999.
69. SenGupta, D. J., P. Y. Lum, Y. Lai, E. Shubochkina, A. H. Bakken, G. Schneider, and J. D. Unadkat. A single glycine mutation in the equilibrative nucleoside transporter gene, hENT1, alters nucleoside transport activity and sensitivity to nitrobenzylthioinosine. *Biochemistry* 41: 1512-9, 2002.
70. Spielman, W. S., and L. J. Arend. Adenosine receptors and signaling in the kidney. *Hypertension* 17: 117-30, 1991.
71. Sundaram, M., S. Y. Yao, J. C. Ingram, Z. A. Berry, F. Abidi, C. E. Cass, S. A. Baldwin, and J. D. Young. Topology of a human equilibrative, nitrobenzylthioinosine

(NBMPR)-sensitive nucleoside transporter (hENT1) implicated in the cellular uptake of adenosine and anti-cancer drugs. *J Biol Chem* 276: 45270-5, 2001.

72. Sundaram, M., S. Y. Yao, A. M. Ng, C. E. Cass, S. A. Baldwin, and J. D. Young. Equilibrative nucleoside transporters: mapping regions of interaction for the substrate analogue nitrobenzylthioinosine (NBMPR) using rat chimeric proteins. *Biochemistry* 40: 8146-51, 2001.

73. Sundaram, M., S. Y. Yao, A. M. Ng, M. Griffiths, C. E. Cass, S. A. Baldwin, and J. D. Young. Chimeric constructs between human and rat equilibrative nucleoside transporters (hENT1 and rENT1) reveal hENT1 structural domains interacting with coronary vasoactive drugs. *J Biol Chem* 273: 21519-25, 1998.

74. Takechi, T., K. Koizumi, H. Tsujimoto, and M. Fukushima. Screening of differentially expressed genes in 5-fluorouracil-resistant human gastrointestinal tumor cells. *Jpn J Cancer Res* 92: 696-703, 2001.

75. Valdes, R., M. A. Ortega, F. J. Casado, A. Felipe, A. Gil, A. Sanchez-Pozo, and M. Pastor-Anglada. Nutritional regulation of nucleoside transporter expression in rat small intestine. *Gastroenterology* 119: 1623-30, 2000.

76. Vickers, M. F., R. S. Mani, M. Sundaram, D. L. Hogue, J. D. Young, S. A. Baldwin, and C. E. Cass. Functional production and reconstitution of the human equilibrative nucleoside transporter (hENT1) in *Saccharomyces cerevisiae*. Interaction of inhibitors of nucleoside transport with recombinant hENT1 and a glycosylation-defective derivative (hENT1/N48Q). *Biochem J* 339: 21-32, 1999.

77. Vickers, M. F., J. D. Young, S. A. Baldwin, M. J. Ellison, and C. E. Cass. Functional production of mammalian concentrative nucleoside transporters in *Saccharomyces cerevisiae*. *Mol Membr Biol* 18: 73-9, 2001.
78. Visser, F., M. F. Vickers, A. M. Ng, S. A. Baldwin, J. D. Young, and C. E. Cass. Mutation of residue 33 of human equilibrative nucleoside transporters 1 and 2 alters sensitivity to inhibition of transport by dilazep and dipyridamole. *J Biol Chem* 277: 395-401, 2002.
79. Walsh, P., D. W. Sifton, L. Murray, G. L. Kelly, N. Deloughery, S. Reilly, and S. W. Lehrer. *Physician's Desk Reference*. Montvale: Medical Economics Inc, 2002.
80. Wang, J., and K. M. Giacomini. Characterization of a bioengineered chimeric Na⁺-nucleoside transporter. *Mol Pharmacol* 55: 234-40, 1999.
81. Wang, J., and K. M. Giacomini. Molecular determinants of substrate selectivity in Na⁺-dependent nucleoside transporters. *J Biol Chem* 272: 28845-8, 1997.
82. Wang, J., and K. M. Giacomini. Serine 318 is essential for the pyrimidine selectivity of the N2 Na⁺-nucleoside transporter. *J Biol Chem* 274: 2298-302, 1999.
83. Wang, J., M. E. Schaner, S. Thomassen, S. F. Su, M. Piquette-Miller, and K. M. Giacomini. Functional and molecular characteristics of Na⁽⁺⁾-dependent nucleoside transporters. *Pharm Res* 14: 1524-32, 1997.
84. Wang, J., S. F. Su, M. J. Dresser, M. E. Schaner, C. B. Washington, and K. M. Giacomini. Na⁽⁺⁾-dependent purine nucleoside transporter from human kidney: cloning and functional characterization. *Am J Physiol* 273: F1058-65, 1997.
85. Ward, J. L., A. Sherali, Z. P. Mo, and C. M. Tse. Kinetic and pharmacological properties of cloned human equilibrative nucleoside transporters, ENT1 and ENT2, stably

expressed in nucleoside transporter-deficient PK15 cells. Ent2 exhibits a low affinity for guanosine and cytidine but a high affinity for inosine. *J Biol Chem* 275: 8375-81, 2000.

86. Williams, M., and M. F. Jarvis. Purinergic and pyrimidineric receptors as potential drug targets. *Biochem Pharmacol* 59: 1173-85, 2000.

87. Williams, T. C., A. J. Doherty, D. A. Griffith, and S. M. Jarvis. Characterization of sodium-dependent and sodium-independent nucleoside transport systems in rabbit brush-border and basolateral plasma-membrane vesicles from the renal outer cortex. *Biochem J* 264: 223-31, 1989.

88. Williams, T. C., and S. M. Jarvis. Multiple sodium-dependent nucleoside transport systems in bovine renal brush-border membrane vesicles. *Biochem J* 274: 27-33, 1991.

89. Williams, T. C., and S. M. Jarvis. Na(+)-dependent purine and pyrimidine nucleoside transporters in bovine outer renal cortex brush-border-membrane vesicles. *Biochem Soc Trans* 18: 684-5, 1990.

90. Wright, E. M., D. D. Loo, E. Turk, and B. A. Hirayama. Sodium cotransporters. *Curr Opin Cell Biol* 8: 468-73, 1996.

91. Wu, X., G. Yuan, C. M. Brett, A. C. Hui, and K. M. Giacomini. Sodium-dependent nucleoside transport in choroid plexus from rabbit. Evidence for a single transporter for purine and pyrimidine nucleosides. *J Biol Chem* 267: 8813-8, 1992.

92. Yao, S. Y., C. E. Cass, and J. D. Young. Transport of the antiviral nucleoside analogs 3'-azido-3'-deoxythymidine and 2',3'-dideoxycytidine by a recombinant nucleoside transporter (rCNT) expressed in *Xenopus laevis* oocytes. *Mol Pharmacol* 50: 388-93, 1996.

93. Yao, S. Y., A. M. Ng, W. R. Muzyka, M. Griffiths, C. E. Cass, S. A. Baldwin, and J. D. Young. Molecular cloning and functional characterization of nitrobenzylthioinosine (NBMPR)-sensitive (es) and NBMPR-insensitive (ei) equilibrative nucleoside transporter proteins (rENT1 and rENT2) from rat tissues. *J Biol Chem* 272: 28423-30, 1997.
94. Yao, S. Y., A. M. Ng, M. F. Vickers, M. Sundaram, C. E. Cass, S. A. Baldwin, and J. D. Young. Functional and Molecular Characterization of Nucleobase Transport by Recombinant Human and Rat Equilibrative Nucleoside Transporters 1 and 2. *Chimeric constructs reveal a role for the ENT2 helix 5-6 region in nucleobase translocation. J Biol Chem* 277: 24938-48, 2002.
95. Yeaman, C., K. K. Grindstaff, and W. J. Nelson. New perspectives on mechanisms involved in generating epithelial cell polarity. *Physiol Rev* 79: 73-98, 1999.
96. Zubay, G. *Biochemistry*. Dubunque, IA: Wm. C. Brown Publishers, 1993.

CHAPTER 2

LOCALIZATION OF CONCENTRATIVE NUCLEOSIDE TRANSPORTERS, SPNT AND CNT1, IN RENAL EPITHELIAL CELLS²

Introduction

Nucleosides and nucleoside analogs are used in the treatment of neoplasms, viral infections, and cardiac arrhythmias. These compounds are hydrophilic and are transported across lipid membrane barriers by specific transporter proteins. There are two main classes of nucleoside transporters, equilibrative and concentrative. Concentrative nucleoside transporters are Na⁺-dependent and are present in renal and intestinal epithelium and in liver (39). Based on substrate selectivity, several types of concentrative nucleoside transporters have been characterized: purine-selective (N1), pyrimidine-selective (N2) (30, 38) and broadly selective (N3, N4, and N5) (7, 10, 11). N1 and N2 type transport have both been functionally observed in kidney vesicles (16-19). Transporters exhibiting N1 and N2 type characteristics, termed SPNT (or CNT2) and CNT1, respectively, have been cloned from various mammalian species (human, rat, and pig) (8, 12, 28, 31, 40) and are members of the SLC28 family.

Nucleoside transporters appear to play major roles in the kidney. Both equilibrative and concentrative nucleoside transport activities have been observed in renal epithelium where they are hypothesized to act sequentially to mediate the transepithelial flux of nucleosides. Equilibrative transport mechanisms have been primarily observed in

² This chapter has been published previously: Mangravite, L.M., J. H. Lipschutz, K. E. Mostov, and K. M. Giacomini. "Localization of GFP-Tagged concentrative nucleoside transporters, SPNT-GFP and CNT1-GFP, in renal polarized epithelial cells." *Am J Physiol Renal Physiol* 280:F879-F885, 2001. Reprinted with permission.

basolateral membrane vesicle preparations whereas concentrative mechanisms have been observed in apical membrane vesicles suggesting that nucleosides are transported in a reabsorptive direction (9, 10, 16-19). This model of reabsorptive flux is further substantiated by renal clearance studies in humans demonstrating active reabsorption of nucleosides (15, 27). In contrast, evidence of secretion of nucleoside analogs challenges such reabsorptive schemes, but may be explained by interaction of these analogs with secretory transporters in the kidney (1, 25, 26).

In addition to their role in transepithelial flux, nucleoside transporters are also thought to modify adenosine signaling in the kidney. Adenosine acts via adenosine receptors (A_1 , A_{2A} , A_{2B} , and A_3) to modify kidney function and has been implicated in the metabolic regulation of glomerular filtration rate (GFR), renin release, erythropoietin production, adrenergic transmission, urine flow, and solute excretion. Receptor function has been localized to the renal tubule (42). Termination of receptor activity, by decreasing the level of adenosine in the vicinity of these receptors, is thought to occur by two mechanisms: 1) enzymatic deamination of adenosine and subsequent transporter-mediated internalization of inosine and 2) transporter-mediated internalization of adenosine (9). Recent studies describe A_1 -like receptor activity on the apical membrane and A_2 -like activity on the basolateral membrane (6, 33). Localization of nucleoside transporters to the apical or basolateral membrane is important in understanding their role in modulating adenosine action in the kidney.

To clearly understand the role of nucleoside transporters in the kidney in mediating the transepithelial flux of nucleosides and nucleoside analogs, it is critical to localize the transporters to the apical or basolateral membrane within renal epithelial

cells. Such studies are also important in understanding the inter-relationships between nucleoside transporters and adenosine receptor subtypes and the role of transporters in modulating the effects of adenosine in the kidney. Localization of transporters using Madin-Darby canine kidney (MDCK) cells, a polarized renal cell line, has mimicked *in vivo* localization in many transporter protein studies (3, 23, 24, 37). In this study we tagged the cloned nucleoside transporters, SPNT and CNT1, with green fluorescent protein (GFP) and expressed the resultant fusion proteins in MDCK cells. Stable expression of SPNT-GFP and CNT1-GFP in MDCK cells provides a method of visualizing the transporters to conclusively determine localization.

Materials and Methods

Materials. Cell culture media and supplements were purchased from the UCSF Cell Culture Facility (San Francisco, CA). G418 and blasticidin were purchased from CalBioChem (La Jolla, CA). pEGFP-C1 was obtained from Clontech (Palo Alto, Ca) and pcDNA3 and pcDNA6/V5-His/lacZ were purchased from Invitrogen (Carlsbad, CA). The pADtet7 vector and tet-off MDCK were a generous gift from Dr. Yoram Altschuler (UCSF, San Francisco, CA) but are available from Clontech (Palo Alto, CA) (2). The EMBL strain of MDCK was a kind gift from Dr. Karl Matlin (U Cincinnati, Cincinnati, OH). Texas-red conjugated phalloidin was purchased from Molecular Probes (Eugene, OR). Vectashield was supplied by Vector Laboratories, Inc (Burlingame, CA). Transwell polycarbonate cell culture filters and polycarbonate cell culture plates were purchased from Corning Costar Corporation (Corning, NY). Bradford reagent was supplied by Bio-Rad (Hercules, CA) and Pierce (Rockford, IL) provided albumin standard. Radiolabeled

uridine, inosine and thymidine were purchased from Moravек Biochemicals (Brea, CA). All other chemicals were purchased from Sigma (St Louis, MO).

Plasmid construction. Rat SPNT and CNT1 were subcloned into the pcDNA3 vector by adding an *EcoRV* site to the 5' end and a *NotI* site to the 3' end using the polymerase chain reaction. Both rat SPNT and CNT1 were subcloned into eGFP-C1 by adding a *BglII* site to the 5' end and a *Sall* site to the 3' end using the same method. SPNT-GFP was isolated from eGFP-C1 by adding an *EcoRI* site upstream to GFP and a *XbaI* site on the 3' end of SPNT and was subcloned into the pADtet7 expression vector. All sequences were confirmed by automated sequence analysis at the Biomolecular Resource Center (UCSF, San Francisco, CA).

Cell Culture. All cells were maintained in minimum essential medium (MEM) Eagle's with Earle's balanced salt solution (BSS) supplemented with 5% heat inactivated fetal bovine serum (FBS), 100 units/ml penicillin, and 100 µg/ml streptomycin in 5% CO₂, 95% air. Cells were transfected with pcDNA3-CNT1, pcDNA3-SPNT, eGFP-C1-CNT1, pADtet7-SPNT, or empty vector by the calcium phosphate method as previously described (4). pADtet7-SPNT was cotransfected with pcDNA6/V5-His/lacZ at a ratio of 100:1 to confer resistance to blasticidin. pcDNA3-CNT1 was cotransfected with eGFP-C1 at the same ratio so positive clones could be selected by fluorescence. Three days after transfection, stable clones were selected in media containing both 10 µg/ml blasticidin and 20 ng/ml doxycycline (for the pADtet7-SPNT vector) or 0.7 mg/ml G418. After 10-14 days, individual stable clones were isolated and positive clones further selected by immunocytochemistry and by ³H-uridine uptake.

Uptake measurements. Unpolarized cells were seeded at 5×10^4 cells/well in 24-well Costar polycarbonate plates and allowed to reach confluence over 3-4 days. Uptake measurements were made as previously described (35). Cells were washed at room temperature in either Na^+ buffer (128 mM NaCl, 4.73 mM KCl, 1.25 mM CaCl_2 , 1.25 mM MgSO_4 , 5 mM Hepes-Tris, pH 7.4) or in Na^+ -free buffer in which choline chloride is substituted for NaCl. Buffer was aspirated and cells were incubated in 10 μM nucleoside (0.1 μM radiolabeled nucleoside and 10 μM unlabeled nucleoside) for a specific time (1-2 minutes unless otherwise noted). All uptakes were carried out in the presence of 10 μM nitrobenzylthioinosine (NBMPR) and either in the presence or in the absence of Na^+ . Uptake was stopped by aspiration of reaction mix and three washes in ice-cold Na^+ -free buffer. Cells were solublized in 1 M NaOH for 2 hours, neutralized with 1 M HCl and counted on a Beckman Scintillation Counter. All studies were performed in triplicate. Data are reported as a mean \pm standard deviation (SD). All assays are repeated with empty vector or untransfected controls. In all cases, empty vector controls mirrored untransfected controls and are not reported. For all studies, 2-3 wells/plate were solublized and assayed for protein content using the Bradford method (35).

Inhibition studies. Inhibition assays were carried out for 1-4 minutes in triplicate. Briefly, ^3H -uridine uptake was measured in the presence of unlabeled uridine at concentrations varying between 0 mM and 2 mM in the presence or absence of Na^+ . Data are presented as mean \pm standard error of the mean (SEM). Data were fit to the equation $V = V_o/[1 + (I/I_{C50})^n]$ where V is uptake of ^3H -uridine in the presence of unlabeled uridine, V_o is ^3H -uridine uptake in absence of unlabeled uridine, I is the unlabeled uridine concentration and n is the Hill coefficient.

Localization uptake studies. To determine the uptake of nucleosides across the apical or basolateral membrane, the following procedure was used. Individual stable clones were polarized by growth on Transwell filters at a confluent density for 7 days with regular media changes. Prior to the experiment, each filter was washed on both the apical and basolateral sides with either Na⁺ or Na⁺-free buffer. In some cases, transepithelial electrical resistance (TEER) values were taken prior to uptake using a MILLICELL-ERS (Millipore Corp, Bedford, MA) equilibrated in Na⁺ Buffer. Radiolabeled nucleoside at the same concentrations as stated above was added to either the apical or basolateral side and nucleoside-free buffer was added to the opposite side. 10 μM NBMPR was added to both sides. Cells were incubated for 1-2 minutes. Radiolabeled nucleoside was aspirated and filters washed three times with ice-cold Na⁺-free buffer. Filters were air-dried, removed from plastic support and counted on a Beckman Scintillation counter. Two filters from each plate were solublized as described above and assayed for protein content.

Data analysis. All experiments were performed in triplicate on at least three separate occasions. For determination of statistical significance, the Student's unpaired t-test was used and p < 0.05 was considered significant (Kaleidagraph, V.3.0, Abelbeck/Synergy Software, Reading, PA). For determination of intracellular uridine concentrations following uptake on polarized MDCK, the following values were used for all calculations: an intracellular volume (total cell volume minus nucleus and vesicles) of 897 femtoliters/cell as determined by Butor and Davoust and 500,000 cells/Transwell filter as determined by Hemocytometer (5).

Confocal microscopy Samples grown on filters for 7 days as stated above were fixed with 4% paraformaldehyde, permeablized with 0.025% (w/v) saponin in phosphate buffered saline, stained with Texas-red conjugated phalloidin for visualization of actin, and mounted on slides in Vectashield mounting medium. Samples were analyzed using a BioRad MRC-1024 confocal microscope.

Transient transfection of LLC-PK₁. LLC-PK₁ cells were maintained in M-199 with Earle's BSS (UCSF Cell Culture Facility, San Francisco, CA) supplemented with 3% heat inactivated FBS, 100 units/ml penicillin, and 100 µg/ml streptomycin in 5% CO₂, 95% air. Cells were grown on Transwell filters with a 0.4 µm pore diameter for 72 hours, and then transfected in OPTIMEM Reduced Serum Medium (UCSF Cell Culture Facility, San Francisco, CA) using LipofectAMINE2000 (Gibco BRL, Rockville, MD). Cells were then grown 24 or 48 hours before being fixed and stained for confocal microscopy as described above.

Results

Stable expression of SPNT-GFP and CNT1-GFP in epithelial cells. To study the intracellular distribution of SPNT and CNT1, we constructed GFP fusion proteins. Using a PCR-based strategy, we tagged the N-terminus of each transporter with a genetically stabilized form of the *Aequorea victoria* GFP to generate SPNT-GFP and CNT1-GFP. Each tagged transporter was stably expressed in MDCK cells (Figure 1A and 1B). MDCK cells have low background concentrative nucleoside transport activity and form uniform, tight monolayers. The SPNT-GFP clone was capable of being expressed in a doxycycline repressible fashion but for the purpose of these studies was expressed

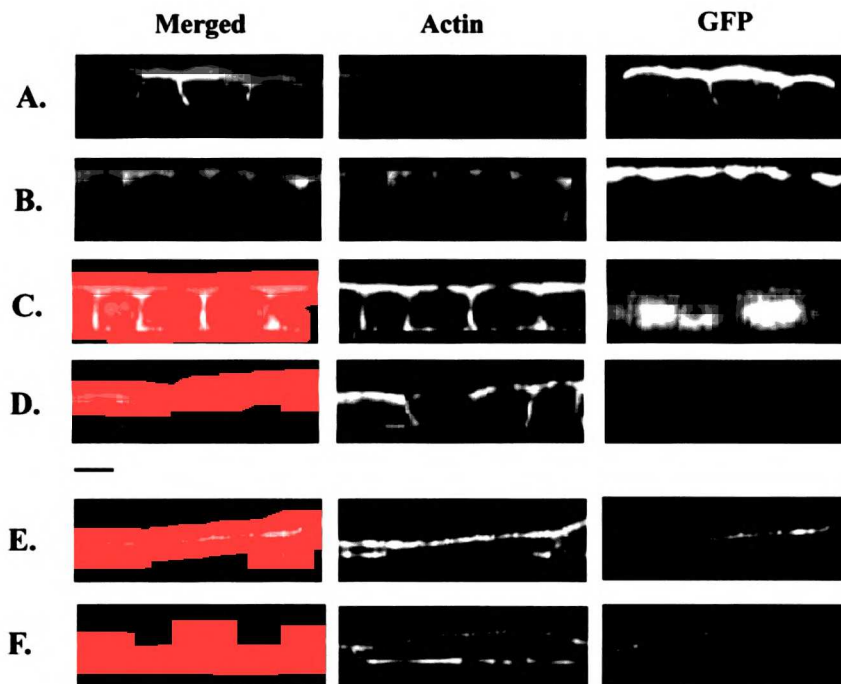


Figure 1. Localization of SPNT-GFP and CNT1-GFP in MDCK and LLC-PK₁ cells.

SPNT-GFP (A), CNT1-GFP (B), isolated GFP (C) and untransfected (D) MDCK clones were polarized by growth on filters for 7 days. The cells were fixed, permeablized, stained for actin with Texas-red conjugated-X phalloidin, and visualized using confocal fluorescence microscopy. SPNT-GFP (E) and CNT1-GFP (F) LLC-PK₁ cells were transiently transfected as described in the Methods section and prepared for confocal microscopy in the same manner as the MDCK cells. The first column shows the two images merged with GFP or GFP fusion protein stained green and actin stained red, the second column shows actin and the third column shows GFP or GFP fusion protein. Vertical optical sections are shown with the apical membrane on top.

Bar, 10 μ m.

continuously in the same manner as the other clones. In addition, we constructed stable transfections of wild-type SPNT and CNT1 and all empty vectors. Na⁺-dependent uptake of ³H-uridine in cells expressing SPNT-GFP or CNT1-GFP was significantly increased over uptake in untransfected or empty vector containing cells (data not shown). TEER values did not differ significantly between transfected and untransfected cells indicating no difference in monolayer tightness. Time-dependent Na⁺-stimulated uptake was linear at early times and plateaued at 10 minutes for both clones (data not shown).

Subsequently, all activity assays were performed for 1-2 minutes unless otherwise noted. Na⁺-dependent ³H-uridine uptake by CNT1- and SPNT-transfected cells (both tagged and untagged) grown in Transwells was concentrative with a final cellular uridine concentration approximately 10 times larger than the extracellular concentration.

Functionality of SPNT-GFP and CNT1-GFP (substrate specificity and inhibition profile of uridine transport) was investigated to determine (1) whether the tagged-transporters were functionally active and (2) whether the GFP tag kinetically altered the activity of the transporters.

We examined the substrate selectivity of the tagged transporters by observing the uptake of several radiolabeled endogenous nucleosides (³H-uridine, ³H-inosine, ³H-thymidine). These were chosen because inosine is a model purine nucleoside, thymidine is a model pyrimidine nucleoside and uridine is transported by all subtypes of nucleoside transporters. Significant uptake of ³H-uridine and ³H-inosine but not ³H-thymidine was observed in cells expressing SPNT-GFP whereas uptake of ³H-uridine and ³H-thymidine but not ³H-inosine was observed in cells expressing CNT1-GFP (Figure 2). No significant uptake was observed in untransfected cells or empty vector clones. These

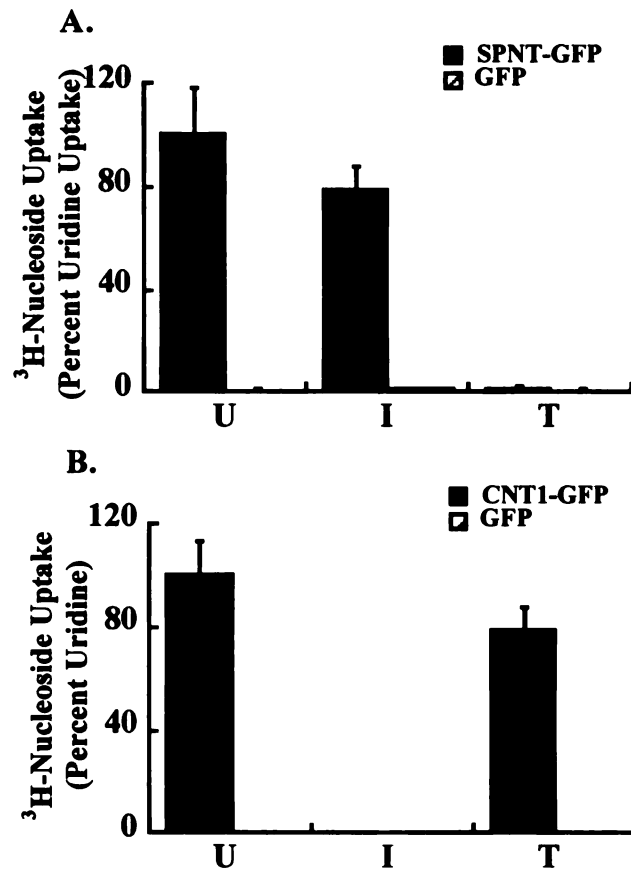


Figure 2. Uptake of ^3H -uridine, ^3H -inosine, and ^3H -thymidine in transfected MDCK cells. Uptake of $0.1\ \mu\text{M}$ ^3H -nucleoside (Control, uridine; I, inosine; T, thymidine) was measured at 25°C in the presence of $10\ \mu\text{M}$ NBMPR and $10\ \mu\text{M}$ of unlabeled nucleoside in (A.) SPNT-GFP cells (solid bars) and untransfected cells (hatched bars) and (B.) CNT1-GFP cells (solid bars) and untransfected cells (hatched bars). All compounds were studied in the presence of Na^+ . Data are presented as percent of ^3H -uridine uptake (pmol/min/mg protein) in presence of Na^+ and represent the average of three experiments in triplicate. Uridine uptake was 318.17 ± 63.2 pmol/mg/min for SPNT-GFP and 413 ± 52.3 pmol/mg/min for CNT1-GFP.

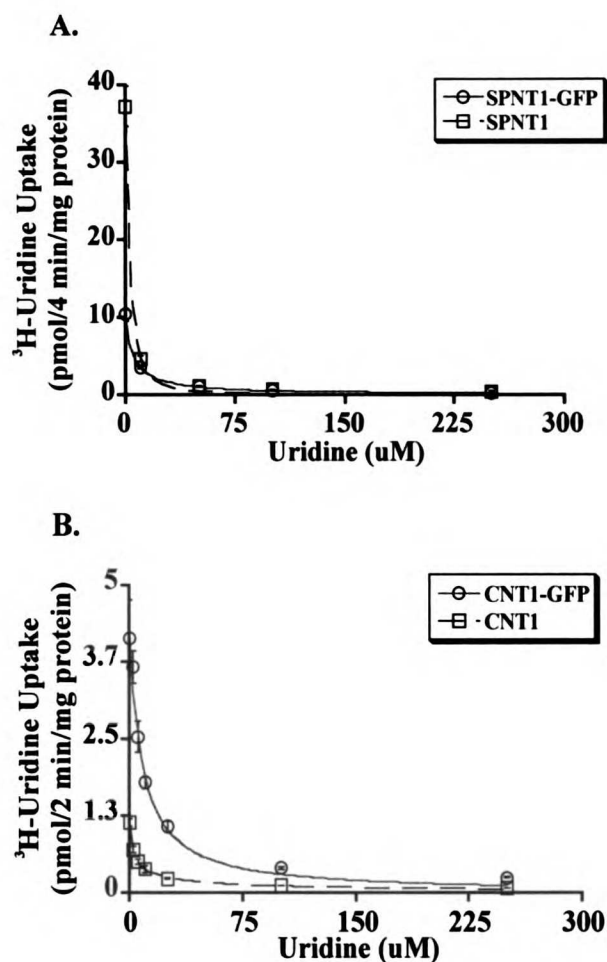


Figure 3. Inhibition of ³H-uridine uptake by unlabeled uridine in transfected MDCK cells. IC₅₀ studies of ³H-uridine uptake in the presence of unlabeled uridine at increasing concentrations in (A.) SPNT1-GFP cells (circles) and SPNT1 cells (squares) and (B.) CNT1-GFP cells (circles) and CNT1 cells (squares). Each point represents the mean ± SEM (n=3) from one representative experiment. IC₅₀ values were obtained by fitting the data to the equation $V = V_0/[1 + (I/IC_{50})]^n$. All fits were carried out using a nonlinear fitting routine in Kaleidagraph and values were compared using the Student's unpaired t-test (p<0.05).

results are consistent with the expected substrate selectivity of SPNT and CNT1 and indicate that the GFP tag does not alter selectivity of these transporters. The IC_{50} of uridine as an inhibitor of 3H -uridine uptake was $3.97 \pm 0.86 \mu M$ for SPNT-GFP and $5.51 \pm 1.45 \mu M$ for untagged SPNT (Figure 3A). The IC_{50} of uridine was $11.0 \pm 1.53 \mu M$ for CNT1-GFP and $3.13 \pm 0.37 \mu M$ for untagged CNT1 (Figure 3B). While these values are statistically different, they represent only modest differences in transport activity.

Localization of SPNT-GFP and CNT1-GFP in polarized MDCK cells. SPNT-GFP and CNT1-GFP transfected MDCK cells were grown as a polarized monolayer on a permeable filter support and examined by confocal fluorescence microscopy. MDCK were stained with Texas Red-conjugated phalloidin, a toxin which binds to actin filaments, to provide a basic outline of each cell. Vertical optical sections of both clones visualized at 488 nm show that SPNT-GFP and CNT1-GFP predominantly stain on the apical membrane (Figure 1A and 1B). In the case of SPNT-GFP, those cells that are most highly transfected as determined by fluorescence levels show low levels of basolateral staining as well. In contrast, isolated GFP clones display a cytosolic pattern of expression and untransfected cells do not display any GFP staining (Figure 1C and 1D). These data indicate the GFP-tagged transporters predominantly localize to the apical membrane domain in MDCK cells.

To determine whether CNT1-GFP and SPNT-GFP showed a similar pattern of distribution in a proximal tubule cell line, we transiently transfected LLC-PK₁ cells and examined the proteins using confocal microscopy (Figure 1E and 1F). In general, we observed a transfection efficiency of about 20% for both SPNT-GFP and CNT1-GFP. The patterns of distribution for both fusion proteins as well as GFP were identical to

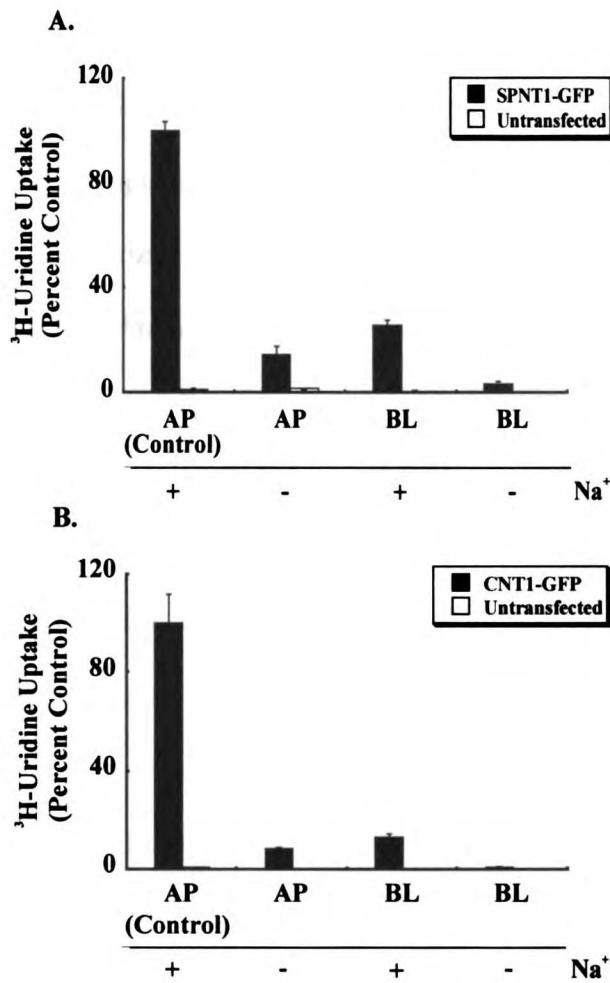


Figure 4. Functional localization of SPNT1-GFP and CNT1-GFP in MDCK cells. (A) SPNT1-GFP cells (solid bars) and untransfected cells (open bars) and (B) CNT1-GFP cells (solid bars) and untransfected cells (open bars) were polarized by growth on 0.4 μm filters for 7 days. ^3H -uridine uptake was measured from either apical (columns labeled AP) or basolateral (columns labeled BL) side in presence or absence of Na^+ . Data are presented as percent of apical uptake in presence of Na^+ and represent the average of 4 experiments (each performed in triplicate). Control is ^3H -uridine uptake from the apical side in presence of Na^+ .

those observed in stably transfected MDCK. That is, GFP showed a cytoplasmic distribution, whereas both CNT1-GFP and SPNT-GFP were predominately localized to the apical membrane with SPNT-GFP displaying a small amount of basolateral signal.

To further confirm apical localization, ³H-uridine uptake from both apical and basolateral surfaces of polarized cells was examined. Na⁺-dependent transport was seen primarily at the apical membrane in SPNT-GFP and CNT1-GFP cells (Figure 4A and 4B) as well as in SPNT and CNT1 cells (data not shown). Low levels of Na⁺-dependent nucleoside transport at the basolateral membrane were observed for both tagged and untagged SPNT and CNT1. For CNT1-GFP and CNT1, Na⁺-dependent basolateral uptake was 10 times lower than Na⁺-dependent apical uptake. For SPNT-GFP and SPNT, Na⁺-dependent basolateral uptake was a fourth of its respective apical uptake. Basolateral activity may indicate low levels of basolateral localization. None of the empty vector clones exhibited uridine uptake significantly different from that in untransfected cells.

Discussion

MDCK is the epithelial cell line most extensively used for studies of membrane trafficking pathways and has accurately predicted the *in vivo* localization of many transporters (3, 23, 24, 37). These cells are capable of direct and indirect protein targeting to both the basolateral and the apical membrane (32, 34). The present work describes the construction of two fusion proteins, SPNT-GFP and CNT1-GFP, and their stable transfection into MDCK cells. We demonstrated that the GFP-tag does not alter the substrate selectivity or functional localization of these transporters and only modestly affects kinetic characteristics of the tagged transporters in comparison to untagged

transporters. Confocal imaging and functional studies indicated that both tagged transporters are primarily localized to the apical membrane in MDCK and LLC-PK₁ cells though SPNT-GFP appears to have low levels of basolateral localization as well. This may be a result of saturation of the pathway of membrane traffic to the apical membrane, as has been described previously for other proteins (22). It may also reflect a dual role for SPNT on both membranes. By stably expressing fluorescent-labeled SPNT and CNT1 in these cells, we have determined their subcellular localization (Figure 1) and provided a model for addressing further questions regarding the cellular role of these transporters.

Renal clearance studies of nucleosides in humans indicate that adenosine is actively reabsorbed whereas deoxyadenosine and other nucleoside analog drugs (deoxyfluorouridine (dFUR), zidovudine (AZT), and zalcitabine (ddC)) are actively secreted (14, 15, 29). Secretory flux of deoxyadenosine as well as several other nucleoside analog drugs has been linked to xenobiotic transporters including organic cation and organic anion transporters (1, 25, 26). Our observation that SPNT and CNT1 predominantly localize to the apical membrane is consistent with studies in isolated renal apical membrane vesicles, and suggests that these transporters play a role in the reabsorption of adenosine and other nucleosides rather than the secretion of deoxyadenosine and nucleoside analog drugs.

These findings also implicate CNT1 and, in particular, SPNT in the adenosine pathway of renal auto-regulation by placing them in proximity to the A₁ receptor. Northern blot analysis indicates that A₁ is the most abundant adenosine receptor type in the kidney (41). Functional studies in the presence of adenosine receptor agonists and

antagonists indicate that A₁-type activity stimulates a majority of the known renal adenosine effects including GFR and renin release (20, 21). In addition, A₁-receptor antagonists have been shown in animal studies to limit severity of acute renal failure (36). Nucleoside transporters may serve to terminate adenosine receptor signaling by decreasing local concentrations of extracellular adenosine (13). Interestingly, stable transfection of the A₁ receptor in MDCK cells demonstrates that approximately 80% of this receptor localizes to the apical membrane with the remaining 20% appearing on the basolateral membrane similar to the results found for SPNT (33). While CNT1 is observed mainly in tissue where nucleoside salvage would be expected, SPNT has a much wider tissue distribution and is in high abundance within the heart, an organ with a large degree of adenosine receptor activity (7). Thus, SPNT may serve the additional function of modulating A₁-receptor mediated effects of adenosine in the renal tubule and elsewhere by internalizing adenosine as well as its deaminated metabolite, inosine.

In summary, the localization of SPNT-GFP and CNT1-GFP to the apical membrane of MDCK and LLC-PK₁ cells supports the model of renal nucleoside reabsorption and suggests a role for these transporters in the modification of adenosine signaling at the A₁ receptor. In addition the stably transfected cells provide a model for visualization of SPNT and CNT1 which may be used in the tracking of individual nucleoside transporters within mammalian cells. Localization under normal physiologic conditions provides a starting point from which to begin exploring the trafficking pathways and regulatory responses of concentrative nucleoside transporters. For the first time, we are capable of observing the mobility of these transporters in response to physiologic factors.

References

1. Aiba, T., Y. Sakurai, S. Tsukada, and T. Koizumi. Effects of probenecid and cimetidine on the renal excretion of 3'-azido-3'-deoxythymidine in rats. *J Pharmacol Exp Ther* 272: 94-9, 1995.
2. Barth, A. I., A. L. Pollack, Y. Altschuler, K. E. Mostov, and W. J. Nelson. NH₂-terminal deletion of beta-catenin results in stable colocalization of mutant beta-catenin with adenomatous polyposis coli protein and altered MDCK cell adhesion. *J Cell Biol* 136: 693-706, 1997.
3. Brandsch, M., V. Ganapathy, and F. H. Leibach. H(+)-peptide cotransport in Madin-Darby canine kidney cells: expression and calmodulin-dependent regulation. *Am J Physiol* 268: F391-7, 1995.
4. Breitfeld, P. P., J. E. Casanova, J. M. Harris, N. E. Simister, and K. E. Mostov. Expression and analysis of the polymeric immunoglobulin receptor in Madin-Darby canine kidney cells using retroviral vectors. *Methods Cell Biol* 32: 329-37, 1989.
5. Butor, C., and J. Davoust. Apical to basolateral surface area ratio and polarity of MDCK cells grown on different supports. *Exp Cell Res* 203: 115-27, 1992.
6. Casavola, V., L. Guerra, S. J. Reshkin, K. A. Jacobson, F. Verrey, and H. Murer. Effect of adenosine on Na⁺ and Cl⁻ currents in A6 monolayers. Receptor localization and messenger involvement. *J Membr Biol* 151: 237-45, 1996.
7. Cass, C. E. Nucleoside transport, in *Drug Transport in Antimicrobial and Anticancer Chemotherapy*. 403-451, New York: Marcel Dekker, 1995.

8. Che, M., D. F. Ortiz, and I. M. Arias. Primary structure and functional expression of a cDNA encoding the bile canalicular, purine-specific Na(+)-nucleoside cotransporter. *J Biol Chem* 270: 13596-9, 1995.
9. Franco, R., J. J. Centelles, and R. K. Kinne. Further characterization of adenosine transport in renal brush-border membranes. *Biochim Biophys Acta* 1024: 241-8, 1990.
10. Gutierrez, M. M., and K. M. Giacomini. Substrate selectivity, potential sensitivity and stoichiometry of Na(+)-nucleoside transport in brush border membrane vesicles from human kidney. *Biochim Biophys Acta* 1149: 202-8, 1993.
11. Huang, Q. Q., C. M. Harvey, A. R. Paterson, C. E. Cass, and J. D. Young. Functional expression of Na⁺-dependent nucleoside transport systems of rat intestine in isolated oocytes of *Xenopus laevis*. Demonstration that rat jejunum expresses the purine-selective system N1 (cif) and a second, novel system N3 having broad specificity for purine and pyrimidine nucleosides. *J Biol Chem* 268: 20613-9, 1993.
12. Huang, Q. Q., S. Y. Yao, M. W. Ritzel, A. R. Paterson, C. E. Cass, and J. D. Young. Cloning and functional expression of a complementary DNA encoding a mammalian nucleoside transport protein. *J Biol Chem* 269: 17757-60, 1994.
13. Klabunde, R. E., and D. G. Althouse. Adenosine metabolism in dog whole blood: effects of dipyridamole. *Life Sci* 28: 2631-41, 1981.
14. Klecker, R. W., Jr., J. M. Collins, R. C. Yarchoan, R. Thomas, N. McAtee, S. Broder, and C. E. Myers. Pharmacokinetics of 2',3'-dideoxycytidine in patients with AIDS and related disorders. *J Clin Pharmacol* 28: 837-42, 1988.
15. Kuttesch, J. F., Jr., and J. A. Nelson. Renal handling of 2'-deoxyadenosine and adenosine in humans and mice. *Cancer Chemother Pharmacol* 8: 221-9, 1982.

16. Le Hir, M., and U. C. Dubach. Concentrative transport of purine nucleosides in brush border vesicles of the rat kidney. *Eur J Clin Invest* 15: 121-7, 1985.
17. Le Hir, M., and U. C. Dubach. Sodium gradient-energized concentrative transport of adenosine in renal brush border vesicles. *Pflugers Arch* 401: 58-63, 1984.
18. Le Hir, M., and U. C. Dubach. Uphill transport of pyrimidine nucleosides in renal brush border vesicles. *Pflugers Arch* 404: 238-43, 1985.
19. Le Hir, M., U. C. Dubach, and S. Angielski. Transport of adenosine by kidney brush border vesicles. *Contrib Nephrol* 41: 417-9, 1984.
20. Libert, F., S. N. Schiffmann, A. Lefort, M. Parmentier, C. Gerard, J. E. Dumont, J. J. Vanderhaeghen, and G. Vassart. The orphan receptor cDNA RDC7 encodes an A1 adenosine receptor. *EMBO J* 10: 1677-82, 1991.
21. Mahan, L. C., L. D. McVittie, E. M. Smyk-Randall, H. Nakata, F. J. Monsma, Jr., C. R. Gerfen, and D. R. Sibley. Cloning and expression of an A1 adenosine receptor from rat brain. *Mol Pharmacol* 40: 1-7, 1991.
22. Marmorstein, A. D., K. G. Csaky, J. Baffi, L. Lam, F. Rahaal, and E. Rodriguez-Boulan. Saturation of, and competition for entry into, the apical secretory pathway. *Proc Natl Acad Sci U S A* 97: 3248-53, 2000.
23. Masuda, S., H. Saito, H. Nonoguchi, K. Tomita, and K. Inui. mRNA distribution and membrane localization of the OAT-K1 organic anion transporter in rat renal tubules. *FEBS Lett* 407: 127-31, 1997.
24. Masuda, S., A. Takeuchi, H. Saito, Y. Hashimoto, and K. Inui. Functional analysis of rat renal organic anion transporter OAT-K1: bidirectional methotrexate transport in apical membrane. *FEBS Lett* 459: 128-32, 1999.

25. Nelson, J. A., J. R. Kuttesch, Jr., and B. H. Herbert. Renal secretion of purine nucleosides and their analogs in mice. *Biochem Pharmacol* 32: 2323-7, 1983.
26. Nelson, J. A., E. Vidale, and M. Enigbokan. Renal transepithelial transport of nucleosides. *Drug Metab Dispos* 16: 789-92, 1988.
27. Newby, A. C. Adenosine and the concept of retaliatory metabolites. *Trends Biochem Sci* 9: 42-44, 1984.
28. Pajor, A. M. Sequence of a pyrimidine-selective Na⁺/nucleoside cotransporter from pig kidney, pkCNT1. *Biochim Biophys Acta* 1415: 266-9, 1998.
29. Patel, B. A., C. K. Chu, and F. D. Boudinot. Pharmacokinetics and saturable renal tubular secretion of zidovudine in rats. *J Pharm Sci* 78: 530-4, 1989.
30. Plagemann, P. G., and J. M. Aran. Characterization of Na⁽⁺⁾-dependent, active nucleoside transport in rat and mouse peritoneal macrophages, a mouse macrophage cell line and normal rat kidney cells. *Biochim Biophys Acta* 1028: 289-98, 1990.
31. Ritzel, M. W., S. Y. Yao, M. Y. Huang, J. F. Elliott, C. E. Cass, and J. D. Young. Molecular cloning and functional expression of cDNAs encoding a human Na⁺-nucleoside cotransporter (hCNT1). *Am J Physiol* 272: C707-14, 1997.
32. Saunders, C., J. R. Keefer, C. A. Bonner, and L. E. Limbird. Targeting of G protein-coupled receptors to the basolateral surface of polarized renal epithelial cells involves multiple, non-contiguous structural signals. *J Biol Chem* 273: 24196-206, 1998.
33. Saunders, C., J. R. Keefer, A. P. Kennedy, J. N. Wells, and L. E. Limbird. Receptors coupled to pertussis toxin-sensitive G-proteins traffic to opposite surfaces in Madin-Darby canine kidney cells. A1 adenosine receptors achieve apical and alpha 2A adrenergic receptors achieve basolateral localization. *J Biol Chem* 271: 995-1002, 1996.

34. Saunders, C., and L. E. Limbird. Disruption of microtubules reveals two independent apical targeting mechanisms for G-protein-coupled receptors in polarized renal epithelial cells. *J Biol Chem* 272: 19035-45, 1997.
35. Schaner, M. E., J. Wang, S. Zevin, K. M. Gerstin, and K. M. Giacomini. Transient expression of a purine-selective nucleoside transporter (SPNTint) in a human cell line (HeLa). *Pharm Res* 14: 1316-21, 1997.
36. Suzuki, F., J. Shimada, H. Mizumoto, A. Karasawa, K. Kubo, H. Nonaka, A. Ishii, and T. Kawakita. Adenosine A1 antagonists. 2. Structure-activity relationships on diuretic activities and protective effects against acute renal failure. *J Med Chem* 35: 3066-75, 1992.
37. Sweet, D. H., D. S. Miller, and J. B. Pritchard. Localization of an organic anion transporter-GFP fusion construct (rROAT1-GFP) in intact proximal tubules. *Am J Physiol* 276: F864-73, 1999.
38. Vijayalakshmi, D., and J. A. Belt. Sodium-dependent nucleoside transport in mouse intestinal epithelial cells. Two transport systems with differing substrate specificities. *J Biol Chem* 263: 19419-23, 1988.
39. Wang, J., M. E. Schaner, S. Thomassen, S. F. Su, M. Piquette-Miller, and K. M. Giacomini. Functional and molecular characteristics of Na(+)-dependent nucleoside transporters. *Pharm Res* 14: 1524-32, 1997.
40. Wang, J., S. F. Su, M. J. Dresser, M. E. Schaner, C. B. Washington, and K. M. Giacomini. Na(+)-dependent purine nucleoside transporter from human kidney: cloning and functional characterization. *Am J Physiol* 273: F1058-65, 1997.

41. Weaver, D. R., and S. M. Reppert. Adenosine receptor gene expression in rat kidney. *Am J Physiol* 263: F991-5, 1992.
42. Yamaguchi, S., S. Umemura, K. Tamura, T. Iwamoto, N. Nyui, T. Ishigami, and M. Ishii. Adenosine A1 receptor mRNA in microdissected rat nephron segments. *Hypertension* 26: 1181-5, 1995.

CHAPTER 3
SORTING OF SPNT IN RENAL EPITHELIUM
IS INDEPENDENT OF N-GLYCOSYLATION³

Introduction

Carrier-mediated transport of nucleosides and nucleoside analogs is achieved by two families of nucleoside transporters, concentrative and equilibrative. The concentrative nucleoside transporter (CNT, SLC28) family consists of three known mammalian members (CNT1, SPNT or CNT2, and CNT3) which mediate active transport of nucleosides down the sodium gradient (1, 4, 13). SPNT is a purine-selective concentrative nucleoside transporter found in abundance in renal epithelium where it is expected to play a role in reabsorption (11). SPNT is predominantly localized to the apical membrane in renal epithelial cells (MDCK and LLC-PK₁) (6). Interestingly, approximately one-fifth of the SPNT protein expressed was found on the basolateral membrane. In comparison, CNT1 was completely confined to the apical membrane (6). Presence of SPNT on both membranes of renal epithelium suggests a secondary role for this transporter in addition to nucleoside salvage.

We were particularly interested in investigating the molecular determinants responsible for localization of SPNT. Sorting signals for apical membrane proteins vary widely and are poorly understood but, for some membrane proteins, glycosylation has been documented as essential (7, 12). Analysis of SPNT as well as CNT1 and CNT3

³ This chapter has been accepted for publication as a manuscript entitled, "Sorting of Rat SPNT in Renal Epithelium is Independent of N-Glycosylation", in *Pharm Res*.

sequences indicates that these family members are differentially glycosylated. In this study, we examined the role of glycosylation as a potential sorting signal for SPNT in renal epithelium.

Materials and Methods

Materials. Cell culture media and supplements were purchased from the Cell Culture Facility (UCSF, San Francisco, CA). The EMBL MDCK II strain was a kind gift from Dr. Karl Matlin (U Cincinnati, Cincinnati, OH). chemiluminescence (ECL) detection was illuminated using Western Lightning (Perkin Elmer, Boston, MA). Complete Mini Protease Inhibitor Cocktail was purchased from Roche (Palo Alto, CA) and radiolabeled inosine from Morevak Biochemicals (Brea, CA). All other chemicals were purchased from Sigma (St. Louis, MO).

Site-directed mutagenesis. The Stratagene QuikChange Site-Directed Mutagenesis kit was used to construct mutant cDNA following the manufacturer's protocol using wild type rSPNT in eGFP-C1 (Clontech, Palo Alto, CA) as template. The N603T mutants were altered by an A to C mutation at base pair 2079 (GenBank accession number U25055), the N606T by an A to C alteration at position 2088, and the N625T by an A to C at position 2145. All sequences were confirmed by direct DNA sequencing. Single mutant constructs were used as templates to construct double and triple mutants (N603T/N606T, N606T/N625T, or N603T/N606T/N625T).

Construction of stably transfected MDCK. Cells were maintained in MEM Eagle's with Earle's balanced salt solution (BSS) supplemented with 5% fetal bovine serum, 100 U/ml penicillin, and 100 µg/ml streptomycin. Cells were transfected with mutant SPNT-GFP

cDNA using the calcium phosphate method as described previously (6). Cells were selected by growth in media containing 0.7 mg/ml geneticin (Gibco, Grand Island, NY) and maintained in this media for the remainder of experiments. Positive clones were further selected by Western blot, functional uptake, and fluorescence microscopy. For all experiments, cells were permeablized by growth for 4-7 days on polycarbonate Transwell filters (Corning Costar, Corning, NY).

Western blot. Samples were lysed by agitation in SDS buffer (2% SDS in PBS with protease inhibitor), and centrifuged at 14,000 RPM for 20 minutes. Supernatant was removed, assayed for protein content using the DC protein assay (BioRad, Hercules, CA), and combined with loading buffer (15 mM TRIS pH 6.8, 1% SDS, 25 mM EDTA, 65 mM DTT, 0.025% bromophenol blue, 6% glycerol). Five micrograms of protein was loaded per sample on a 10% BioRad ready gel and separated by electrophoresis. Protein was transferred to PVDF membrane (BioRad), blocked in 5% milk, incubated first in mouse anti-GFP primary antibody (1:1000, Roche, Palo Alto, CA), then in goat anti-mouse IgG-HRP conjugated secondary antibody (1:3000, BioRad) and signal was detected by the ECL method.

Confocal microscopy. Cells were fixed with 4% paraformaldehyde, permeablized with 0.025% (w/v) saponin, stained with Texas-red conjugated phalloidin (Molecular Probes, Eugene, OR) for visualization of actin, and mounted on slides in Vectashield mounting medium (Vector Laboratories, Burlingame, CA). Cells were visualized using a BioRad MRC-1024 laser scanning confocal microscope.

Functional localization and statistical analysis. Functional localization was performed as described previously (6). Briefly, cells were exposed to either Na⁺ buffer (128 mM

NaCl, 4.73 mM KCl, 1.25 mM CaCl₂, 1.25 mM MgSO₄, 5 mM HEPES-Tris, pH 7.4) or Na⁺-free buffer (in which choline chloride is substituted for NaCl) containing 0.1 μM ³H-inosine (specific activity = 25.4 Ci/mMol), 10 μM inosine and 10 μM NBMPR on either the apical or the basolateral membrane for 2 minutes. Reaction was terminated by washing samples three times in ice cold Na⁺-free buffer. Samples were air dried and lysed by shaking for 30 minutes in 300 μl 10% SDS. Samples were counted on a Beckman Scintillation Counter (Anaheim, CA). All experiments were repeated four times (in duplicate each time). For each experiment, the ratio of apical uptake to basolateral uptake (A:B) was calculated. These were averaged and statistically analyzed by analysis of variance (ANOVA), using the "Primer to Biostatistics" program supplied by Stanton Glantz (UCSF, San Francisco, CA) (p < 0.05 was considered statistically significant).

Results

SPNT but not CNT1 localization is sensitive to tunicamycin. Preliminary experiments indicated that administration of tunicamycin for 24 hours caused a small decrease in molecular mass of SPNT and CNT1, characteristic of deglycosylation. When viewed by confocal microscopy, this shift was associated with partial internalization of SPNT but not CNT1 (data not shown). The SPNT amino acid sequence contains five putative N-glycosylation sites, two of which (N439 and N539) are predicted to be located in transmembrane domains and are unlikely to be glycosylated. The other three sites (N603, N606, and N625) are located in the extracellular C-terminal tail (3). Alignment of the C-terminal tail of human and rat CNTs indicated that these three sites are unique to SPNT

(Figure 1). Two of these three glycosylation sites are conserved across species (N606 and N625) while the third (N603) is specific to rat and mouse SPNT.

Stable transfections of deglycosylated SPNT mutants in MDCK. Using site-directed mutagenesis, the three unique glycosylation sites in SPNT-GFP were removed. We began by making single mutations (N603T, N606T, and N625T) and stably transfecting into MDCK cells. Positive clones were selected by immunoblot analysis, confocal microscopy, and functional analysis for maximal protein expression and function. In addition, two double mutants (N603T/N606T and N606T/N625T) and a triple mutant containing none of the putative glycosylation sites were constructed and transfected into MDCK. All mutant SPNT-GFP proteins demonstrated a reduction in molecular mass indicative of deglycosylation (Figure 2). Wild-type tagged SPNT has a molecular mass of approximately 115 kDa, representing ~70 kDa SPNT plus ~30 kDa GFP plus glycosylation. The N603T and N606T mutants both demonstrated minimal mobility shifts of approximately 5-7 kDa. Interestingly, the N603T and N606T single mutant clones appeared to contain less protein than wildtype or other mutant clones. It is unclear whether this is a consequence of transfection or whether deglycosylation at these sites affects protein stability. The N625T mutant had a more pronounced decrease in size (~15 kDa) indicating that this site is more heavily glycosylated. Western blot analysis of the double and triple mutants indicated that the effects of deglycosylation on protein size were additive. The molecular masses of these mutants were smaller than either wild type or single mutant proteins.

Deglycosylation does not affect localization of SPNT mutants. Localization of SPNT glycosylation mutants was examined by immunofluorescence and functional analysis. In

```

rCNT3    ----AINCHHVLE---SSKLVSNTTEVASCCQGLFNSTVARGPNDVLPGG-----NFSLY
rCNT1    PRGVEVDCVSLLN----QTVSSSSFEVYLCCRQVFQSTSS-----EFSQV
rSPNT    PRGAETDCVSFLN----TFTRTYETYVCCRELFQSTLLGTNMPSFSGPWQDKESSLR
hSPNT1   PRGAEADCVSFPN----TSFTNRITYETYMCCRGLFQSTSLNGTNPPSFSGPWEDKEFSAM
hCNT1    PRGAEVDCMSLLN----TTLSSSSFEIYQCCREAFQSVNP-----EFSPE
hCNT3    ----DINCHHVLENAFNSTFPGN'TTKVIACCQSLLSSTVAKGPGEVIPGG-----NHSLY

```

```

rCNT3    TLKSCCNLLKPPTLNCGWIPNIP
rCNT1    ALDNCCRFYN--HTVCT-----
rSPNT    NLAKCCDLYT--STVCA-----
hSPNT1   ALTNCCGFYN--NTVCA-----
hCNT1    ALDNCCRFYN--HTICAQ-----
hCNT3    SLKGCCTLLNPSTFNCNGISNTF

```

Figure 1. Multiple alignments of predicted extracellular C-terminal tail of CNTs. The glycosylation sites in all sequences are highlighted in light gray. The glycosylation sites unique to rat SPNT, which were mutated in this study, are highlighted in dark gray (rSPNT sites N603, N606, and N625).

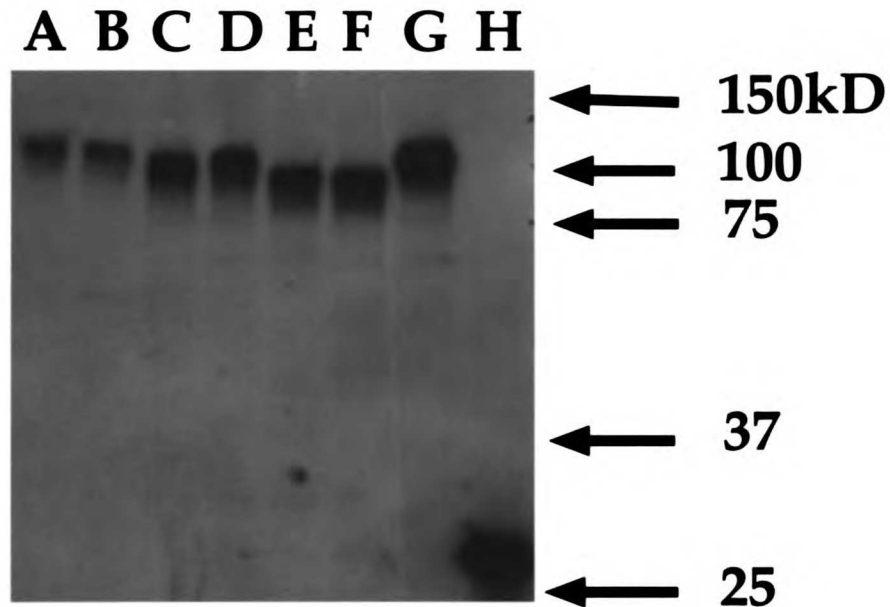


Figure 2. Western blot analysis of SPNT glycosylation mutants. MDCK stably transfected with SPNT mutants N603T (A), N606T (B), N625T (C), N603T/N606T (D), N606T/N625T (E), N603T/N606T/N625T (F), wild type SPNT (G), or GFP (H) were polarized by growth for seven days on permeabilized support and prepared for Western blot as described in Materials and Methods. Five micrograms of protein per lane were loaded on a 10% SDS-PAGE gel and protein was separated by electrophoresis, transferred to PVDF and probed with GFP antibody. Weight of molecular standards is indicated by arrows to right of gel.

all cases, experiments were repeated on more than one positive clone with similar results. Localization of single, double, and triple mutants mirrored that of wild type SPNT-GFP. Visualization by confocal microscopy indicated that all clones localized primarily to the apical membrane with minor populations residing on the basolateral membrane (Figure 3). For the N603T and N606T clones, basolateral signal was present but difficult to view due to low levels of protein expression.

In all cases, sodium-dependent nucleoside uptake was greater across the apical membrane than across the basolateral membrane (Figure 4). Statistical analysis of the ratios of apical to basolateral function (A: B ratios, Figure 4), performed using Analysis of Variance (ANOVA), indicated that these ratios did not differ significantly ($p < 0.05$).

Discussion

SPNT is the most uniformly expressed of the concentrative nucleoside transporters. It is abundant throughout the gastrointestinal tract and present in liver and kidney where it is expected to play a role in nucleoside reabsorption. In addition, SPNT is widely expressed in small amounts throughout the rest of the body including tissues in which signaling via adenosine receptors is important such as heart, testis, and lung (2, 11). In fact, the A₁ adenosine receptor, considered the key adenosine receptor in the kidney, exhibits a similar localization pattern to SPNT when expressed in MDCK (14). Expression of SPNT is dependent on cell cycle, up-regulated by exposure to PKC activating molecules, and affected by growth factors including insulin and glucagon (10).

Differential localization of SPNT in comparison to CNT2 or CNT3 in renal epithelial cells suggests that this protein has an alternate sorting mechanism. Recent

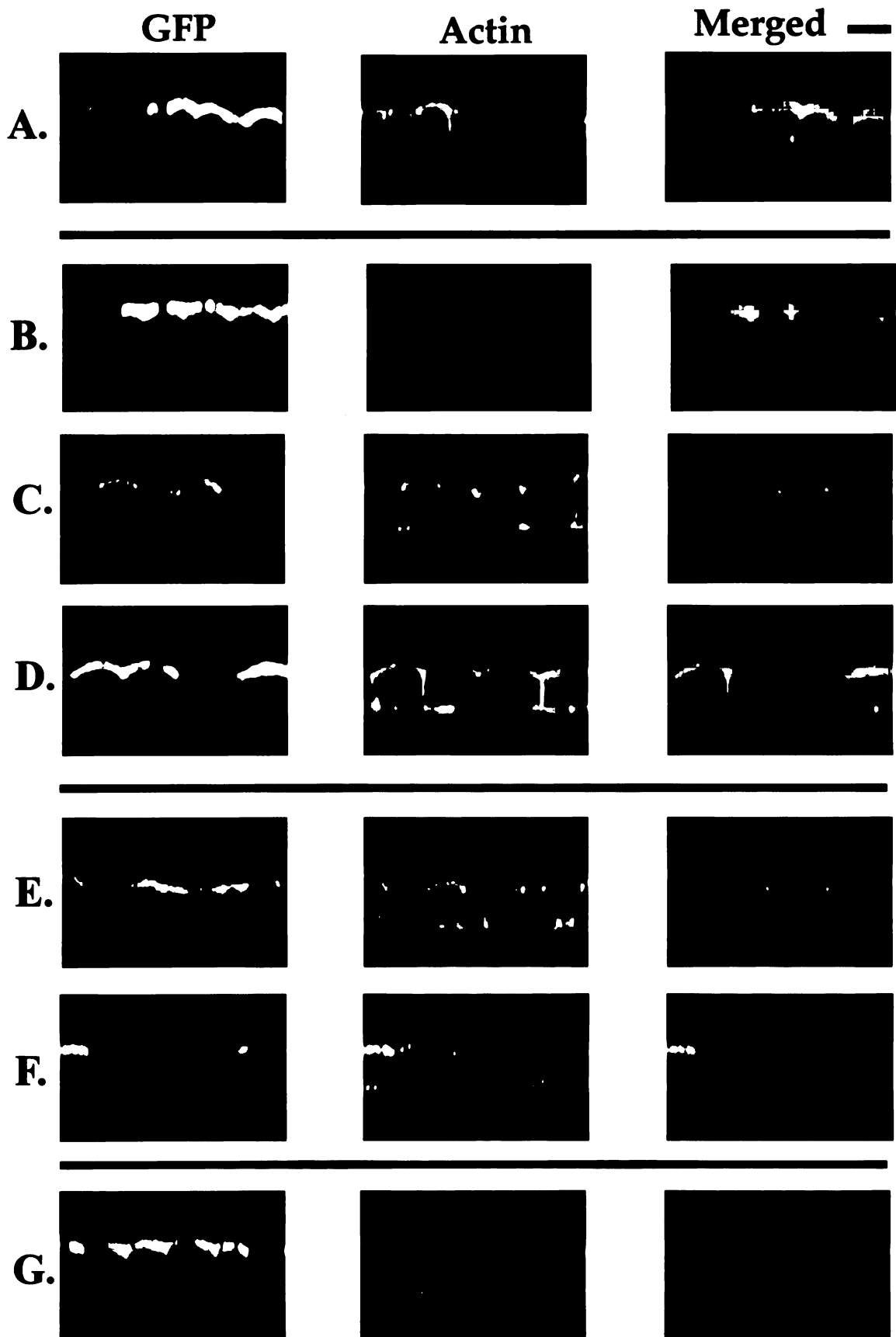


Figure 3. Localization of SPNT glycosylation mutants in MDCK. MDCK stably transfected with wild type (A.) or mutant SPNT (N603T, B.; N606T, C.; N625T, D.; N603T/N606T, E.; N606T/N625T, F.; N603T/N606T/N625T, G.) were polarized by growth on permeable support, fixed, permeablized, stained for actin with Texas-red conjugated-X Phalloidin, and visualized by laser scanning confocal microscopy. Vertical lines separate wild type, single, double, and triple mutants. Left column: GFP. Middle column: Actin. Right column: Merged image. Vertical optical sections are shown with apical membrane on top. Bar, 10 μ m.

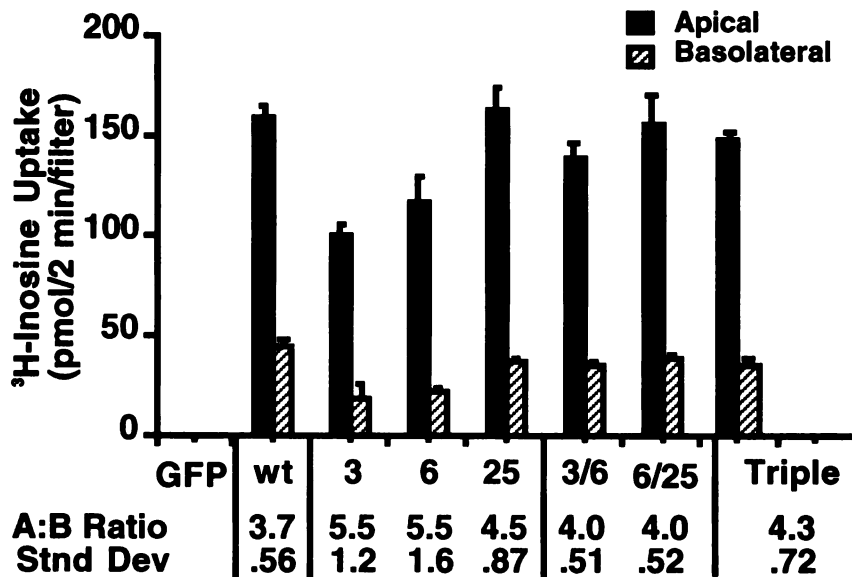


Figure 4. Functional localization of SPNT glycosylation mutants. MDCK cells stably transfected with GFP, wild type SPNT [wt], or the glycosylation mutants N603T [3], N606T [6], N625T [25], N603T/N606T [3/6], N606T/N625T [6/25], or N603T/N606T/N625T [Triple] were polarized by growth on permeable support. ^3H -inosine uptake was measured across either the apical or basolateral membrane in the presence of Na^+ . Data represent the average of four experiments ($n = 2$). The averaged ratio of apical to basolateral uptake (A:B ratio) for each mutant is listed below each column.

observations from Pastor-Anglada suggest that SPNT sorts differently from CNT1 in hepatocytes as well (9). Sorting signals within membrane proteins vary but often act by selective interaction with trafficking machinery specific for movement to one type of membrane or vesicle. These signals tend to be discrete motifs within the protein and can often be identified. Within epithelial cells, proteins are not simply sent to the plasma membrane but specifically contain signals appropriate for targeting to either the apical or basolateral membrane.

While basolateral sorting signals often depend on a specific amino acid motif, apical sorting signals are less well characterized. They may involve anything from structure within a transmembrane domain, as is seen for the influenza virus hemagglutinin protein, to post-translational modifications such as glycosylation as in the case of the high affinity glycine transporter, GLYT1 (5, 8). SPNT has three conserved glycosylation sites, all of which were not found in CNT1 and CNT3. To examine the importance of N-glycosylation on sorting of SPNT, we observed the effect of removing these glycosylation sites on localization. We determined localization by both confocal microscopy and functional analysis. Our data indicated that sorting of SPNT is independent of glycosylation. Glycosylation may play a role in other aspects of SPNT biology such as protein turnover or stability. The molecular determinants responsible for sorting of SPNT remain to be identified.

References

1. Che, M., D. F. Ortiz, and I. M. Arias. Primary structure and functional expression of a cDNA encoding the bile canalicular, purine-specific Na(+)-nucleoside cotransporter. *J Biol Chem* 270: 13596-9, 1995.
2. Felipe, A., R. Valdes, B. Santo, J. Lloberas, J. Casado, and M. Pastor-Anglada. Na+-dependent nucleoside transport in liver: two different isoforms from the same gene family are expressed in liver cells. *Biochem J* 330: 997-1001, 1998.
3. Hamilton, S. R., S. Y. Yao, J. C. Ingram, D. A. Hadden, M. W. Ritzel, M. P. Gallagher, P. J. Henderson, C. E. Cass, J. D. Young, and S. A. Baldwin. Subcellular distribution and membrane topology of the mammalian concentrative Na+-nucleoside cotransporter rCNT1. *J Biol Chem* 276: 27981-8, 2001.
4. Huang, Q. Q., S. Y. Yao, M. W. Ritzel, A. R. Paterson, C. E. Cass, and J. D. Young. Cloning and functional expression of a complementary DNA encoding a mammalian nucleoside transport protein. *J Biol Chem* 269: 17757-60, 1994.
5. Lin, S., H. Y. Naim, A. C. Rodriguez, and M. G. Roth. Mutations in the middle of the transmembrane domain reverse the polarity of transport of the influenza virus hemagglutinin in MDCK epithelial cells. *J Cell Biol* 142: 51-7, 1998.
6. Mangravite, L. M., J. H. Lipschutz, K. E. Mostov, and K. M. Giacomini. Localization of GFP-tagged concentrative nucleoside transporters in a renal polarized epithelial cell line. *Am J Physiol Renal Physiol* 280: F879-85, 2001.
7. Martinez-Maza, R., I. Poyatos, B. Lopez-Corcuera, N. u. E, C. Gimenez, F. Zafra, and C. Aragon. The role of N-glycosylation in transport to the plasma membrane and sorting of the neuronal glycine transporter GLYT2. *J Biol Chem* 276: 2168-73, 2001.

8. Olivares, L., C. Aragon, C. Gimenez, and F. Zafra. The role of N-glycosylation in the targeting and activity of the GLYT1 glycine transporter. *J Biol Chem* 270: 9437-42, 1995.
9. Pastor-Anglada, M., F. J. Casado, R. Valdes, J. Mata, J. Garcia-Manteiga, M. Molina, A. Felipe, B. del Santo, J. F. Mata, B. Santo, J. Lloberas, and J. Casado. Complex regulation of nucleoside transporter expression in epithelial and immune system cells. *Mol Membr Biol* 18: 81-5, 2001.
10. Pastor-Anglada, M., A. Felipe, F. J. Casado, B. del Santo, J. F. Mata, and R. Valdes. Nucleoside transporters and liver cell growth. *Biochem Cell Biol* 76: 771-7, 1998.
11. Pennycooke, M., N. Chaudary, I. Shuralyova, Y. Zhang, and I. R. Coe. Differential expression of human nucleoside transporters in normal and tumor tissue. *Biochem Biophys Res Commun* 280: 951-9, 2001.
12. Petrecca, K., R. Atanasiu, A. Akhavan, and A. Shrier. N-linked glycosylation sites determine HERG channel surface membrane expression. *J Physiol* 515: 41-8, 1999.
13. Ritzel, M. W., A. M. Ng, S. Y. Yao, K. Graham, S. K. Loewen, K. M. Smith, R. G. Ritzel, D. A. Mowles, P. Carpenter, X. Z. Chen, E. Karpinski, R. J. Hyde, S. A. Baldwin, C. E. Cass, and J. D. Young. Molecular identification and characterization of novel human and mouse concentrative Na⁺-nucleoside cotransporter proteins (hCNT3 and mCNT3) broadly selective for purine and pyrimidine nucleosides (system cib). *J Biol Chem* 276: 2914-27, 2000.
14. Saunders, C., J. R. Keefer, A. P. Kennedy, J. N. Wells, and L. E. Limbird. Receptors coupled to pertussis toxin-sensitive G-proteins traffic to opposite surfaces in

Madin-Darby canine kidney cells. A1 adenosine receptors achieve apical and alpha 2A adrenergic receptors achieve basolateral localization. *J Biol Chem* 271: 995-1002, 1996.

CHAPTER 4

LOCALIZATION AND SORTING OF HUMAN EQUILIBRATIVE NUCLEOSIDE TRANSPORTERS, hENT1 AND hENT2, IN RENAL EPITHELIAL CELLS⁴

Introduction

Nucleoside transporters are polytopic membrane proteins that mediate both the uptake and release of hydrophilic nucleosides and nucleoside analogs across lipophilic membranes. They are highly abundant in the kidney where they are hypothesized to play a major role in the salvage of endogenous nucleosides used for nucleotide synthesis.

Two major classes of nucleoside transporters, equilibrative nucleoside transporters (ENT, SLC29) and concentrative nucleoside transporters (CNT, SLC28), have been characterized from a variety of species including human and rat (12, 13, 33, 34, 41, 47, 48). The CNT family are secondary active transporters that couple cellular transport of nucleosides to an internally directed sodium- or proton-gradient (10, 33, 47). In contrast, the ENT family mediates passive transport of nucleosides. Classically, the ENT family can be further subdivided into two types of transporters (*es* and *ei*) based on their sensitivity to inhibition by nitrobenzylthioinosine (NBMPR); *es*-type transport is sensitive to NBMPR while *ei*-type transport is not (2, 48). Recently, two members of the ENT family have been cloned and functionally characterized: ENT1 that mediates *es*-type transport and ENT2 that mediates *ei*-type transport (15, 16, 48).

Members of both the CNT and ENT family are present in renal epithelium that

⁴ This chapter has been accepted for publication as a manuscript entitled, "Localization of Human Equilibrative Nucleoside Transporters, hENT1 and hENT2, in Renal Epithelial Cells" at *Am J Physiol Renal Physiol*

forms the barrier between the tubular lumen and the circulatory system (11, 23, 25, 45, 46). These transporters are hypothesized to act in series to mediate the vectorial transport of nucleosides through this epithelium in a reabsorptive direction, providing a means to salvage nucleosides from the filtrate. The ability of the epithelial cells to perform this function depends on the asymmetric intracellular distribution of these nucleoside transporters. Early studies using apical and basolateral membrane vesicles from renal epithelium in animal models indicate that transport at the apical membrane is predominantly concentrative while basolateral transport is predominantly equilibrative (3, 23, 26, 30, 37, 40, 46). Some studies additionally report equilibrative nucleoside transport activity on the apical membrane(6, 9). Molecular localization studies in our laboratory provided the first direct evidence that CNT1 and CNT2 are localized predominantly to the apical membrane in renal cells (27). This result is supported by recent immunohistochemical studies demonstrating that CNT1 is on the apical membrane of rat kidney (14). To date, there is no information concerning the intracellular localization of ENT1 or ENT2. Knowledge of the localization of these transporters will enhance our understanding of how ENT1 and ENT2 work in concert with the CNT family to mediate transepithelial flux of nucleosides and nucleoside analogs within the kidney. Further, this information will contribute to understanding the differential functions of these two transporters.

In addition, we are interested in understanding the basic mechanisms which govern the intracellular trafficking of ENT1 and ENT2. In polarized cells, plasma membrane proteins are sorted in the trans golgi network and specifically sent to either the apical or basolateral membrane (1). Basolateral targeting appears to be triggered by

distinct amino acid sequences within the protein itself which interact with the sorting machinery (50). Some of these targeting motifs (such as the tyrosine motif (NPXY) or dileucine repeat) are related to signals for clathrin coated pit localization. These signals overlap with those used for endosomal recycling and endocytosis (1). Some proteins contain basolateral targeting motifs unrelated to clathrin coated pits such as the R/HXXY motif seen in the cation-dependent mannose 6-phosphate receptor (CD-MPR) (8). While the exact mechanisms of action of these unrelated motifs are unknown, their structural orientation appears to allow for interaction with the basolateral sorting machinery. Apical targeting is less well understood but appears to be based on segregation of apical proteins into vesicles or rafts enriched with lipids preferentially delivered to the apical membrane. For some proteins it appears that incorporation into these rafts is based on glycosylation motifs or GPI-anchors (1, 32).

The goal of this study was to determine the localization of both hENT1 and hENT2 within renal epithelial cells. We used MDCK cells that have been successfully used to study *in vivo* intracellular localization of a variety of renal transporters (4, 28, 29, 39). Additionally, we sought to determine the molecular sequence responsible for the intracellular sorting of hENT1 and hENT2.

Materials and Methods

Materials. Cell culture media and supplements were purchased from the UCSF Cell Culture Facility (San Francisco, CA). pEGFP-C1 was purchased from Clontech (Palo Alto, CA) and vector pOX was a gift from Andrew T. Gray (University of California, San Francisco). The EMBL MDCK II strain was a gift from Dr. Karl Matlin (U

Cincinnati, Cincinnati, OH). Texas-red conjugated phalloidin was purchased from Molecular Probes (Eugene, OR). Transwell polycarbonate cell culture filters and polycarbonate cell culture plates were purchased from Corning Costar Corporation (Corning, NY). Bradford reagent was purchased from Bio-Rad (Hercules, CA). Radiolabeled adenosine and thymidine were from Moravsek Biochemicals (Brea, CA). All other chemicals were supplied by Sigma (St. Louis, MO).

Plasmid construction. hENT1, hENT2 and the splice variant, hENT2A, were cloned by Polymerase Chain Reaction (PCR) using primers flanking the Open Reading Frame (ORF) of hENT1 and hENT2. The primers were designed based on published hENT1 and hENT2 cDNA sequences (7, 13). For hENT1, the sense primer was: 5'-gggaaaaccgagaacaccatcaccatg-3', the antisense primer was: 5'-agtccttctgtccatcctttgtcacac-3'. For hENT2, the sense primer was: 5'-ggcgcacccgcccggcggccatggcg-3', and the antisense primer was: 5'-gagcctggagggccacttcagagcag-3'. hENT1 was then subcloned in-frame into pEGFP-C1 vector by adding a *Sall* site to the 5' end and a *SacII* site to the 3' end. hENT2 and hENT2A were subcloned in-frame into pEGFP-C1 vector by adding a *Sall* site to the 5' end and an *Apal* site to the 3' end. All plasmid constructions and DNA sequences were confirmed by enzyme digestion analyses and by automated sequencing at the Biomolecular Resource Center at the University of California, San Francisco.

Site-directed mutagenesis. Mutations of hENT1 (R453A and Δ RAIV) and of hENT2 (L455R and Δ LL) were constructed with QuickChangeTM Site-directed Mutagenesis Kit (Stratagene, La Jolla, CA), using wild type hENT1 cDNA and hENT2 cDNA as the

templates. The sequences of these mutants were confirmed by DNA sequencing at the Biomolecular Resource Center at the University of California, San Francisco.

Stable Transfection of MDCK. MDCK cells were grown in MEM Eagle's with Earle's BSS supplement, 5% heat inactivated FBS, 100 units/ml penicillin and 100 units/ml streptomycin in a humidified atmosphere of 5% CO₂, 95% air at 37°C. Cells were transfected with 1 µg DNA and 16 µg Effectene (Qiagen, Valencia, CA). Cells were grown for 48 hours and then diluted into media supplemented with 700 µg/ml G418. Clones were picked after two weeks of growth in selection media and positive clones were chosen by Western blot, confocal microscopy, and functional uptake of ³H-nucleoside.

Transient transfection of LLC-PK₁. LLC-PK₁ cells were grown in M-199 Eagle's with Earle's BSS supplement, 3% heat inactivated FBS, 100 units/ml penicillin and 100 units/ml streptomycin in a humidified atmosphere of 5% CO₂, 95% air at 37°C. LLC-PK₁ cells were transiently transfected following the procedure described previously (27). Briefly, LLC-PK₁ cells were grown on Transwell filters with 0.4 µm pore for 48 hours. Cells were then transfected with 0.8 µg DNA (pEGFP-C1-wild type hENTs or mutant hENTs) and 2 µg Lipofectamine 2000 (Gibco BRL, Rockville, MD) in OPTIMEM reduced serum medium (UCSF Cell Culture Facility, San Francisco, CA) and were then grown an additional 48 hours before being prepared for confocal fluorescence microscopy.

Confocal microscopy. Samples were prepared for confocal microscopy as described previously (27, Chapter 2). Samples were grown for 4-7 days on a permeable support and then fixed with 4-8% paraformaldehyde, permeablized with 0.025% (w/v) saponin in

phosphate buffered saline, stained with Texas-red conjugated phalloidin for visualization of actin, and mounted on slides in Vectashield mounting medium (Vector Labs, Burlingame, CA). Samples were analyzed using a Bio-Rad MRC-1024 laser scanning confocal microscope.

Functional uptake in MDCK. Stably transfected MDCK were grown for 5-7 days on a permeable support and then assayed for membrane specific functionality as described previously (27, Chapter 2). Briefly, cells were treated with 0.1 μM ^3H -inosine in choline buffer (128 mM choline, 4.73 mM KCl, 1.25 mM CaCl_2 , 1.25 mM MgSO_4 , 5 mM HEPES, pH 7.4) in the absence or presence of 1mM inosine. All buffers in hENT2 experiments also contained 10 μM NBMPR to reduce background levels of endogenous *es*-type function. Reaction mix was applied to either the apical or basolateral membrane for 2 minutes, removed, and cells were washed three times in ice-cold choline buffer to terminate the reaction. Cellular uptake of ^3H -inosine was measured by lysing cells and counting in a Beckman Scintillation Counter. All experiments were repeated in duplicate on three separate occasions.

Immunoblot analysis. Transfected cells that had been polarized by growth for 4-7 days on transwells were lysed by agitation in SDS buffer (2% SDS in PBS with protease inhibitor), and centrifuged at 14,000 RPM for 20 minutes. Supernatant was removed, assayed from protein content using the DC protein assay (BioRad, Hercules, CA), and combined with loading buffer (15 mM TRIS pH 6.8, 1% SDS, 25 mM EDTA, 65 mM DTT, 0.025% bromophenol blue, 6% glycerol). Five micrograms of protein was loaded per sample on a 10% BioRad ready gel and separated by electrophoresis. Protein was transferred to PVDF membrane (BioRad), blocked in 5% milk, incubated first in mouse

anti-GFP primary antibody (1:1000, Roche, Palo Alto, CA), then in goat anti-mouse IgG-HRP conjugated secondary antibody (1:3000, BioRad) and signal was detected by the ECL method.

Expression and functional analysis in *Xenopus laevis* oocytes. To study the function of wild type and mutant hENTs and GFP-tagged hENTs, DNA of these transporters were subcloned into pOX vector by adding a *Sall* site to the 5' end and an *XbaI* site to the 3' end. pOX contains the 5' and 3' untranslated regions of the *Xenopus* β -globin gene flanking the insert (17). hENT and GFP-tagged hENT cRNA was synthesized using T3 polymerase (Stratagene, La Jolla, CA) following the manufacturer's protocol. Oocytes were harvested and treated as described previously (47). Fifty nanoliters of cRNA (~0.4 ng/nl) or water was injected individually into defolliculated oocytes. Oocytes were incubated at 18°C for 30-40 hr and then uptake assays were performed for 40 minutes at 25°C in 100 μ l of transport buffer (2 mM KCl, 1 mM CaCl₂, 10 mM HEPES) containing various concentrations of [³H]-labeled nucleosides (Moravek Biochemicals, Brea, CA). Reaction was terminated by washing oocytes five times in 3 ml ice-cold choline buffer. Oocytes were lysed individually in 10% sodium dodecyl sulfate (SDS) and the amount of radiolabeled nucleoside transported into each oocyte was determined by liquid scintillation counting.

Statistics and data analysis. Groups of 8-10 cRNA-injected or water-injected oocytes were used for each experiment. Uptake values are expressed as mean \pm S.E. For kinetic studies, uptake rates (V) determined at different substrate concentrations (S) were fit to the Michaelis-Menten equation: $V = V_{\max} \cdot S / (K_m + S)$, where V_{\max} is the maximal uptake rate, and K_m is the Michaelis-Menten constant (the substrate concentration at $V_{\max}/2$).

Fits were carried out using a nonlinear least-squares regression-fitting program (Kaleidagraph, V.3.0, Abelbeck/Synergy Software, Reading, PA). Kinetic experiments were repeated several times in different batches of oocytes; data for one representative experiment are presented in this study. Statistical analysis was carried out by comparing the uptakes from tested compounds with those from controls in the same experiments using a two-tailed, two sample equal variance t-test. Results with the probability of $p < 0.05$ were considered statistically significant.

Results

Localization of hENT1 and hENT2 in polarized renal epithelial cells. In order to visualize hENT1 and hENT2 in the absence of protein-specific antibodies, we tagged the amino-terminus of hENT1 and hENT2 with green fluorescence protein (GFP). Kinetic studies in *Xenopus laevis* oocytes indicated there were no significant differences in the binding between tagged and untagged transporters (Table 1), suggesting that the GFP tag does not kinetically alter the function of these transporters.

Immunofluorescent analysis of tagged and untagged hENT1 and hENT2 stably transfected MDCK cells indicated that both transporters localized predominantly to the basolateral membrane (Figure 1). Vertical optical sections indicated additional presence of a small portion of hENT1 on the apical membrane (Figure 1A.). Apical presence of hENT2 was not observed (Figure 1B.). hENT1-mediated transport of inosine was observed at both the apical and basolateral membranes whereas hENT2-mediated transport was isolated to the basolateral membrane (Figure 2). Results were replicated using multiple positive stable clones for each transporter.

Table 1. Apparent K_m and V_{max} of adenosine

Clone	K_m (pmole/oocyte/40min)	V_{max} (pmole/oocyte/40min)
hENT1	62.0 ±18.4	115 ±23.
GFP-hENT1	62.0 ±18.4	181 ±33
GFP-hENT1	62.0 ±18.4	180 ±34
GFP-hENT1	78.0 ±22.2	164 ±30

hENT1, GFP-hENT1, hENT2, and GFP-hENT2 mediated uptake of adenosine at

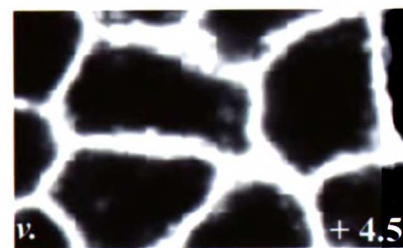
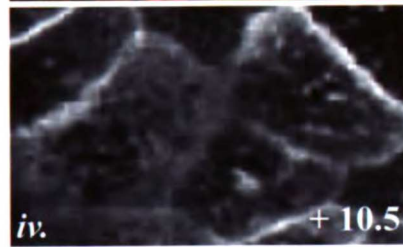
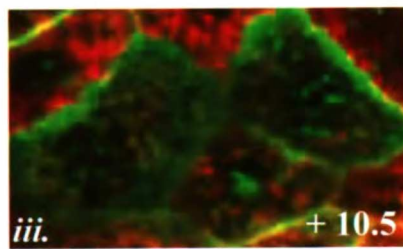
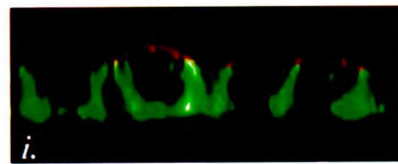
concentrations ranging from 1 μ M to 2 mM were measured as described in Materials and

Methods. Uptake values are expressed as mean \pm S.E (experiments were performed on 8-

10 oocytes/point). These experiments were repeated several times and apparent K_m and

V_{max} from one representative experiment are given.

A. ENT1



B. ENT2

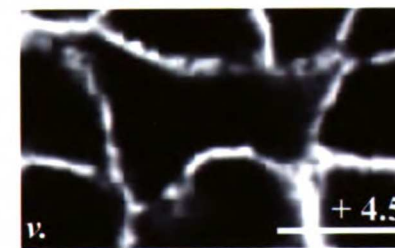
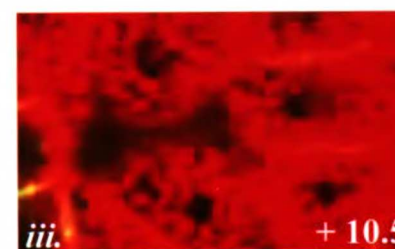
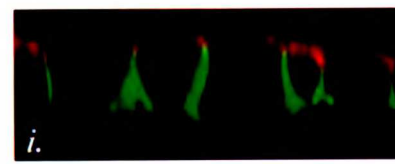


Figure 1. Immunofluorescent localization of wild type ENT1 and ENT2 in MDCK. MDCK stably transfected with ENT1-GFP (A.) or ENT2-GFP (B.) were fixed, permeablized, stained with Texas-red conjugated phalloidin, and visualized by confocal fluorescence microscopy. Vertical optical sections (*i.* and *ii.*) with apical membrane on top (Bar, 10 μ m). Slices through the xy-plane are shown in *iii.-v.* Distance from plastic support (below basolateral membrane) are indicated in microns. Images *iii.* and *iv.* show apical membrane. Images *i.* and *iii.* are shown with GFP-tagged protein in green and phalloidin-stained F-actin in red. All other images display only the GFP-tagged protein. Bar, 10 μ m.

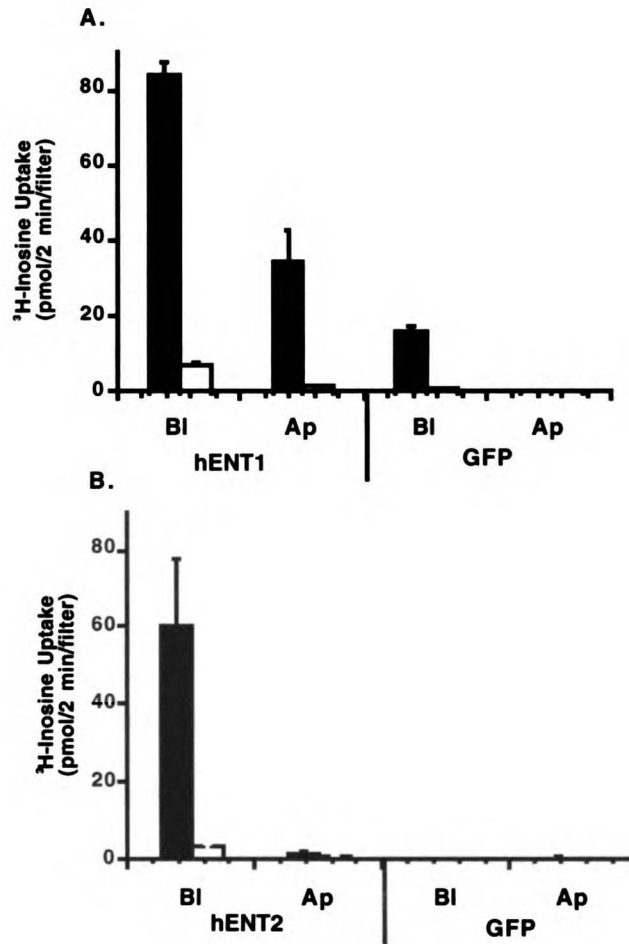


Figure 2. Functional localization of GFP-tagged wild type hENT1 and hENT2 in MDCK. hENT1-GFP (A.), hENT2-GFP (B.) or GFP (both A. and B.) stably transfected cells were polarized by growth on permeabilized filters for 5-7 days. Uptake of ³H-inosine was measured for two minutes from either the apical (Ap) or basolateral (Bl) membrane in the absence of sodium and in either the presence (solid bars) or absence (open bars) of inosine (1mM). NBMPR (10 μM) was present in solutions used for functional analysis of hENT2 (B.). Each experiment was repeated in duplicate on three or four separate occasions.

Basolateral targeting is independent of the carboxy-terminal tail of both hENT1 and hENT2. We were interested in investigating the molecular determinants responsible for polarized localization of hENT1 and hENT2. Based on hydropathy plot analysis and topology studies, hENT1 and hENT2 are each predicted to have eleven transmembrane domains with a four amino acid carboxy-terminal tail (Figure 3A.) (12, 13, 38). The carboxy-terminus of both transporters contained a motif implicated in basolateral targeting: an R/HXXV motif in hENT1 (RAIV) and a dileucine repeat in hENT2 (LL). No other targeting motifs were obvious in either sequence at either terminus. We investigated the significance of these two sequences on polarized trafficking of the proteins via mutagenesis studies.

The R/HXXV sequences in hENT1 was mutagenized in two ways: 1) a single mutation was made at position 453 removing the arginine (R453A) or 2) the entire carboxy-terminal tail was truncated (Δ RAIV). Both mutants were stably transfected into MDCK and produced full length protein as demonstrated by Western blot (Figure 4). Neither mutation had a visible effect on localization of hENT1 (Figure 3B.) nor was there a effect on hENT1-mediated transport of inosine at the basolateral membrane (data not shown).

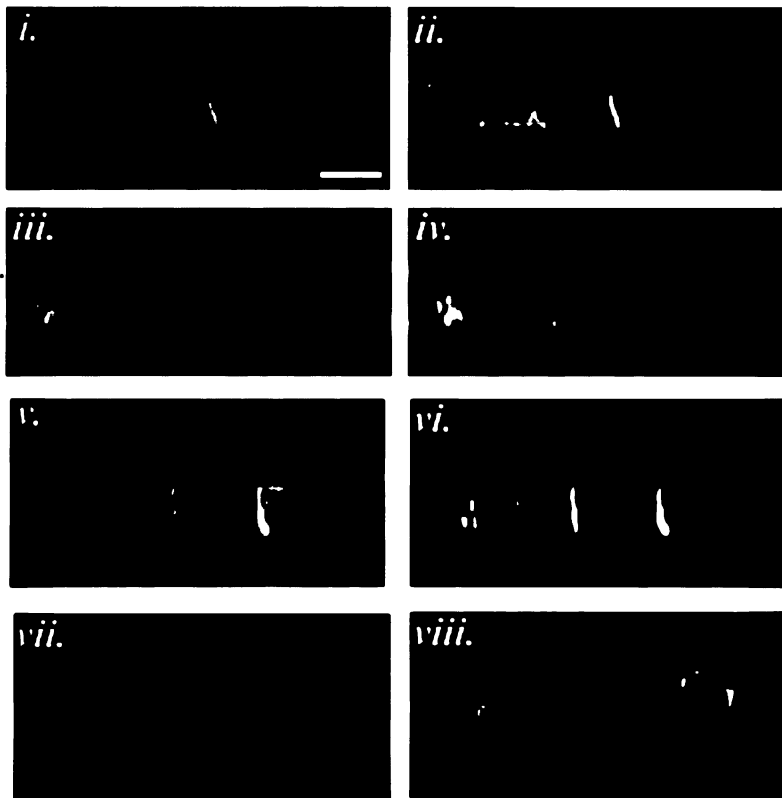
The dileucine repeat in hENT2 was also mutated by both point mutation (L455R) and truncation (Δ LL) (Figure 3A.) and stably transfected into MDCK. Transfection efficiencies were extremely low (<10% of cells were transfected). L455R protein levels were too low to be detected by Western blot (Figure 4). Δ LL protein levels were

A.

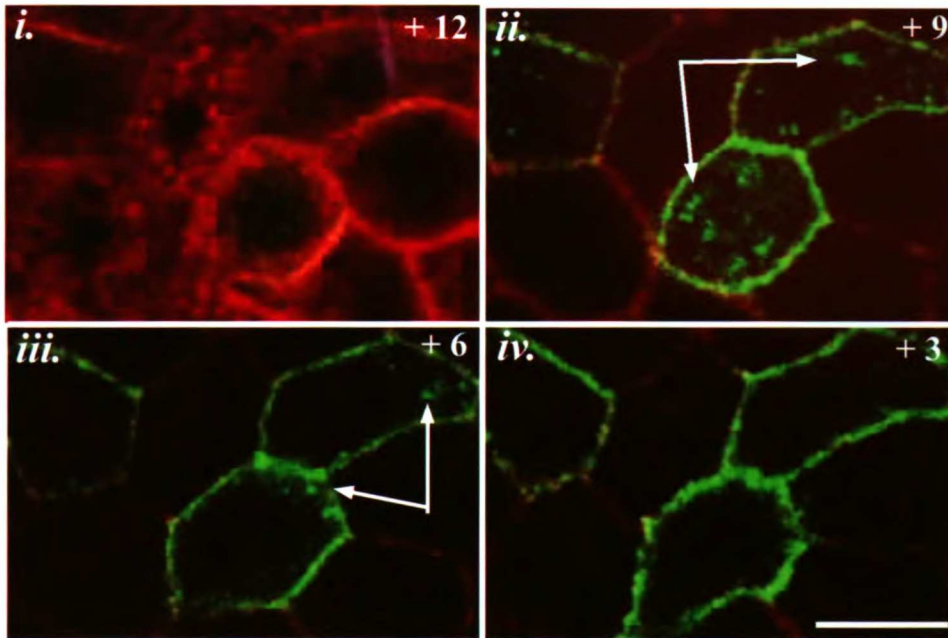
hENT1 ■--FLCLGLALGAVFSFLF**RAIV**

hENT2 ■--FLALGLSCGASLSFLFKAL**L**

B.



C.



D.

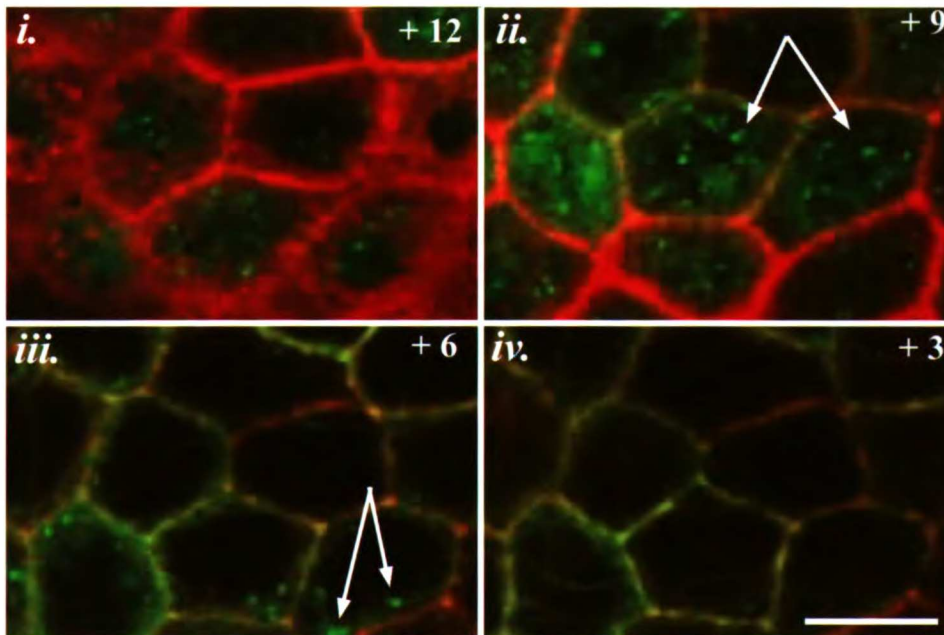


Figure 3. Expression and localization of mutagenized ENT1 and ENT2 in MDCK. (A.) Sequence analysis of carboxy-termini of hENT1 and hENT2. Predicted transmembrane domains are underlined, targeting motifs are emboldened, and single amino acids which were mutated are enlarged. (B.) Immunofluorescence of polarized MDCK stably transfected with (i and ii) ENT1 R453A, (iii and iv) ENT1 Δ RAIV, (v and vi) ENT2 L455R, and (vii and viii) ENT2 Δ LL. Vertical optical images shown with apical membrane on top. Bar, 10 μ m. (i, iii, v, and vii) show GFP-tagged protein as green and phalloidin-stained F-actin as red. (ii, iv, vi, and viii) show just the GFP-tagged protein from the picture to their lefthand side. (C.) Immunofluorescent Z-series of ENT2 L455R. xy-sections spaced 3 μ m are shown in series. Position of each image relative to the plastic support below the basolateral membrane is indicated in each picture in microns. Bar, 10 μ m. Red indicates phalloidin-stained F-actin and green indicates GFP-tagged protein. Arrows indicate vesicular staining. (D.) Immunofluorescent Z-series of ENT2 Δ LL. Images are arranged exactly as seen in section D.

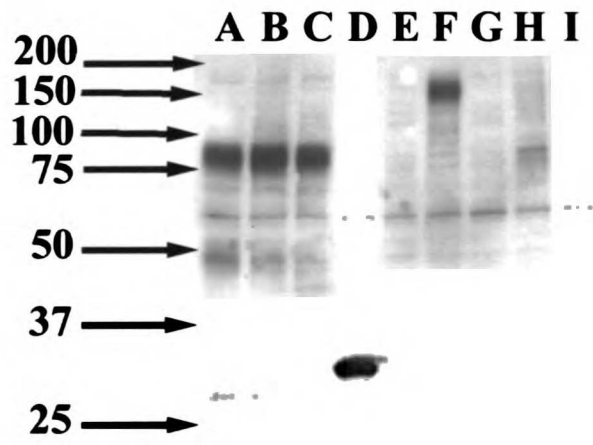


Figure 4. Immunoblot analysis of hENT1 and hENT2 protein in MDCK. MDCK stably transfected with wt hENT1 (A), hENT1 R453A (B), hENT1 DRAIV (C), GFP (D), untransfected (E), wt hENT2 (F), hENT2 L455R (G), hENT2 DLL (H), or hENT2A (I) were polarized by growth for seven days on permeabilized support and prepared for Western blot as described in Materials and Methods. Five micrograms of protein per lane were loaded on a 10% SDS-PAGE gel and protein was separated by electrophoresis, transferred to PVDF and probed with GFP antibody. Arrows to left of gel indicate weights of molecular standards.

detectable and yielded a single band smaller in size than wild type hENT2 but equivalent to wild type hENT1 (Figure 4). Wild type ENT2 clones produced a protein of abnormally large mass (~140 kDa) compared to ENT1 (80 kDa). Evidence for large ENT2 has been seen in other studies as well (18, 37).

Both hENT2 L455R and Δ LL trafficked exclusively to the basolateral membrane with no apparent apical localization. However, surface expression was drastically reduced (Figure 3B.). The L455R mutant displayed some vesicular staining in MDCK (Figure 3C.). The Δ LL mutant displayed significant vesicular staining (Figure 3D.), indicating the dileucine motif is important for surface expression. This was also true when these proteins were transfected into LLC-PK₁ cells, a renal epithelial cell line originating from proximal tubule (Figure 5). Vesicular retention may occur by alteration of protein stability, surface delivery, or surface retention.

Functional localization studies could not be performed on the mutated hENT2 stable MDCK clones due to low transfection efficiencies. Therefore, further studies analyzing the effect of these mutations on hENT2 function were carried out using heterologous expression in oocytes (Figure 6). Neither truncation of hENT1 (Δ RAIV) nor single mutation (L455R) of hENT2 altered the functional activity of these proteins. In contrast, the hENT2 truncated mutant (Δ LL) showed significant reduction in function, suggesting that the dileucine motif is essential for surface expression of hENT2 in oocytes as well.

Identification of a hENT2 variant. In the process of cloning hENT2, using primers flanking the ORF of the published hENT2 cDNA sequence (7), we found a variant, termed hENT2A (GenBank accession no. AF401235). We determined this to be a splice

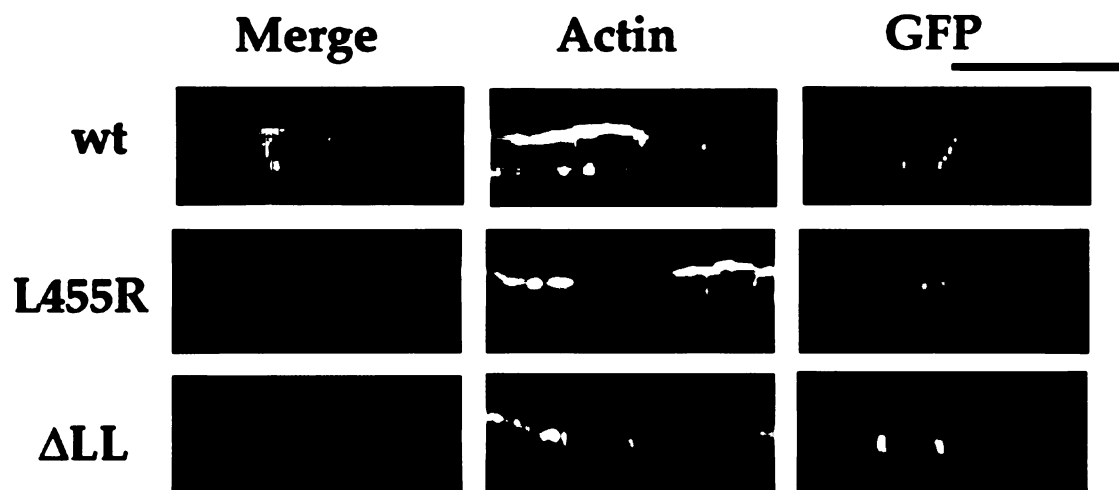


Figure 5. Localization of hENT2 wt and mutants in LLC-PK₁. LLC-PK₁ cells were transiently transfected with hENT2 wt, hENT2-L455R, or hENT2-DLL, as described in Materials section, and prepared for confocal microscopy in the same manner as MDCK cells. Left column: merged image. Middle column: Actin. Right column: GFP-tagged transporter. Vertical optical sections shown with apical membrane on top. Bar, 50 μ m.

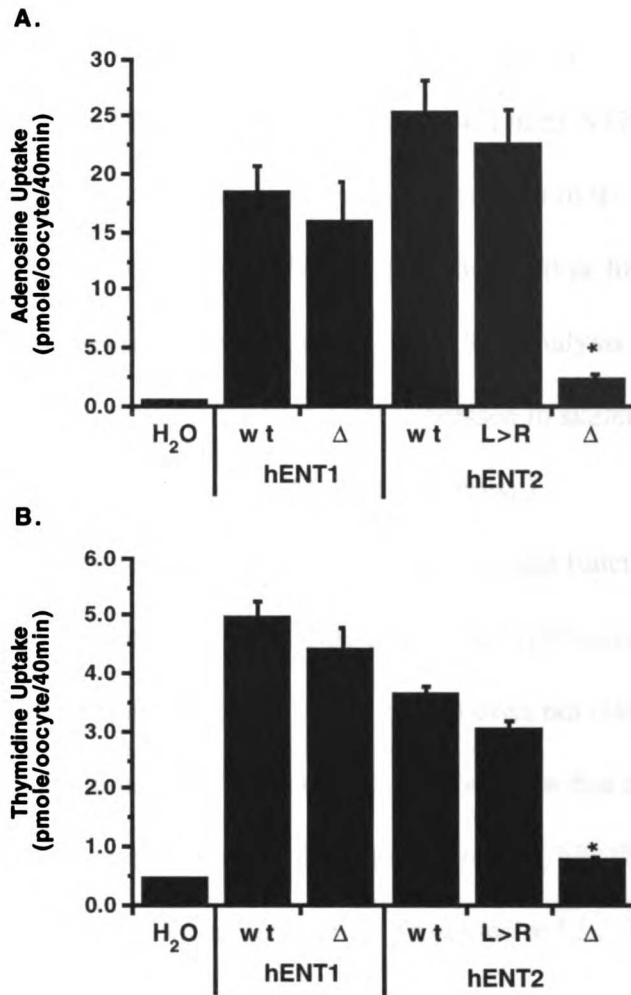


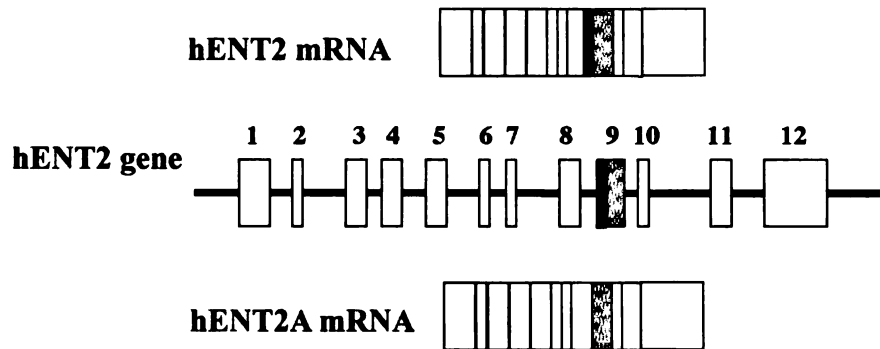
Figure 6. Effect of mutations on hENT1- and hENT2- mediated uptake of adenosine and thymidine in oocytes. Uptake of (A.) ³H-adenosine (10 μM) and (B.) ³H-thymidine (10 μM) was measured at 25°C for 40 min in oocytes (8-10 per data point) injected with H₂O or cRNA for GFP-tagged hENT1 (wt), hENT1-ΔRAIV (Δ), hENT2 (wt), hENT2-L455R (L>R), or hENT2-ΔLL (Δ). Data are expressed as mean ± S.E. and an asterisk (*) indicates results that are statistically different from GFP-tagged wild type control (p< 0.05).

variant based on the genomic sequence of hENT2 (GenBank accession no. AF034102), which has 12 exons and 11 introns. hENT2A uses a different splicing site on the 5' end of exon 9, causing a 40 bp deletion (positions 1103-1142) in hENT2A mRNA (Figure 7). This out-of-frame deletion introduces a premature stop codon in the ORF, encoding a truncated variant which is 156 amino acids shorter than wild type hENT2, and has an alternative COOH terminus sequence (Figure 8). RT-PCR analysis of several tissues found that both wild type and variant hENT2 are expressed in skeletal muscle, liver, lung, brain, kidney, heart, pancreas, and placenta (data not shown).

hENT2A was heterologously expressed in oocytes and functionally studied. The variant did not take up adenosine or thymidine under our experimental conditions (Figure 9A.). This lack of activity may suggest that the variant does not retain the domains necessary for nucleoside transport. Alternatively, it is possible that the variant is not properly trafficking to the membrane. To further explore this, hENT2A was tagged with GFP, stably expressed in MDCK and transiently expressed in LLC-PK₁ cells in the same manner described earlier. hENT2A did not sort to the plasma membrane in either of these cell lines (Figure 9B. and 9C.).

Several splice variants of other membrane transporters have been found to have dominant negative effects on the function of wild type transporters (19, 44). We tested the effect of expression of hENT2A on function of wild type hENT2 by coinjecting equal amounts of cRNA for both transporters into oocytes and measuring nucleoside uptake. Uptake in oocytes expressing hENT2 and hENT2A did not differ from that observed in oocytes expressing wild type hENT2 alone (Figure 9A.).

A.



B.

hENT2wt splicing:

*tggtcccag//atctggctgacagcgcctgtgccttgtgtggcttcacagtcaccctgtccgtctccccccatcacagcc
atggtgaccagctccaccagtcctgggaagtgga//gtgagtgt*

hENT2A splicing:

*tggtcccagatctggctgacagcgcctgtgccttgtgtggcttcacag//tcaccctgtccgtctccccccatcacagccatggtg
accagctccacc **agtcctgggaagtgga**//gtgagtgt*

Figure 7. Sequence analysis of hENT2 and hENT2A. (A.) Schematic representation of hENT2 and hENT2A mRNA and gene organization. Lines and boxes in hENT2 gene represent introns and exons, respectively. Exons are numbered. Exon 9 is colored light grey with the 40bp in exon 9 which is deleted in hENT2A mRNA colored dark grey. (B.) 5' and 3' Exon-intronic splicing sites of exon 9 in hENT2 and hENT2A. Exon region is in bold and italic, and the 40bp region that is deleted in hENT2A mRNA is underlined. The portion of the hENT2A sequence which differs from hENT2 is emboldened.

```

1                               I                               50
hENT2  MARGDAPRDS YHLVGISFFI LGLGTL LPWN FFITAIPYFQ ARLAGAGNST
hENT2A MARGDAPRDS YHLVGISFFI LGLGTL LPWN FFITAIPYFQ ARLAGAGNST

51                               II                              100
hENT2  ARILSTNHTG PEDAFNFNW VTL LSQLPLL LFTLLNSFLY QCVPETVRIL
hENT2A ARILSTNHTG PEDAFNFNW VTL LSQLPLL LFTLLNSFLY QCVPETVRIL

101          III              IV              150
hENT2  GSLLAILLLF ALTAALVKVD MSPGPFFSIT MASVCFINSF SAVLQGSLEFG
hENT2A GSLLAILLLF ALTAALVKVD MSPGPFFSIT MASVCFINSF SAVLQGSLEFG

151                               V                               200
hENT2  QLGTMPSTYS TLFLSGQGLA GIFAALAMLL SMASGVDAET SALGYFITPY
hENT2A QLGTMPSTYS TLFLSGQGLA GIFAALAMLL SMASGVDAET SALGYFITPC

201          VI              250
hENT2  VGILMSIVCY LSLPHLKFAR YYLANKSSQA QAQELETKAE LLQSDENGIP
hENT2A VGILMSIVCY LSLPHLKFAR YYLANKSSQA QAQELETKAE LLQSDENGIP

251                               300
hENT2  SSPQKVALTL DLDLEKEPES EPDEPQKPGK PSVFTVFQKI WLTALCLVLV
hENT2A SSPQKVALTL DLDLEKEPES EPDEPQKPGK PSVFTVFQKS PCPSSPPSQP

301          VII              VIII              350
hENT2  FVTLSVFP A ITAMVTSSTS PGKWSQFFNP ICCFLLFNIM DWLGRSLTSY
hENT2A W~~~~~ ~~~~~~ ~~~~~~ ~~~~~~ ~~~~~~ ~~~~~~

351                               IX                              400
hENT2  FLWPEDESR L LPLLVCLRFL FVPLFMLCHV PQRSRLPILF PQDAYFITFM
hENT2A ~~~~~~ ~~~~~~ ~~~~~~ ~~~~~~ ~~~~~~

401          X              XI              450
hENT2  LLFAVSNGYL VSLTMCLAPR QVLPHEREVA GALMTFFLAL GLSCGASLSF
hENT2A ~~~~~~ ~~~~~~ ~~~~~~ ~~~~~~ ~~~~~~

451
hENT2  LFKALL
hENT2A ~~~~~~

```

Figure 8. Protein sequences of hENT2 and hENT2A. Wild type hENT2 has 456 amino acid residues. Due to the premature stop codon induced by the out of frame 40 bp deletion in the ORF of hENT2, hENT2A has only 301 amino acid residues and its COOH terminus sequence is changed. Predicted transmembrane domains are overscored and numbered with roman numerals.

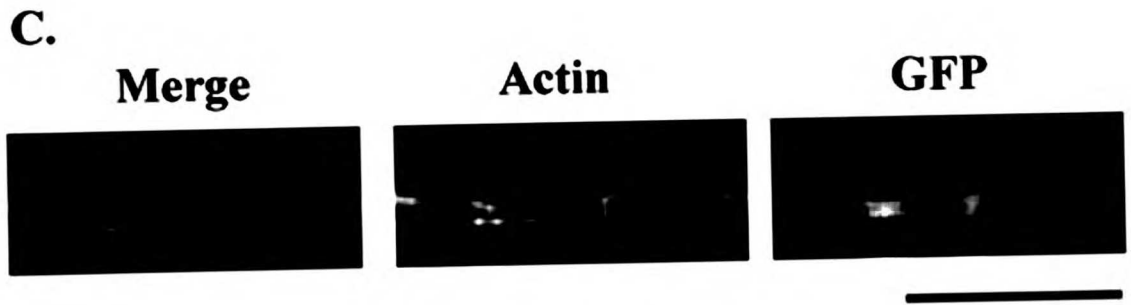
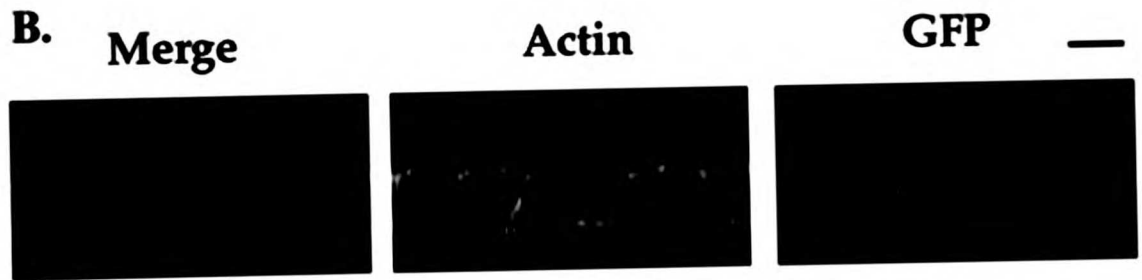
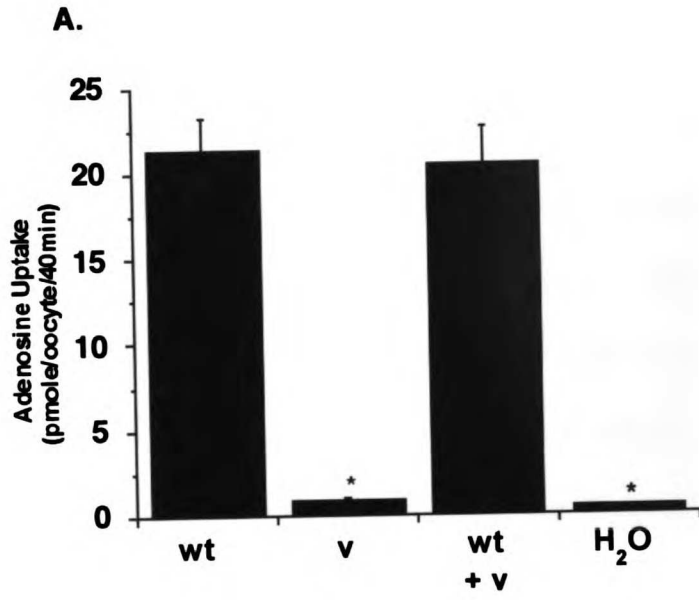


Figure 9. Function and localization of the splice variant, hENT2A. (A.) Uptake of 10 μM ^3H -adenosine was measured at 25°C for 40 min in oocytes injected with H_2O or with 20 ng of cRNA for hENT2 (wt), hENT2A (v), or both hENT2 and hENT2A (20 ng each) (wt + v). Data are expressed as mean \pm S.E of 8-10 oocytes. An asterisk (*) indicates results that are statistically different from wild type control ($p < 0.05$). (B.) MDCK stably transfected with hENT2A-GFP were fixed, stained with Texas-red conjugated phalloidin, and visualized by laser scanning confocal microscopy. Bar, 10 μm . (C.) LLC-PK₁ transiently transfected with hENT2-GFP and visualized in the same manner. Left column: merged image. Middle column: Actin stain. Right column: GFP protein. Bar, 10 μm .

Discussion

Past studies have attempted to localize equilibrative nucleoside transport within epithelia but with conflicting results. Both the absence and presence of *es*-type transport activity (presumably hENT1) in brush border membrane vesicles (BBM) have been reported (5, 9, 24). In contrast, *ei*-type activity (presumably hENT2) was reported to reside only on the basolateral membrane (5). Because functional studies in isolated plasma membrane vesicles may be confounded by the presence of multiple transport activities or contamination with other membranes, data localizing transporters using functional activity are difficult to interpret. In this study, we directly examined the localization of GFP-tagged hENT1 and hENT2 in renal epithelial cells. Our data demonstrate that hENT1 and hENT2 are present and functional on the basolateral membrane (Figures 1 and 2). Interestingly, hENT1 also appears in small amounts on the apical membrane where it is also functional. Function of hENT1 on the apical membrane in MDCK was also demonstrated recently by Lai *et al.* (22). Previous data from this laboratory demonstrated that the concentrative nucleoside transporters, CNT1 and CNT2, are predominantly localized to the apical membrane in renal epithelial cells (27, Chapter 2). Together, these data provide a picture of asymmetrically localized CNTs and ENTs working in concert to salvage nucleosides and nucleoside analogs from the tubular filtrate. *In vivo* studies showing that adenosine is reabsorbed in the kidney support this model (21).

We were additionally interested in examining the molecular determinants responsible for basolateral targeting of these two transporters. The carboxy-terminal tail of hENT1 contained an R/HXXY motif (RAIV) which has been implicated in basolateral

sorting of CD-MPR (8, 51). Neither mutation nor truncation of this sequence affected hENT1 levels on the basolateral membrane (Figure 3). In contrast, the carboxy-terminal tail of hENT2 contained a dileucine repeat. This motif is implicated as a signal in both basolateral sorting and endosomal recycling of a large number of proteins (1, 16). Both mutation and truncation of the dileucine affected surface expression of hENT2 but in both cases, all protein which reached the plasma membrane remained confined to the basolateral membrane (Figure 3). This indicates that this motif is important for maintaining steady-state expression of hENT2 on the plasma membrane. While this does not implicate the dileucine as a targeting motif, the repeat may be important in endosomal recycling or surface retention of hENT2. Understanding the mechanisms which govern steady-state surface expression of these proteins will give us insight into how they might be regulated within the cell.

Differential sorting sequences and localization patterns of hENT1 and hENT2 further substantiate the idea that these two transporters are maintained and regulated by distinct mechanisms within the cell. hENT1 is found ubiquitously throughout the body and is thought to be the major transporter involved in uptake of nucleosides for DNA synthesis (31). hENT1 is also implicated in terminating adenosine signals in the vicinity of adenosine receptors . Within the renal epithelium the A1 adenosine receptor, which also localizes to both membranes in MDCK, is thought to be the major receptor involved in adenosine signaling (36). Conditions of chronic hypoxia selectively downregulate ENT1 function, as a means to increase extracellular adenosine levels at the site of receptor activation (20). Symbiosis between hENT1 and the A1 adenosine receptor may explain the presence of hENT1 on the apical membrane.

In contrast, hENT2 is expressed in far lower amounts in all tissues except skeletal muscle. It has a lower affinity for most physiologic nucleosides with the exception of inosine, an adenosine metabolite (32, 43). Recent data indicate that it also interacts with nucleoside bases, preferring the purinergic base hypoxanthine (49). For this reason, it has been proposed that hENT2 is involved in mechanisms requiring heavy adenosine metabolism such as ATP depletion in skeletal muscle caused by strenuous exercise (7, 49). Within the kidney, hENT2's purely basolateral localization suggests that its major role is to function in concert with CNTs in the salvage of nucleosides and nucleobases from the filtrate.

The hENT2 splice variant (hENT2A) contains a 40 bp deletion in the mRNA that introduces a premature stop codon, removing 156 amino acid residues from the COOH terminus of the transporter. Confocal microscopy of MDCK and LLC-PK₁ expressing GFP-tagged hENT2A indicates that the variant is not expressed on the surface of these cells. Further, our data demonstrated that the variant was not functional nor did it affect function of the wild type hENT2, as has been demonstrated for spliced isoforms of other membrane proteins (19, 35, 42, 44). The role of hENT2A is unknown.

In summary, we report that cellular hENT2 is localized exclusively to the basolateral membrane and that hENT1 is localized primarily to the basolateral membrane in renal epithelial cells. The C-terminal dileucine repeat in hENT2 is implicated in surface expression of this protein. Neither this dileucine motif nor the RXXY motif in hENT1 appear to be important for basolateral targeting. In addition, we found a splice

variant of hENT2 that is expressed in multiple tissues, does not have nucleoside transport activity, and has no effect on the activity of wild type hENT2.

References

1. Aroeti, B., H. Okhrimenko, V. Reich, and E. Orzech. Polarized trafficking of plasma membrane proteins: emerging roles for coats, SNAREs, GTPases and their link to the cytoskeleton. *Biochim Biophys Acta* 1376: 57-90, 1998.
2. Belt, J. A., and L. D. Noel. Nucleoside transport in Walker 256 rat carcinosarcoma and S49 mouse lymphoma cells. Differences in sensitivity to nitrobenzylthioinosine and thiol reagents. *Biochem J* 232: 681-8, 1985.
3. Betcher, S. L., J. N. Forrest, Jr., R. G. Knickelbein, and J. W. Dobbins. Sodium-adenosine cotransport in brush-border membranes from rabbit ileum. *Am J Physiol* 259: G504-10, 1990.
4. Brandsch, M., V. Ganapathy, and F. H. Leibach. H⁺-peptide cotransport in Madin-Darby canine kidney cells: expression and calmodulin-dependent regulation. *Am J Physiol* 268: F391-7, 1995.
5. Chandrasena, G., R. Giltay, S. D. Patil, A. Bakken, and J. D. Unadkat. Functional expression of human intestinal Na⁺-dependent and Na⁺-independent nucleoside transporters in *Xenopus laevis* oocytes. *Biochem Pharmacol* 53: 1909-18, 1997.
6. Ciruela, F., J. Blanco, E. I. Canela, C. Lluís, R. Franco, and J. Mallol. Solubilization and molecular characterization of the nitrobenzylthioinosine binding sites from pig kidney brush-border membranes. *Biochim Biophys Acta* 1191: 94-102, 1994.
7. Crawford, C. R., D. H. Patel, C. Naeve, and J. A. Belt. Cloning of the human equilibrative, nitrobenzylmercaptopyrine riboside (NBMPR)-insensitive nucleoside transporter ei by functional expression in a transport-deficient cell line. *J Biol Chem* 273: 5288-93, 1998.

8. Distel, B., U. Bauer, R. Le Borgne, and B. Hoflack. Basolateral sorting of the cation-dependent mannose 6-phosphate receptor in Madin-Darby canine kidney cells. Identification of a basolateral determinant unrelated to clathrin-coated pit localization signals. *J Biol Chem* 273: 186-93, 1998.
9. Franco, R., J. J. Centelles, and R. K. Kinne. Further characterization of adenosine transport in renal brush-border membranes. *Biochim Biophys Acta* 1024: 241-8, 1990.
10. Gerstin, K. M., M. J. Dresser, J. Wang, and K. M. Giacomini. Molecular cloning of a Na⁺-dependent nucleoside transporter from rabbit intestine. *Pharm Res* 17: 906-10, 2000.
11. Griffith, D. A., A. J. Doherty, and S. M. Jarvis. Nucleoside transport in cultured LLC-PK1 epithelia. *Biochim Biophys Acta* 1106: 303-10, 1992.
12. Griffiths, M., N. Beaumont, S. Y. Yao, M. Sundaram, C. E. Boumah, A. Davies, F. Y. Kwong, I. Coe, C. E. Cass, J. D. Young, and S. A. Baldwin. Cloning of a human nucleoside transporter implicated in the cellular uptake of adenosine and chemotherapeutic drugs. *Nat Med* 3: 89-93, 1997.
13. Griffiths, M., S. Y. Yao, F. Abidi, S. E. Phillips, C. E. Cass, J. D. Young, and S. A. Baldwin. Molecular cloning and characterization of a nitrobenzylthioinosine-insensitive (ei) equilibrative nucleoside transporter from human placenta. *Biochem J* 328: 739-43, 1997.
14. Hamilton, S. R., S. Y. Yao, J. C. Ingram, D. A. Hadden, M. W. Ritzel, M. P. Gallagher, P. J. Henderson, C. E. Cass, J. D. Young, and S. A. Baldwin. Subcellular distribution and membrane topology of the mammalian concentrative Na⁺-nucleoside cotransporter rCNT1. *J Biol Chem* 276: 27981-8, 2001.

15. Handa, M., D. Choi, R. M. Caldeiro, R. O. Messing, A. S. Gordon, and I. I. Diamond. Cloning of a novel isoform of the mouse NBMPR-sensitive equilibrative nucleoside transporter (ENT1) lacking a putative phosphorylation site. *Gene* 262: 301-7, 2001.
16. Heilker, R., M. Spiess, and P. Crottet. Recognition of sorting signals by clathrin adaptors. *Bioessays* 21: 558-67, 1999.
17. Jegla, T., and L. Salkoff. A novel subunit for shal K⁺ channels radically alters activation and inactivation. *J Neurosci* 17: 32-44, 1997.
18. Karim-Jimenez, Z., N. Hernando, J. Biber, and H. Murer. Requirement of a leucine residue for (apical) membrane expression of type IIb NaPi cotransporters. *Proc Natl Acad Sci U S A* 97: 2916-21, 2000.
19. Kitayama, S., T. Ikeda, C. Mitsuata, T. Sato, K. Morita, and T. Dohi. Dominant negative isoform of rat norepinephrine transporter produced by alternative RNA splicing. *J Biol Chem* 274: 10731-6, 1999.
20. Kobayashi, S., H. Zimmermann, and D. E. Millhorn. Chronic hypoxia enhances adenosine release in rat PC12 cells by altering adenosine metabolism and membrane transport. *J Neurochem* 74: 621-32, 2000.
21. Kuttesch, J. F., Jr., and J. A. Nelson. Renal handling of 2'-deoxyadenosine and adenosine in humans and mice. *Cancer Chemother Pharmacol* 8: 221-9, 1982.
22. Lai, Y., A. D. Bakken, and J. D. Unadkat. Simultaneous expression of hCNT1-CFP and hENT1-YFP in Mardin-Darby canine kidney (MDCK) cells: Localization and vectorial transport studies. *J Biol Chem* 277: 37711-17, 2002.

23. Le Hir, M. Evidence for separate carriers for purine nucleosides and for pyrimidine nucleosides in the renal brush border membrane. *Renal Physiol Biochem* 13: 154-61, 1990.
24. Le Hir, M., and U. C. Dubach. Concentrative transport of purine nucleosides in brush border vesicles of the rat kidney. *Eur J Clin Invest* 15: 121-7, 1985.
25. Lee, C. W., C. I. Cheeseman, and S. M. Jarvis. Na⁺- and K⁺-dependent uridine transport in rat renal brush-border membrane vesicles. *Biochim Biophys Acta* 942: 139-49, 1988.
26. Lee, C. W., C. I. Cheeseman, and S. M. Jarvis. Transport characteristics of renal brush border Na⁽⁺⁾- and K⁽⁺⁾-dependent uridine carriers. *Am J Physiol* 258: F1203-10, 1990.
27. Mangravite, L. M., J. H. Lipschutz, K. E. Mostov, and K. M. Giacomini. Localization of GFP-tagged concentrative nucleoside transporters in a renal polarized epithelial cell line. *Am J Physiol Renal Physiol* 280: F879-85, 2001.
28. Masuda, S., H. Saito, H. Nonoguchi, K. Tomita, and K. Inui. mRNA distribution and membrane localization of the OAT-K1 organic anion transporter in rat renal tubules. *FEBS Lett* 407: 127-31, 1997.
29. Masuda, S., A. Takeuchi, H. Saito, Y. Hashimoto, and K. Inui. Functional analysis of rat renal organic anion transporter OAT-K1: bidirectional methotrexate transport in apical membrane. *FEBS Lett* 459: 128-32, 1999.
30. Mun, E. C., K. J. Tally, and J. B. Matthews. Characterization and regulation of adenosine transport in T84 intestinal epithelial cells. *Am J Physiol* 274: G261-9, 1998.

31. Pennycooke, M., N. Chaudary, I. Shuralyova, Y. Zhang, and I. R. Coe. Differential expression of human nucleoside transporters in normal and tumor tissue. *Biochem Biophys Res Commun* 280: 951-9, 2001.
32. Petrecca, K., R. Atanasiu, A. Akhavan, and A. Shrier. N-linked glycosylation sites determine HERG channel surface membrane expression. *J Physiol* 515: 41-8, 1999.
33. Ritzel, M. W., A. M. Ng, S. Y. Yao, K. Graham, S. K. Loewen, K. M. Smith, R. G. Ritzel, D. A. Mowles, P. Carpenter, X. Z. Chen, E. Karpinski, R. J. Hyde, S. A. Baldwin, C. E. Cass, and J. D. Young. Molecular identification and characterization of novel human and mouse concentrative Na⁺-nucleoside cotransporter proteins (hCNT3 and mCNT3) broadly selective for purine and pyrimidine nucleosides (system cib). *J Biol Chem* 276: 2914-27, 2001.
34. Ritzel, M. W., S. Y. Yao, M. Y. Huang, J. F. Elliott, C. E. Cass, and J. D. Young. Molecular cloning and functional expression of cDNAs encoding a human Na⁺-nucleoside cotransporter (hCNT1). *Am J Physiol* 272: C707-14, 1997.
35. Sairam, M. R., L. G. Jiang, T. A. Yarney, and H. Khan. Follitropin signal transduction: alternative splicing of the FSH receptor gene produces a dominant negative form of receptor which inhibits hormone action. *Biochem Biophys Res Commun* 226: 717-22, 1996.
36. Saunders, C., J. R. Keefer, A. P. Kennedy, J. N. Wells, and L. E. Limbird. Receptors coupled to pertussis toxin-sensitive G-proteins traffic to opposite surfaces in Madin-Darby canine kidney cells. A1 adenosine receptors achieve apical and alpha 2A adrenergic receptors achieve basolateral localization. *J Biol Chem* 271: 995-1002, 1996.

37. Scharrer, E., and B. Grenacher. Active intestinal absorption of nucleosides by Na⁺-dependent transport across the brush border membrane in cows. *J Dairy Sci* 84: 614-9, 2001.
38. Sundaram, M., S. Y. Yao, J. C. Ingram, Z. A. Berry, F. Abidi, C. E. Cass, S. A. Baldwin, and J. D. Young. Topology of a human equilibrative, nitrobenzylthioinosine (NBMPR)-sensitive nucleoside transporter (hENT1) implicated in the cellular uptake of adenosine and anti-cancer drugs. *J Biol Chem* 276: 45270-5, 2001.
39. Sweet, D. H., D. S. Miller, and J. B. Pritchard. Localization of an organic anion transporter-GFP fusion construct (rROAT1-GFP) in intact proximal tubules. *Am J Physiol* 276: F864-73, 1999.
40. Vijayalakshmi, D., and J. A. Belt. Sodium-dependent nucleoside transport in mouse intestinal epithelial cells. Two transport systems with differing substrate specificities. *J Biol Chem* 263: 19419-23, 1988.
41. Wang, J., S. F. Su, M. J. Dresser, M. E. Schaner, C. B. Washington, and K. M. Giacomini. Na⁺-dependent purine nucleoside transporter from human kidney: cloning and functional characterization. *Am J Physiol* 273: F1058-65, 1997.
42. Wang, Y., and R. J. Miksicek. Identification of a dominant negative form of the human estrogen receptor. *Mol Endocrinol* 5: 1707-15, 1991.
43. Ward, J. L., A. Sherali, Z. P. Mo, and C. M. Tse. Kinetic and pharmacological properties of cloned human equilibrative nucleoside transporters, ENT1 and ENT2, stably expressed in nucleoside transporter-deficient PK15 cells. Ent2 exhibits a low affinity for guanosine and cytidine but a high affinity for inosine. *J Biol Chem* 275: 8375-81, 2000.

44. Watanabe, K., T. Fukuchi, H. Hosoya, T. Shirasawa, K. Matuoka, H. Miki, and T. Takenawa. Splicing isoforms of rat Ash/Grb2. Isolation and characterization of the cDNA and genomic DNA clones and implications for the physiological roles of the isoforms. *J Biol Chem* 270: 13733-9, 1995.
45. Williams, T. C., A. J. Doherty, D. A. Griffith, and S. M. Jarvis. Characterization of sodium-dependent and sodium-independent nucleoside transport systems in rabbit brush-border and basolateral plasma-membrane vesicles from the renal outer cortex. *Biochem J* 264: 223-31, 1989.
46. Williams, T. C., and S. M. Jarvis. Multiple sodium-dependent nucleoside transport systems in bovine renal brush-border membrane vesicles. *Biochem J* 274: 27-33., 1991.
47. Xiao, G., J. Wang, T. Tangen, and K. M. Giacomini. A novel proton-dependent nucleoside transporter, CeCNT3, from *Caenorhabditis elegans*. *Mol Pharmacol* 59: 339-48, 2001.
48. Yao, S. Y., A. M. Ng, W. R. Muzyka, M. Griffiths, C. E. Cass, S. A. Baldwin, and J. D. Young. Molecular cloning and functional characterization of nitrobenzylthioinosine (NBMPR)-sensitive (es) and NBMPR-insensitive (ei) equilibrative nucleoside transporter proteins (rENT1 and rENT2) from rat tissues. *J Biol Chem* 272: 28423-30, 1997.
49. Yao, S. Y., A. M. Ng, M. F. Vickers, M. Sundaram, C. E. Cass, S. A. Baldwin, and J. D. Young. Functional and molecular characterization of nucleobase transport by recombinant human and rat equilibrative nucleoside transporters 1 and 2. Chimeric constructs reveal a role for the ENT2 helix 5-6 region in nucleobase translocation. *J Biol Chem* 277: 24938-48, 2002.

50. Yeaman, C., K. K. Grindstaff, and W. J. Nelson. New perspectives on mechanisms involved in generating epithelial cell polarity. *Physiol Rev* 79: 73-98, 1999.
51. Zegers, M. M., and D. Hoekstra. Mechanisms and functional features of polarized membrane traffic in epithelial and hepatic cells. *Biochem J* 336: 257-69, 1998.

CHAPTER 5

LOCALIZATION OF CNT3, A BROADLY SELECTIVE CONCENTRATIVE NUCLEOSIDE TRANSPORTER, IN RENAL EPITHELIAL CELLS⁵

Introduction

Nucleosides are hydrophilic compounds important physiologically as precursors for nucleotides. Naturally occurring nucleosides require carrier-mediated transport to cross cellular membranes. Many nucleoside analogs, which are used as chemotherapeutic agents in the treatments of cancers and viral infections, also rely heavily on nucleoside transporters to enter and leave cells.

Transepithelial flux of nucleosides and nucleoside analogs within the renal epithelium depends on expression and polarized distribution of nucleoside transporters. Our current model predicts reabsorption of nucleosides via two families of nucleoside transporters. Concentrative nucleoside transporters (CNT1 and SPNT) localize predominantly to the apical membrane of renal epithelial cells where they mediate the first step in salvage, concentrating luminal nucleosides within the cells (13). Equilibrative nucleoside transporters (ENT1 and ENT2) localize predominantly to the basolateral membrane where they mediate downhill movement of nucleosides out of the epithelium and back into the systemic circulation (see Chapter 4). Naturally occurring nucleosides tend to follow this pathway, undergoing active absorption within the kidney. Most nucleoside analogs, however, tend to undergo active secretion. This is likely due to several factors: 1) interaction of analogs with efflux pumps such as organic cation

⁵ This work was done with help from Ilaria Badagnani.

transporters increases secretion and 2) lower affinity of nucleoside transporters for analogs of nucleosides decreases reabsorption.

Expression profiling indicates CNT3, the recently cloned broadly selective CNT, is expressed in low levels within the kidney. This transporter interacts with a broad range of nucleoside analogs and may play an important role in renal disposition (14). There is some evidence that broadly selective nucleoside transporters are important on the apical membrane of the renal epithelium. Studies using vesicles prepared from rat kidney tell us that a broad range of nucleosides are transported by a concentrative system without specifying whether this is achieved by one broadly selective system or several more specific systems (2, 7-10, 15). Studies using vesicles prepared from human kidney provide evidence for broadly selective nucleoside transport mechanisms for pyrimidines and also guanosine (4, 5).

In this study, we localized CNT3 within MDCK cells, a renal epithelial cell line. MDCK form a uniform monolayer of polarized epithelial cells that may also serve as a model of the intestinal epithelium and other epithelial tissues throughout the body.

Materials and Methods

Materials. All tissue culture plasticware and transwells were purchased from Corning Costar (Corning, NY). Protease inhibitor cocktail was purchased from Roche Labs (Palo Alto, CA), and ECL chemicals from PerkinElmer (Boston MA). Radiolabeled inosine (25.4 Ci/mMol), ribavirin (14.9 Ci/mMol) and cladribine (17 Ci/mMol) were purchased from Moravек Biochemicals (Brea, CA). Scintillation fluid (EcoLite) was obtained from

ICN Biomedicals (Costa Mesa, CA). All other chemicals were purchased from Sigma (St. Louis, MO).

Cloning of CNT3 and plasmid construction. hCNT3 was cloned by PCR amplification from a cDNA library made using the Superscript First Strand cDNA Synthesis System for RT-PCR (Invitrogen, Carlsbad, CA) with human pancreas poly-A mRNA (Clontech, Palo Alto, CA) as template. Primers were designed to bases 89-114 (sense) and 2196-2170 (antisense) of the known mRNA sequence of hCNT3 (GenBank # AF305210) and synthesized by Invitrogen (50 nmoles/primer, desalted). PCR product was ligated into pGEM-T vector (Promega, Madison, WI) using ExTaq polymerase (TaKaRa via Intergen, Purchase, NY). hCNT3 was then subcloned in-frame into pEGFP-C1 by bioengineering a Bgl II site directly 5' to the start codon and a Sal I site directly 3' of the stop codon. DNA sequence was verified by automated sequencing at the Biochemical Resource Center (BRC, UCSF, San Francisco, CA).

Stable transfection of MDCK. MDCK cells (the EMBL strain) were grown in MEM Eagle's with Earle's BSS supplement, 5% heat inactivated FBS, 100 units/ml Penicillin and 100 units/ml Streptomycin in a humidified atmosphere of 5% CO₂, 95% air at 37°C. Cells were transfected with 1 µg hCNT3-pEGFP-C1 or empty vector and 16 µg Effectene (Qiagen, Valencia, CA). Cells were grown for 48 hours and then diluted into media supplemented with 800 µg/ml geneticin (Invitrogen, Carlsbad, CA). Clones were picked after two weeks of growth in selection media and positive clones were chosen by western blot, confocal microscopy, and functional uptake of ³H-nucleoside. All subsequent experiments were performed on more than one positive clone with comparable results.

Confocal microscopy. Samples were prepared for confocal microscopy as described previously (13, Chapters 2 and 4). Samples were grown for 4-7 days on permeable support and then fixed with 4% paraformaldehyde, permeablized with 0.025% (w/v) saponin in phosphate buffered saline, stained with Texas-red conjugated phalloidin (Molecular Probes, Eugene, OR) for visualization of actin, and mounted on slides in Vectashield mounting medium (Vector Labs, Burlingame, CA). Samples were analyzed using a Bio-Rad MRC-1024 laser scanning confocal microscope.

Functional localization in MDCK. Stably transfected MDCK cells were grown for 5-7 days on permeable support and then assayed for membrane specific functionality as described previously (13, Chapter 2). Briefly, cells were exposed to $0.1 \mu\text{M}$ ^3H -inosine in sodium buffer (128 mM NaCl, 4.73 mM KCl, 1.25 mM CaCl_2 , 1.25 mM MgSO_4 , 5 mM Hepes, pH 7.4) or choline butter (128 mM CholineCl, 4.73 mM KCl, 1.25 mM CaCl_2 , 1.25 mM MgSO_4 , 5 mM Hepes, pH 7.4) containing $10 \mu\text{M}$ cold inosine and $10 \mu\text{M}$ NBMPR (an inhibitor of the endogenous ENT system). Reaction mix was applied to either the apical or basolateral membrane for 2 minutes (with choline buffer in opposite chamber), removed, and cells were washed three times in ice-cold choline buffer to terminate the reaction. Cellular uptake of ^3H -inosine was measured by lysing cells (30 minutes shaking in $300 \mu\text{l}$ 10% SDS) and counting in a Beckman Scintillation Counter. All experiments were repeated 3 times in duplicate.

Functional kinetic analysis in MDCK. MDCK cells transfected with CNT3-GFP or GFP were plated at a density of 5×10^4 cells/well five days prior to experiment. Uptake of $0.1 \mu\text{M}$ ^3H -nucleoside (inosine, ribavirin, or cladribine) was measured for four minutes in sodium butter or choline buffer in the presence of $10 \mu\text{M}$ NBMPR. For kinetic

analysis, varying amounts of inosine (0 μM to 250 μM ; transport plateaus above 250 μM) were also added to the reaction mix. For inhibition studies, 1 mM cold substrate was added to some wells to observe inhibition. The reaction was stopped by removing the reaction mix and washing three times with ice cold choline buffer (1x 1 ml, 2 x 0.5 ml). Cells were lysed for 2 hours in 0.5 ml NaOH and neutralized with 0.5 ml 1M HCl. An aliquot (0.5 ml) was added to 3 ml scintillation fluid and counted on a Beckman Scintillation Counter. In all cases, three wells of cells/plate were lysed in 0.5 ml 1M NaOH for 2 hours, neutralized with 1M HCl, and stored for protein assay. The lysate (100 μl) was assayed using the BioRad DC protein assay with albumin as standard (Pierce, Rockford, IL).

Immunoblot analysis. Transfected cells which had been polarized by growth for 4-7 days on transwells were lysed by agitation in SDS buffer (2% SDS in PBS with protease inhibitor), and centrifuged at 14,000 RPM for 20 minutes. The supernatant was removed, assayed for protein content using the DC protein assay (BioRad, Hercules, CA), and combined with loading buffer (15 mM TRIS pH 6.8, 1% SDS, 25 mM EDTA, 65 mM DTT, 0.025% bromophenol blue, 6% glycerol). Twenty micrograms of protein was loaded per sample on a 10% BioRad ready gel and separated by electrophoresis. Protein was transferred to PVDF membrane (BioRad), blocked in 5% milk, incubated first in mouse anti-GFP primary antibody (1:1000, Roche, Palo Alto, CA), then in goat anti-mouse IgG-HRP conjugated secondary antibody (1:3000, BioRad) and signal was detected by chemiluminescence.

Statistics and data analysis. All functional experiments were repeated at least three times (in duplicate or triplicate) and results averaged. For kinetic analysis, negative

control values were subtracted from functional data and corrected data were fit to the Michaelis-Menten equation: $V=V_{\max} \cdot S/(K_m+S)$ where V = velocity, V_{\max} = maximal velocity, S = substrate concentration, K_m = the Michaelis Menten rate constant (substrate concentration at $V_{\max}/2$). Fits were carried out using a nonlinear least-squares regression-fitting program (Kaleidagraph, V.3.0, Abelbeck/Synergy Software, Reading, PA). Kinetic experiments were repeated several times; data for one representative experiment are presented in this chapter.

Results

Preparation of a GFP-tagged CNT3 stably transfected cell line in MDCK.

hCNT3 was cloned from human pancreas using primers to the known cDNA sequence (GenBank # AF305210). In order to visualize CNT3 in a cellular system, we tagged the N-terminus of the protein with green fluorescence protein (GFP), a 35 kDa protein originally isolated from jellyfish which fluoresces under light at 488 nm. CNT3-GFP was then stably transfected into MDCK, a polarized renal epithelial cell line. Positive clones were selected by resistance to geneticin, and identified by Western blot, functional assay, and fluorescence microscopy. Immunoblotting of CNT3-GFP positive clones demonstrated a major band at approximately 140 kDa, with a minor band at approximately 110 kDa (Figure 1). These bands were unique to CNT3-GFP positive cells and were not present in untransfected or GFP transfected cells. Untagged CNT3 is estimated to have a molecular weight of 77 kDa and to contain four putative glycosylation sites, all located within the extracellular C-terminal tail (14). It is likely

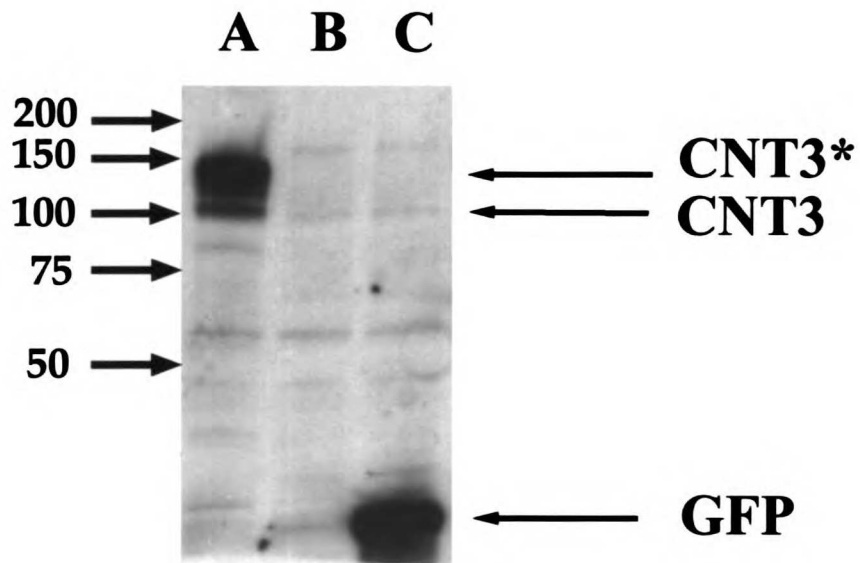


Figure 1. Immunoblot of CNT3-GFP positive MDCK cells. MDCK transfected with CNT3-GFP (A), untransfected (B) or transfected with GFP (C) were lysed, separated by electrophoresis and immunoanalysed with antibody to GFP as described in Materials and Methods. Twenty micrograms of total protein was loaded per lane. Size of molecular standards (in kDa) is indicated by arrows to the left of the blot. Relevant bands are indicated by arrows to right of blot with CNT3* indicating glycosylated protein.

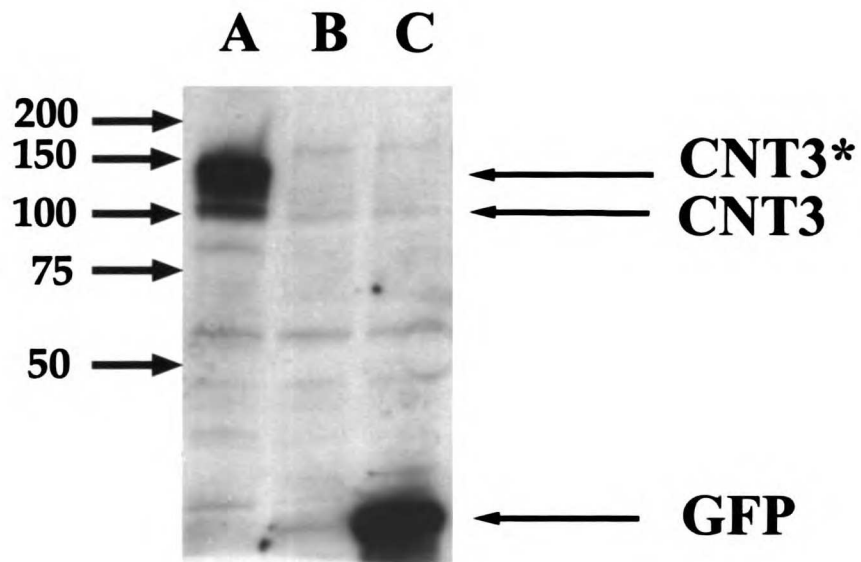


Figure 1. Immunoblot of CNT3-GFP positive MDCK cells. MDCK transfected with CNT3-GFP (A), untransfected (B) or transfected with GFP (C) were lysed, separated by electrophoresis and immunoanalysed with antibody to GFP as described in Materials and Methods. Twenty micrograms of total protein was loaded per lane. Size of molecular standards (in kDa) is indicated by arrows to the left of the blot. Relevant bands are indicated by arrows to right of blot with CNT3* indicating glycosylated protein.

that the 110 kDa band correlates to unglycosylated CNT3-GFP and the larger band to glycosylated CNT3-GFP.

To ensure that addition of the GFP tag did not alter functionality of CNT3, we performed kinetic analysis of transport in CNT3-GFP cells. Michaelis Menten analysis of inosine transport yielded an apparent K_m ($53.8 \pm 10.9 \mu\text{M}$, Figure 2) which was indistinguishable from the previously reported value in cells ($52.5 \pm 12.6 \mu\text{M}$) (14).

Localization of CNT3 in MDCK. Subcellular localization of CNT3-GFP within MDCK was determined by confocal microscopy and functional analysis. Microscopy data indicate that CNT3-GFP is confined to the apical membrane (Figure 3). In addition, sodium-dependent uptake of radiolabeled nucleoside was demonstrated selectively on the apical membrane (Figure 4). Interestingly, removal of sodium from the buffer completely inhibited CNT3-mediated uptake. Residual transport was seen in the absence of sodium in similar experiments using either SPNT or CNT1 transfected cells (13).

Kinetic analysis and drug interactions of CNT3. Because CNT3 has such a broad selectivity, its presence in the intestine and kidney is expected to have an effect on the pharmacokinetics of a wide range of therapeutically relevant nucleoside analogs. We examined the interactions between CNT3 and several clinically used drugs. CNT3 transports both the anti-viral agent ribavirin, a base-modified guanosine analog, and the anticancer agent cladribine, a base-modified deoxyadenosine analog, although at levels far lower than inosine (Figure 5A.). Levels were too low for accurate kinetic analysis. In addition, transport of inosine was partially inhibited by the presence of therapeutically

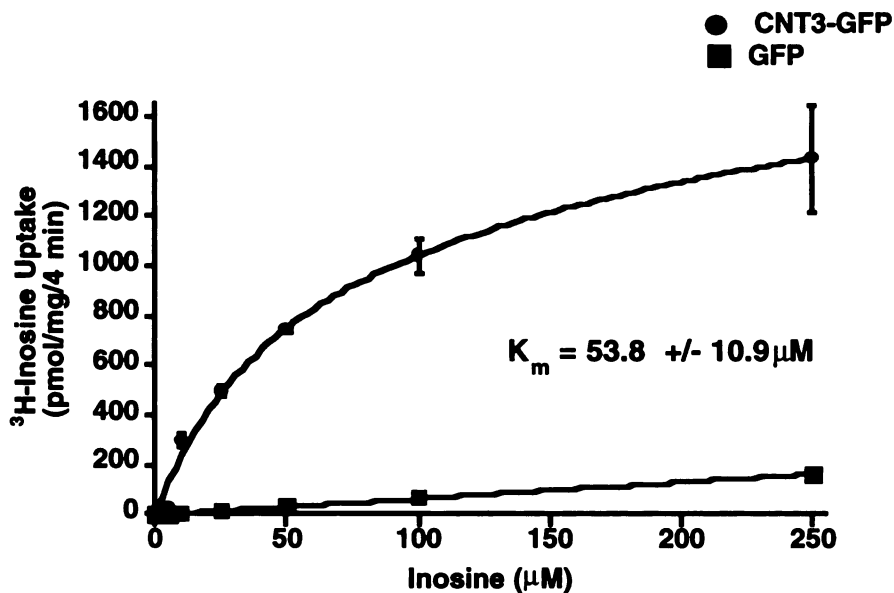


Figure 2. Michaelis-Menten analysis of inosine transport by CNT3-GFP in MDCK.

Transport of ^3H -inosine ($0.1 \mu\text{M}$) was measured by MDCK transfected with CNT3-GFP or GFP in the presence of NBMPR ($10 \mu\text{M}$) and a range of concentrations of unlabeled inosine (0 - $250 \mu\text{M}$). Corrected data (CNT3 data minus GFP control) were analyzed using the equation, $V = V_{\text{max}} * S / (K_m + S)$ where V = velocity, V_{max} = maximal velocity, S = substrate concentration, K_m = Michealis Menten constant (substrate concentration at $V_{\text{max}}/2$) by Kaleidagraph Graphics. K_m is averaged from 4 separate experiments. Graph depicts representative data (performed in triplicate) from one experiment.

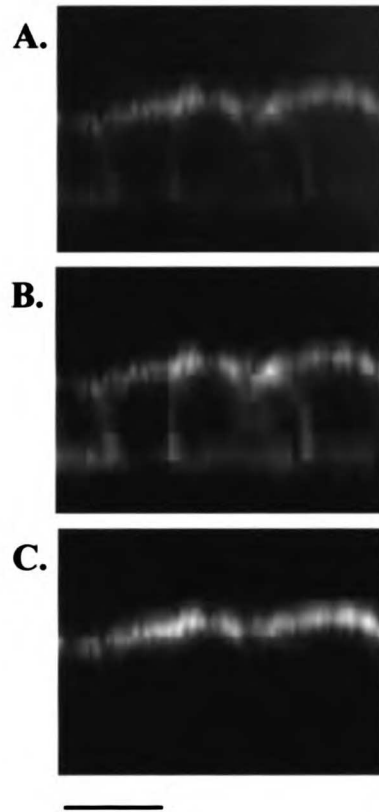


Figure 3. Localization of CNT3-GFP to apical membrane of MDCK. CNT3-GFP transfected cells were polarized by growth on permeable support, fixed, permeablized and stained with Texas-Red conjugated phalloidin. (A.) Red indicates phalloidin-stained actin, green indicates CNT3-GFP. (B.) Shows only actin stain. (C.) Shows only CNT3-GFP. Picture oriented with apical membrane on top. Bar, 10 μm .

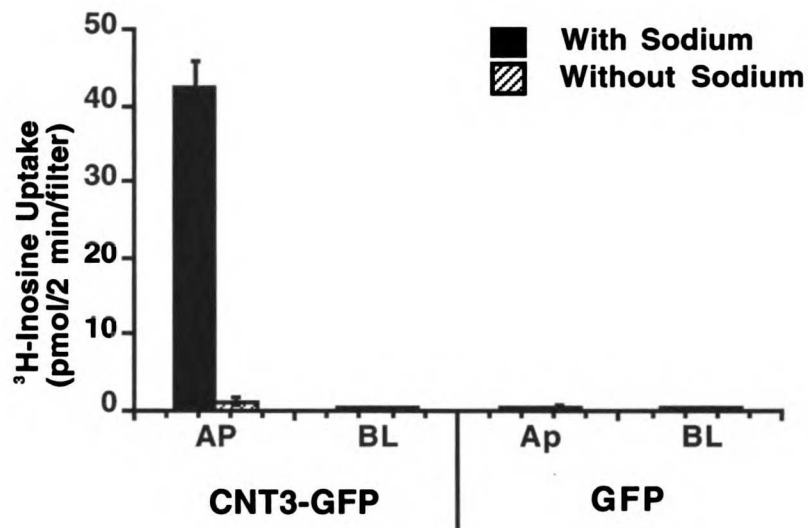


Figure 4. Functional localization of CNT3-GFP to apical membrane. MDCK transfected with CNT3-GFP or GFP were polarized and sodium-dependent transport of ³H-inosine (0.1 μ M) was examined in the presence of NBMPR (10 μ M) at either the apical (AP) or basolateral (BL) membranes. Data represent averages of three experiments each performed in duplicate.

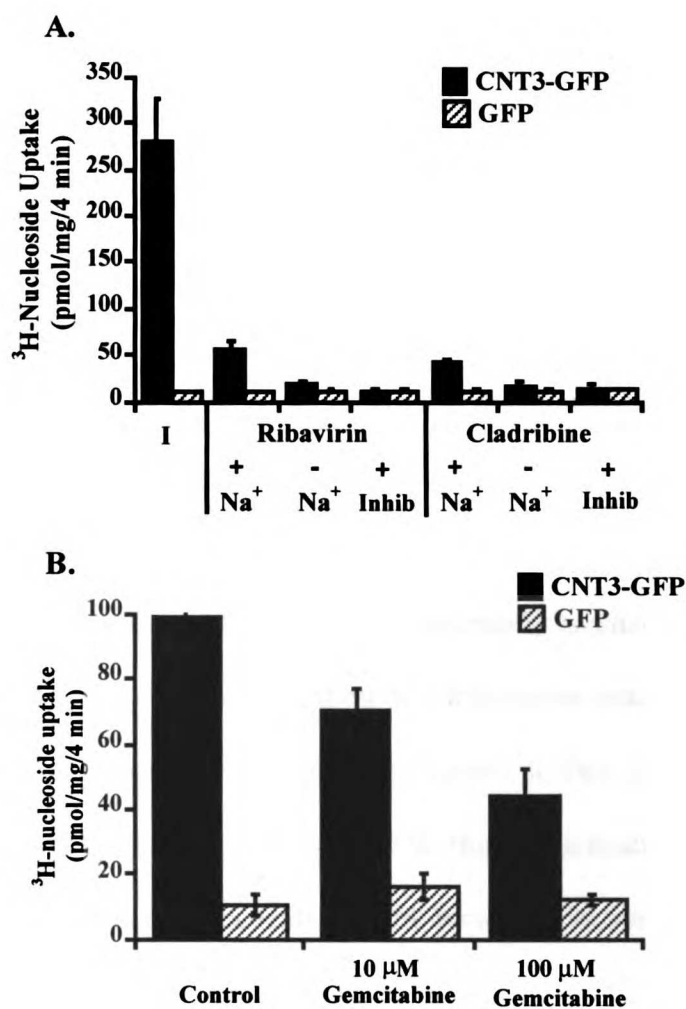


Figure 5. Interaction of CNT3-GFP with clinically relevant nucleoside analogs. (A.) Transport of ³H-nucleoside (0.1 μM) (inosine (I), ribavirin or cladribine) was measured in CNT3-GFP or GFP transfected cells in the presence (+ Na⁺) or absence (- Na⁺) of sodium or in the presence of both sodium and 1 mM unlabelled substrate (+ Inhib). (B.) Transport of ³H-inosine (0.1 μM) in the absence (Control) or presence of 10 μM or 100 μM gemcitabine. Data represent the average of three experiments (n=3 per data point per experiment).

relevant levels of gemcitabine, a ribose-modified cytidine analog used as chemotherapy in pancreatic and non-small cell lung cancers (Figure 5B.). Thus, CNT3 appears to interact with nucleoside analogs and may play a role in the pharmacokinetics of these and other therapeutic compounds.

Discussion

To date, work in this laboratory has shown that two concentrative nucleoside transporters, CNT1 and SPNT, are predominantly localized to the apical membrane of renal epithelium (Chapter 2) and that the two functionally characterized equilibrative nucleoside transporters, ENT1 and ENT2, are predominantly localized to the basolateral membrane (Chapter 4). It is expected that these two transporter families work in concert to mediate salvage of nucleosides from the tubular lumen. In fact, co-transfection of CNT1 and ENT1 in MDCK results in transepithelial flux of adenosine in a reabsorptive direction (6). Understanding the localization of the broadly selective concentrative nucleoside transporter, CNT3, in renal epithelium will add to our model of transepithelial nucleoside flux within the kidney. To this aim, we GFP-tagged the human clone of CNT3 and stably expressed it in MDCK. CNT3-GFP was confined entirely to the apical membrane (Figures 3 and 4). In addition, we demonstrated that three nucleoside analog drugs (ribavirin, cladribine, and gemcitabine) interact with CNT3.

mRNA expression profiling indicates that CNT3 mRNA is present in small amounts in the kidney (14). CNT3 exhibits a Na^+ :nucleoside coupling ratio of 2:1, indicating it concentrates nucleosides ten times more than either CNT1 or SPNT, which

both have coupling ratios of 1:1 (2, 11, 14, 17). Presence of small amounts of CNT3 protein may be important in renal salvage of nucleosides.

Interestingly, removal of Na^+ from our experimental system resulted in complete inhibition of inosine uptake. This differs from results seen in our previous studies in stably transfected cells expressing CNT1 and SPNT, both of which retained a significant portion of function in the absence of Na^+ (13). Electrophysiologic studies of both SPNT and CNT1 indicate that movement of nucleosides across membranes via these proteins can be facilitated by other ions (chloride or protons) and is dependent on membrane potential (1, 3, 12). Chimeric studies replacing estimated TMDs 8-9 of rat CNT1 with the amino acid sequence for TMDs 8-9 of rat SPNT resulted in a protein which lost the requirement of Na^+ for transport, indicating there may be specific molecular determinants for Na^+ -coupled transport (16). The Na^+ coupling mechanism for CNT3 differs from that of SPNT and CNT1 which may explain the higher Na^+ dependence of nucleoside flux by CNT3. Further studies are needed to examine the ionic requirements for CNT3 transport and the molecular determinants involved.

Originally thought to be confined to epithelial cells and primarily important in maintaining levels of endogenous nucleosides within the body, it seems that some of the CNTs (CNT3 in particular) have tissue distributions which indicate other roles within the body. CNT3 is found in low quantities in the kidney and at higher levels in pancreas, bone marrow, mammary gland, trachea, and throughout the intestine (14). Its presence in the intestine suggests that CNT3 may play a role in the absorption of orally administered nucleoside analogs such as ribavirin. In fact, gemcitabine, which we have shown here to interact with CNT3, is the first order chemotherapeutic agent used in treatment of

pancreatic cancer and its uptake in pancreas may be highly dependent on CNT3-mediated transport.

Typically, adverse reactions to clinical treatment with antiviral nucleoside analogs (largely dideoxynucleoside analogs) include pancreatitis, lactic acidosis and hepatomegaly with steatosis, along with occasional peripheral neuropathy, hypotension, or bone marrow suppression. Generally, all of these reactions are thought to be related to the mechanism of action of these drugs, which inhibit viral reverse transcriptase but also cause toxicity by affecting mammalian mitochondrial DNA polymerase. Such mitochondrial toxicity is not cell-type specific, but appears to more strongly affect organs which have high energy demands such as pancreas, bone marrow, and liver. Many of these tissues express high levels of CNT3. Presence of abundant amounts of CNT3 may be playing a role in concentrating nucleoside analogs within these tissues, causing increased toxicity relative to the rest of the body.

In this study, we report construction of MDCK cells stably transfected with GFP-tagged human CNT3, providing the first cellular model for examining CNT3. CNT3 was expressed in these cells predominantly in a glycosylated form, and was confined entirely to the apical membrane where it likely participates in reabsorption of nucleosides within the kidney and absorption within the intestine. We show that CNT3 transports both ribavirin and cladribine, and interacts with gemcitabine. In addition to providing a model for further examination of the trafficking and regulation of CNT3, stably transfected CNT3-MDCK cells provide a means by which to examine the substrate specificity of CNT3 for a wide range of therapeutically relevant nucleoside analogs.

References

1. Dresser, M. J., K. M. Gerstin, A. T. Gray, D. D. Loo, and K. M. Giacomini. Electrophysiological analysis of the substrate selectivity of a sodium-coupled nucleoside transporter (rCNT1) expressed in *Xenopus laevis* oocytes. *Drug Metab Dispos* 28: 1135-40, 2000.
2. Franco, R., J. J. Centelles, and R. K. Kinne. Further characterization of adenosine transport in renal brush-border membranes. *Biochim Biophys Acta* 1024: 241-8, 1990.
3. Gerstin, K. M., M. J. Dresser, and K. M. Giacomini. Specificity of human and rat orthologs of the concentrative nucleoside transporter, SPNT. *Am J Physiol Renal Physiol* 283: F344-9, 2002.
4. Gutierrez, M. M., C. M. Brett, R. J. Ott, A. C. Hui, and K. M. Giacomini. Nucleoside transport in brush border membrane vesicles from human kidney. *Biochim Biophys Acta* 1105: 1-9, 1992.
5. Gutierrez, M. M., and K. M. Giacomini. Substrate selectivity, potential sensitivity and stoichiometry of Na(+)-nucleoside transport in brush border membrane vesicles from human kidney. *Biochim Biophys Acta* 1149: 202-8, 1993.
6. Lai, Y., A. D. Bakken, and J. D. Unadkat. Simultaneous expression of hCNT1-CFP and hENT1-YFP in Mardin-Darby canine kidney (MDCK) cells: Localization and vectorial transport studies. *J Biol Chem* 277: 37711-17, 2002.
7. Le Hir, M., and U. C. Dubach. Concentrative transport of purine nucleosides in brush border vesicles of the rat kidney. *Eur J Clin Invest* 15: 121-7, 1985.
8. Le Hir, M., and U. C. Dubach. Sodium gradient-energized concentrative transport of adenosine in renal brush border vesicles. *Pflugers Arch* 401: 58-63, 1984.

9. Le Hir, M., and U. C. Dubach. Uphill transport of pyrimidine nucleosides in renal brush border vesicles. *Pflugers Arch* 404: 238-43, 1985.
10. Lee, C. W., C. I. Cheeseman, and S. M. Jarvis. Na⁺- and K⁺-dependent uridine transport in rat renal brush-border membrane vesicles. *Biochim Biophys Acta* 942: 139-49, 1988.
11. Lee, C. W., C. I. Cheeseman, and S. M. Jarvis. Transport characteristics of renal brush border Na⁽⁺⁾- and K⁽⁺⁾-dependent uridine carriers. *Am J Physiol* 258: F1203-10, 1990.
12. Lostao, M. P., J. F. Mata, I. M. Larrayoz, S. M. Inzillo, F. J. Casado, and M. Pastor-Anglada. Electrogenic uptake of nucleosides and nucleoside-derived drugs by the human nucleoside transporter 1 (hCNT1) expressed in *Xenopus laevis* oocytes. *FEBS Lett* 481: 137-40, 2000.
13. Mangravite, L. M., J. H. Lipschutz, K. E. Mostov, and K. M. Giacomini. Localization of GFP-tagged concentrative nucleoside transporters in a renal polarized epithelial cell line. *Am J Physiol Renal Physiol* 280: F879-85, 2001.
14. Ritzel, M. W., A. M. Ng, S. Y. Yao, K. Graham, S. K. Loewen, K. M. Smith, R. G. Ritzel, D. A. Mowles, P. Carpenter, X. Z. Chen, E. Karpinski, R. J. Hyde, S. A. Baldwin, C. E. Cass, and J. D. Young. Molecular identification and characterization of novel human and mouse concentrative Na⁺-nucleoside cotransporter proteins (hCNT3 and mCNT3) broadly selective for purine and pyrimidine nucleosides (system cib). *J Biol Chem* 276: 2914-27, 2001.
15. Trimble, M. E., and R. Coulson. Adenosine transport in perfused rat kidney and renal cortical membrane vesicles. *Am J Physiol* 246: F794-803, 1984.

16. Wang, J., and K. M. Giacomini. Molecular determinants of substrate selectivity in Na⁺-dependent nucleoside transporters. *J Biol Chem* 272: 28845-8, 1997.
17. Yao, S. Y., C. E. Cass, and J. D. Young. Transport of the antiviral nucleoside analogs 3'-azido-3'-deoxythymidine and 2',3'-dideoxycytidine by a recombinant nucleoside transporter (rCNT) expressed in *Xenopus laevis* oocytes. *Mol Pharmacol* 50: 388-93, 1996.

CHAPTER 6

CONCLUSIONS AND FUTURE STUDIES

Understanding the molecular mechanisms governing renal transport of nucleosides and their analogs is essential to predicting the renal disposition of these compounds. The advent of cloning technology has allowed for the identification of several candidate proteins that participate in these processes. The most likely candidates in renal disposition of nucleosides are the six recently cloned nucleoside transporters. This dissertation explores in detail the subcellular localization and sorting mechanisms of these proteins as a means to better understand renal disposition of nucleosides. This work also begins to explore the cellular regulation of nucleoside transporters.

Localization of Nucleoside Transporters within Renal Epithelial Cells

To understand the role that nucleoside transporters play in renal handling of nucleosides, it is essential to determine their subcellular distribution within renal epithelium. This information will allow us to develop a model of nucleoside transporter-mediated transepithelial nucleoside flux (Figure 1). To localize each transporter, we have established cell culture models within MDCK, a renal epithelial cell line (Chapters 2, 4, and 5).

The concentrative nucleoside transporters, CNT1, SPNT, and CNT3 localized predominantly to the apical membrane of MDCK (see Chapter 2 and Chapter 5). While CNT1 and CNT3 were entirely confined to the apical membrane, as determined by immunofluorescence and functional analysis of GFP-tagged transporters in MDCK,

A.

Clone	Apical Expression	Basolateral Expression
CNT1	yes	no
SPNT	yes	yes
CNT3	yes	no
ENT1	yes	yes
ENT2	no	yes
ENT3	no	no

B.

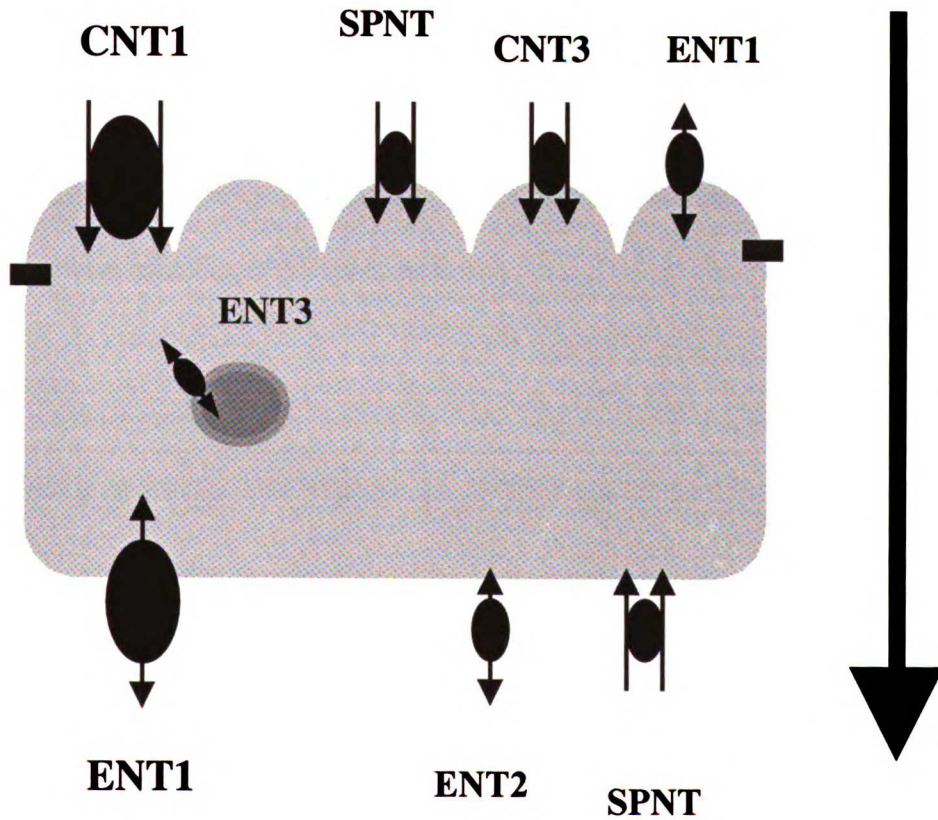


Figure 1. Model of nucleoside transporters within renal epithelium. Localization of transporters, as described within this dissertation, are (A.) described and (B.) displayed visually in a representative renal epithelial cell. ENT1 and CNT1 are larger than the other transporters to indicate their relative abundance within the kidney, as determined by mRNA levels. Rectangles represent tight junctions, separating the apical (top) from basolateral (bottom) membranes. Arrow depicts overall direction of vectorial flux of nucleosides suggested by this model (reabsorptive). Dual arrows on the concentrative transporters indicate substrate plus sodium or protons.

SPNT had significant presence on the basolateral membrane as well. These results were confirmed in a second renal epithelial cell line, LLC-PK₁.

In contrast, the equilibrative nucleoside transporters, ENT1 and ENT2, localized predominantly to the basolateral membrane within MDCK and LLC-PK₁ (Chapter 4). ENT2 was confined entirely to the basolateral membrane whereas ENT1 was predominantly on the basolateral membrane with a small additional presence on the apical membrane. Thus, these transporters primarily control movement of nucleosides between the epithelial cytosol and the interstitium.

Localization of CNTs to the apical membrane and ENTs to the basolateral membrane implicates these transporters in renal reabsorption of nucleosides (Figure 1). Nucleosides filtered into the tubule lumen by the glomeruli are actively removed in two steps. Nucleosides within the filtrate come in contact with CNTs and are actively transported into the cytosol of the surrounding epithelium. As these nucleosides are concentrated within the cells (they are driven across the basolateral membrane) via ENT1 and ENT2.

The newest member of the nucleoside transporter families to be cloned, ENT3, is also transcribed in the kidney (12). ENT3 is 31-33% identical to ENT1 and ENT2. To date, there has been no successful functional analysis of ENT3. Thus, the role of ENT3 in renal handling of nucleosides is not known. Initial studies of GFP-tagged ENT3 within MDCK, carried out by Jennifer Gray in this laboratory, indicated that this protein is sequestered within internal vesicles. Internal localization may indicate protein misfolding or degradation but could also be of physiologic significance. ENT3 has an extended cytosolic N-terminal tail that may be responsible for this differential

localization pattern. Studies are ongoing in this and other laboratories to understand the physiologic implications of ENT3.

Renal Handling of Nucleoside Analogs

Clinical observation of naturally occurring nucleosides and nucleoside analogs indicates that some of these compounds are actively reabsorbed whereas others are actively secreted (Introduction, Table 1). Upon initial observation, one would expect that exposure of nucleoside analogs to the transepithelial flux model described above should result in active reabsorption of all of these compounds. In trying to understand this seemingly conflicting data, there are several important points to consider.

Nucleoside transporters have a much lower affinity for nucleoside analogs than for naturally occurring nucleosides. While extensive analysis of transporter interactions with many of the analogs is limited (Table 1), basic uptake studies indicate that nucleoside analogs are less tolerated. For example, hSPNT1 is intolerant of base or ribose modifications, transporting most nucleoside analogs very poorly (4, 6, 18). In Chapter 5, we compared CNT3-mediated transport of inosine, ribavirin, and cladribine. Our results indicated that CNT3 transports inosine at a rate five times faster than that of either of these analogs (Chapter 5). It appears that our nucleoside reabsorption model is likely to mediate reabsorption of nucleoside analogs at a far slower rate than it does of naturally occurring nucleosides.

Secondly, there are xenobiotic transporters expressed in the kidney that interact with nucleoside analogs. Both organic anion and organic cation transporters have been reported to interact with several of these compounds (Table 2). These proteins recognize

Table 1. Known interactions between nucleoside analogs and nucleoside transporters.

Substrate	Nucleoside Transporter (Kinetic Constant, μM)	References
ddI	rSPNT (<i>46</i>)	(24)
	hSPNT1 (<i>19</i>)	(25)
	hENT2 (2.3)	(33)
Cladribine	rSPNT (<i>13</i>)	(17)
	hSPNT1 (<i>371</i>)	(25)
	hENT1 (71)	(19)
Deoxyadenosine	hCNT1 (<i>46</i>)	(22)
	hSPNT1 (<i>110</i>)	(30)
Gemcitabine	hCNT1 (24)	(18)
	hENT1 (160)	(19)
Deoxycytidine	rCNT1 (150)	(7)
FUdR	rCNT1 (<i>50</i>)	(7)
IUdR	rCNT1 (<i>50</i>)	(7)
AZT	rCNT1 (500)	(5)
ddC	rCNT1 (500)	(33)
Inhibitor		
Dipyridamole	hENT1 (<i>140</i>)	(32)
Dilazep	hENT1 (<i>60</i>)	(32)
	hENT2 (740)	(33)
NBMPR	hENT1 (0.002)	(8)

Kinetic constants are reported in parenthesis. Values are K_m (μM) if emboldened, IC_{50} values (μM) if italicized, and K_i if underscored.

Table 2. Known interactions between nucleoside or nucleotide analogs and secretory transporters in the kidney.

Substrate	Secretory Transporter (Kinetic Constant, μM , if known)	Reference
Deoxytubercidin	rOCT1 (23)	(2)
	rOCT2 (212)	(2)
Cytosine arabinoside (Ara-C)	rOCT1	(2)
Cladribine	rOCT1	(2)
AZT	rOCT1	(2)
	rOAT1 (26)	(20)
	hOAT1 (45)	(27)
	hOAT2 (26)	(27)
	hOAT3 (145)	(27)
Acyclovir	hOAT4 (151)	(27)
	rOAT1 (242)	(29)
	hOCT1 (151)	(27)
	hOAT1 (342)	(27)
Gancyclovir	hOCT1 (516)	(27)
	hOAT1 (895)	(27)
Valcyclovir	hOAT3	(27)
ddC	rOAT1 (3080)	(20)
ddI	rOAT1	(29)
Lamivudine	rOAT1	(29)
Stavudine	rOAT1	(29)
Trifluridine	rOAT1	(29)
Cidofovir	hOAT1 (58)	(10)
Adefovir	hOAT1 (23.8)	(10)
PMEA	hMRP4	(16)
	hMRP5	(23)
6-Thioguanine	hMRP4	(3)
	hMRP5	(23)
6-Mercaptopurine	hMRP4	(3)
	hMRP5	(23)
2-Mercaptopurine	hMRP4	(3)
cAMP	hMRP4 (44.5)	(3)
	hMRP5 (379)	(13)
cGMP	hMRP4 (9.7)	(3)
	hMRP5 (2)	(13)

Kinetic constants shown in parenthesis in μM . Value are K_m if emboldened and K_i if underscored. Abbreviation: PMEA, 9-(2-phosphonylethyladenine).

a wide array of substrates, based on charge and hydrophobicity, and collectively mediate transepithelial flux of xenobiotics, waste and metabolites in a secretory direction.

Transport of nucleoside analogs by these systems would directly oppose any reabsorption occurring via the nucleoside transporter-mediated pathway. In addition, multidrug resistance associated proteins, MRP4 and MRP5, appear to interact with nucleosides and nucleotide monophosphates as well. As such, they would also play a role in renal disposition of these compounds (Table 2) (15).

In general, the renal handling of nucleosides and nucleoside analogs is a complex activity. We cannot predict renal pharmacokinetic parameters of a compound based on one simple transport action. Rather, the overall disposition of each molecule—whether actively reabsorbed or secreted—will be dependent on the compilation of interactions with a wide array of transporter proteins (Figure 2). This is likely true for many nucleoside analogs. Variations in transporter affinity and turnover rate constants would explain the vast variations in renal clearances observed for this class of compounds. In order to obtain a clear understanding of the renal handling of a compound, it will be necessary to understand the individual molecular mechanisms that govern its transport.

Trafficking of Nucleoside Transporters within the Kidney

Differential steady state localization of nucleoside transporters indicates that they may be interacting with the cellular trafficking machinery in individual ways. Newly synthesized membrane proteins in polarized cells are selectively sorted within the trans golgi network (TGN) based on specific structural motifs within the proteins themselves.

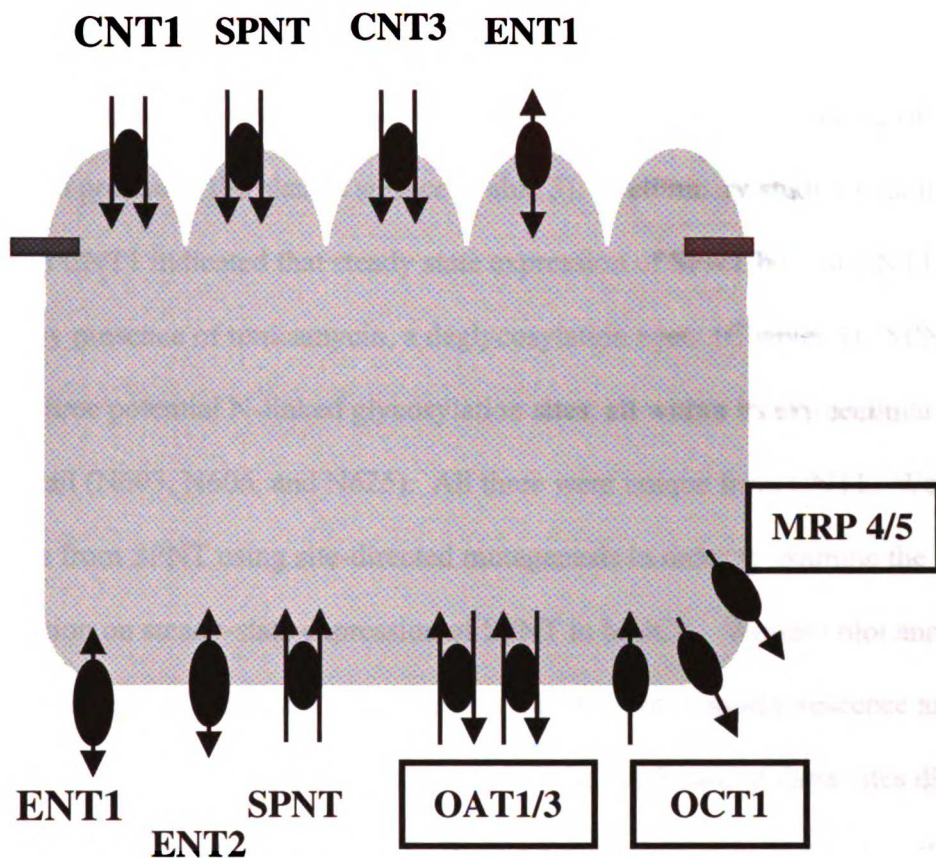


Figure 2. Renal transporters known to interact with nucleoside analogs. Xenobiotic transporters are indicated by a box. To date, the apical transporter responsible for mediating secretion of nucleosides has not been molecularly identified, but may be ENT1.

These motifs interact with membrane-specific sorting machinery and are sent specifically to the basolateral or apical membranes.

To begin to understand the cellular mechanisms that govern steady-state nucleoside transporter expression within the renal epithelium, we identified several targeting motifs within these proteins and examined their role in trafficking of newly synthesized protein at the plasma surface (Table 3). Preliminary studies examining SPNT and CNT1 indicated that steady state expression of SPNT but not CNT1 was affected by presence of tunicamycin, a deglycosylation agent (Chapter 3). SPNT contains three potential N-linked glycosylation sites, all within its extracellular C-terminal tail (N603, N606, and N625). All three were unique from CNT1. We removed these sites from SPNT using site-directed mutagenesis in order to examine the effect of glycosylation on steady-state expression of SPNT in MDCK. Western blot analysis indicated that sites N603 and N625 were glycosylated. Immunofluorescence and functional analysis demonstrated that removal of the N-glycans at these sites did not affect steady state expression of SPNT. Because apical targeting motifs do not follow obvious patterns, further analysis of the SPNT sequence has not provided insight into the nature of its apical sorting signal.

Recent work has indicated that some proteins are initially distributed uniformly on both plasma membranes and then selectively retained in an asymmetric manner by protein-protein interactions. This is typically achieved by linkage to the cytoskeletal scaffolding via a linker protein such as those containing a PSD95/DglA/ZO-1 domain (PDZ)-binding motif. The NaPi IIa transporters, CFTR chloride channel, and MRP2 all interact with PDZ-containing proteins and are retained on the apical membrane of

Table 3. Effects of sorting signals on targeting and steady state expression of NTs.

Transporter	Motif	Involved in Targeting?	Involved in Steady-State Expression?
SPNT	C-terminal glycosylation	No	No
ENT1	--RAIV	No	No
ENT2	--LL	No	Yes

renal epithelial cells (9, 14, 31). Asymmetrical localization achieved by linkage is a newly emerging field and many of the players have not yet been identified.

CNT1 or SPNT may retain polarized expression by linkage to the cytoskeleton. In order to explore this, we examined the effect of depolymerization of the actin and microtubule networks—the two main cytoskeletal components involved in trafficking and internalization of proteins—on nucleoside transporter steady-state localization. We discovered that surface expression of both CNT1 and SPNT were affected by disruption of microtubular networks via addition of nocodazole (Figure 3). This is not surprising as microtubules are known to play an important role both in delivery of newly synthesized proteins to the apical membrane and in endocytotic recycling pathways. Interestingly, disruption of the actin network by cytochalasin D drastically affected steady-state surface expression of CNT1 but not SPNT (Figure 3). This indicates that polarized surface expression of CNT1 may be dependent on actin-linkage.

Because basolateral targeting motifs are more clearly defined, we examined ENT1 and ENT2 for potential targeting motifs (Chapter 4). Typically, basolateral targeting motifs reside in the terminal tails of proteins. The carboxy-terminus of ENT1 and ENT2 each contained a motif associated with targeting: a H/RXXV motif in ENT1 and a dileucine repeat in ENT2. Using mutagenesis techniques, we determined that neither of these motifs were necessary for targeting of these proteins. The dileucine repeat in ENT2, however, was important for steady-state surface expression. Mutagenesis or removal of the dileucine repeat resulted in internal sequestration of ENT2. In addition to functioning as a basolateral targeting motif, the dileucine motif overlaps as a clathrin-coated pit internalization signal, used for endocytotic recycling and lysosomal

A.



B.



Figure 3. Actin and microtubules are important for steady-state expression of SPNT and CNT1. SPNT-GFP (A.) or CNT1-GFP (B.) expressing MDCK cells were polarized by growth on permeable support for 4-7 days and exposed for 15 hours to (i.) fresh media (control), (ii.) cytochalasin D (2 μ M, an actin depolymerizing agent), (iii.) nocodazole (33 μ M, a microfilament depolymerizing agent). Cells were fixed, permeablized, and stained for F-actin with Texas-red conjugated phalloidin. Green, GFP-tagged transporter. Red, actin. Bar, 50 μ m.

degradation pathways (1). The effects of dileucine mutation on ENT2 expression may be occurring via one of these pathways. Further examination of the ENT sequences and mutagenesis studies will be required to determine targeting motifs. Knowledge that ENT3, which has a fifty amino acid N-terminal tail extension, is sequestered internally in vesicles makes the N-terminus a promising site for further exploration (Figure 4). Future studies using truncation mutants could indicate the motifs required for plasma localization of ENT1 and ENT2 and vesicular localization of ENT3.

Cellular Regulation of Nucleoside Transporters

There are limited data on regulation of nucleoside transporters. Of the work that has been done, the majority has focused on hepatic regulation of concentrative nucleoside transporters (21). In addition, there is some indication that CNT1 expression is governed by both cell cycle and nucleotide metabolism (11). ENT1 is downregulated by p38 MAPK inhibitors and upregulated by PKC stimulation (28). Along with this, there is some indication that SPNT and ENT1 function is regulated in lymphocytes by PKC (26). Interestingly PKC-mediated signaling is linked to activation of several adenosine receptors within the kidney. These are G-protein coupled receptors that maintain homeostasis within the kidney in response to extracellular adenosine levels. There are four subtypes of adenosine receptors—A₁, A_{2A}, A_{2B}, and A₃—all of which are expressed to some degree within the kidney. A₁ receptors appear to be the major adenosine receptors within the proximal tubule, where they localize predominantly to the apical membrane. It has been hypothesized that attenuation of adenosine concentrations in the regions local to this receptor is affected by presence of nucleoside transporters. Thus,

```

          1                                                    50
hENT1  .....M TTSHQPQDRY
hENT2  .....M ARGDAPRDSY
hENT3  MAVVSEDDFQ HSSNSTYRRT SSSLRADQEA LLKLLDRPP PGLQRPEDRF

          51          72
hENT1  KAVWLIFFML GLGTLLPWNF FM
hENT2  HLVGISFFIL GLGTLLPWNF FI
hENT3  CGTYIIFSSL GIGSLLPWNF FI

```

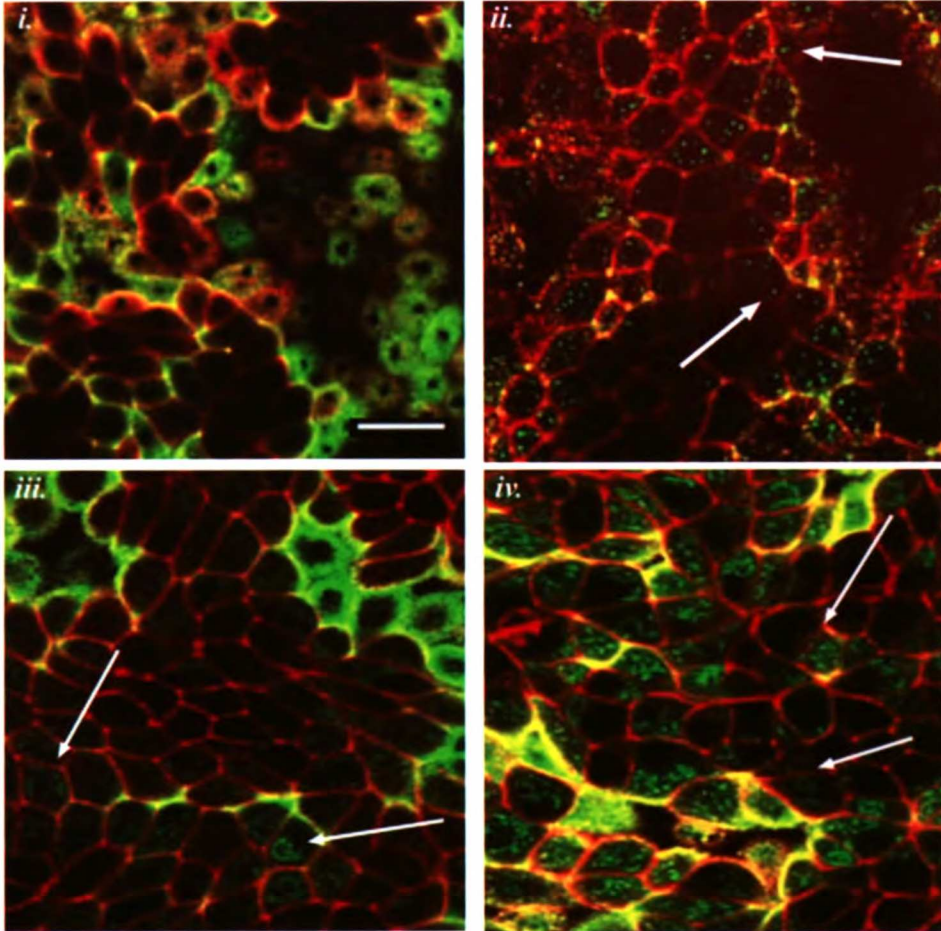
Figure 4. Sequence alignment of N-terminal tails of ENTs. Putative transmembrane domain is overscored. Potential signals in ENT3 are emboldened and highlighted.

regulation of NTs via PKC may serve as a mechanism by which receptors can modulate their own function. Preliminary studies in this laboratory indicated that steady-state expression of CNT1 but not SPNT is affected by PKC stimulation. In fact, both activation and inhibition of PKC resulted in internalization of CNT1 within MDCK (Figure 5). This change was not the result of protein degradation (Figure 5B.) but was coupled to a decrease in nucleoside transport function (Figure 5C.). No effect was seen under the same conditions for SPNT. These effects were not seen acutely; rather, they were seen over a longer time frame. This indicates that the effects of PKC on CNT1 surface expression are likely to be the indirect result of other PKC-mediated alterations within the cell. These studies stand as a first step in understanding how a renal cell might govern the intake of nucleosides.

Summary

In summary, we have examined the subcellular distribution of all known cloned and characterized nucleoside transporters in an effort to understand their role in renal disposition of nucleosides and nucleoside analogs. Our data indicate that nucleoside transporters are primarily involved in reabsorption. The net renal secretion documented clinically for many nucleoside analogs indicates that nucleoside transporters work in concert with other transporters in nucleoside disposition. It is essential to understand the spatial distribution and extent of protein expression for each of these transporters within the kidney in order to fully understand the role that these transporters may play in renal disposition of nucleosides and nucleoside analogs.

A.



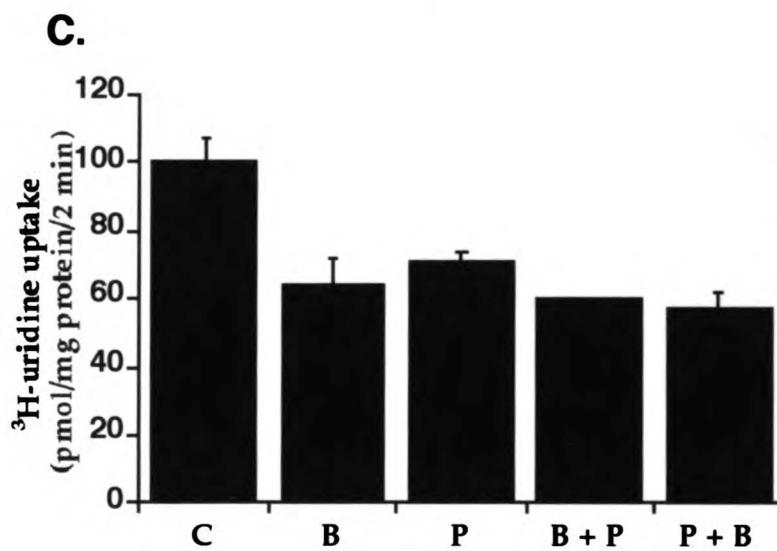
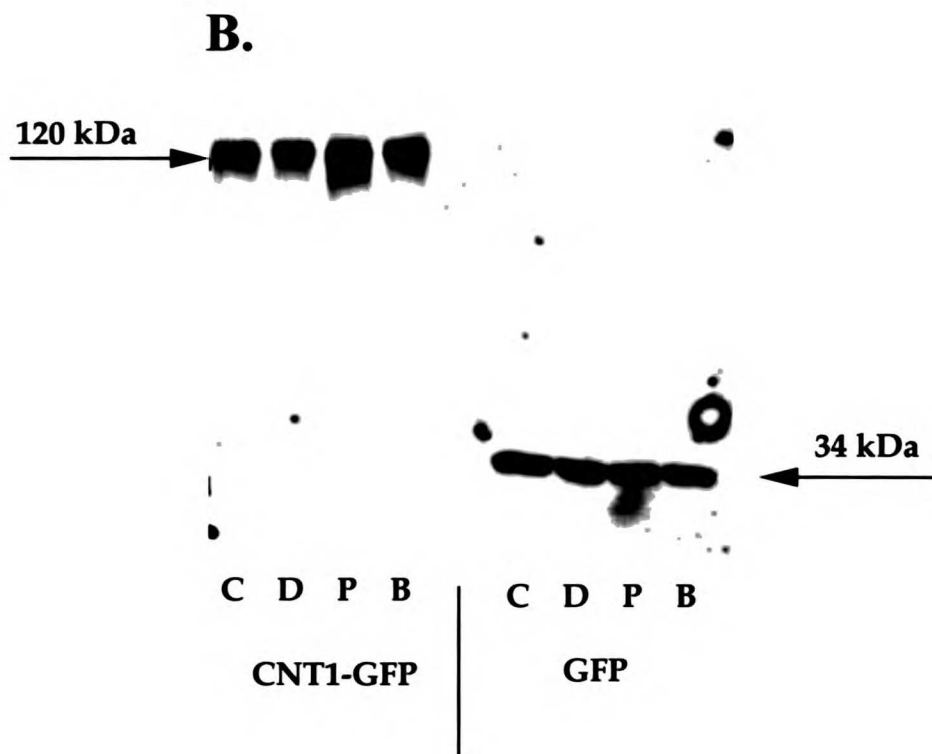


Figure 5. PKC-mediated internalization of CNT1. (A.) CNT1-GFP transfected MDCK were polarized by growth for 4-7 days on permeable support, and then exposed for 2 hours to (i.) fresh media, (ii.) a PKC activator, 4 α -phorbol 12-myristate 13-acetate (PMA, 1 μ M), (iii.) a PKC inhibitor, bisindolylmaleimide I (1 μ M) or (iii.) both (at 37 $^{\circ}$ C, in normal media). Cells were fixed, permeablized, and stained for F-actin with Texas-red conjugated phalloidin. Images were viewed using a BioRad 1024 laser scanning microscope. Green, GFP-tagged transporter. Red, actin. Arrows indicate internalization. Bar, 20 μ m. Both PKC activation and inhibition cause internalization of CNT1-GFP but to different types of vesicles. (B.) Western blot analysis of CNT1-GFP or GFP transfected MDCK exposed for 2 hours to nothing (control, C), vehicle (0.1% DMSO, D), PMA (P), or Bisindolylmaleimide (B). Cells were lysed in 2% SDS, rotated, vortexed, centrifuged, and 10 μ g total protein was loaded per lane. GFP antibody was used as described in Chapter 2, Materials and Methods. Blot indicates that there is no protein degradation of CNT1-GFP under any of the conditions used. (C.) Transport of 3 H-uridine (1 μ M) by CNT1-GFP transfected MDCK exposed for 2 hours to vehicle, PMA (P), Bisindolylmaleimide (B) or both (P + B and B + P). In the cases where both were added, cells were pretreated with one compound for 1 hour (B for B + P, and P for P + B) and then both compounds for a second hour Effects were not additive.

In addition, we have begun to explore the molecular mechanisms responsible for the polarized steady-state expression of SPNT, CNT1, ENT1, and ENT2. Our data indicate that SPNT localization is independent of glycosylation, and ENT1 and ENT2 localization are independent of their carboxy-terminal tails. ENT2 steady-state surface expression is affected by removal of the carboxy-terminal dileucine motif. Protein expression is a dynamic process. Understanding the molecular determinants of steady-state expression and cellular regulation of these transporters will be a useful tool in further understanding renal handling of nucleosides and nucleoside analogs. Further examination of these topics will be essential to understanding the physiologic relevance of nucleoside transporters.

References

1. Aroeti, B., H. Okhrimenko, V. Reich, and E. Orzech. Polarized trafficking of plasma membrane proteins: emerging roles for coats, SNAREs, GTPases and their link to the cytoskeleton. *Biochim Biophys Acta* 1376: 57-90, 1998.
2. Chen, R., J. W. Jonker, and J. A. Nelson. Renal organic cation and nucleoside transport. *Biochem Pharmacol* 64: 185-90, 2002.
3. Chen, Z. S., K. Lee, and G. D. Kruh. Transport of cyclic nucleotides and estradiol 17-beta-D-glucuronide by multidrug resistance protein 4. Resistance to 6-mercaptopurine and 6-thioguanine. *J Biol Chem* 276: 33747-54, 2001.
4. Dresser, M. J., K. M. Gerstin, A. T. Gray, D. D. Loo, and K. M. Giacomini. Electrophysiological analysis of the substrate selectivity of a sodium-coupled nucleoside transporter (rCNT1) expressed in *Xenopus laevis* oocytes. *Drug Metab Dispos* 28: 1135-40, 2000.
5. Fang, X., F. E. Parkinson, D. A. Mowles, J. D. Young, and C. E. Cass. Functional characterization of a recombinant sodium-dependent nucleoside transporter with selectivity for pyrimidine nucleosides (cNT1rat) by transient expression in cultured mammalian cells. *Biochem J* 317 (Pt 2): 457-65, 1996.
6. Gerstin, K. M., M. J. Dresser, and K. M. Giacomini. Specificity of human and rat orthologs of the concentrative nucleoside transporter, SPNT. *Am J Physiol Renal Physiol* 283: F344-9, 2002.

7. Graham, K. A., J. Leithoff, I. R. Coe, D. Mowles, J. R. Mackey, J. D. Young, and C. E. Cass. Differential transport of cytosine-containing nucleosides by recombinant human concentrative nucleoside transporter protein hCNT1. *Nucleosides Nucleotides Nucleic Acids* 19: 415-34, 2000.
8. Griffiths, M., S. Y. Yao, F. Abidi, S. E. Phillips, C. E. Cass, J. D. Young, and S. A. Baldwin. Molecular cloning and characterization of a nitrobenzylthioinosine-insensitive (ei) equilibrative nucleoside transporter from human placenta. *Biochem J* 328: 739-43, 1997.
9. Hernando, N., N. Deliot, S. M. Gisler, E. Lederer, E. J. Weinman, J. Biber, and H. Murer. PDZ-domain interactions and apical expression of type IIa Na/P(i) cotransporters. *Proc Natl Acad Sci U S A* 99: 11957-62, 2002.
10. Ho, E. S., D. C. Lin, D. B. Mendel, and T. Cihlar. Cytotoxicity of antiviral nucleotides adefovir and cidofovir is induced by the expression of human renal organic anion transporter 1. *J Am Soc Nephrol* 11: 383-93, 2000.
11. Huang, M., Y. Wang, M. Collins, J. J. Gu, B. S. Mitchell, and L. M. Graves. Inhibition of nucleoside transport by p38 MAPK inhibitors. *J Biol Chem* 277: 28364-7, 2002.
12. Hyde, R. J., C. E. Cass, J. D. Young, and S. A. Baldwin. The ENT family of eukaryote nucleoside and nucleobase transporters: recent advances in the investigation of

structure/function relationships and the identification of novel isoforms. *Mol Membr Biol*

18: 53-63, 2001.

13. Jedlitschky, G., B. Burchell, and D. Keppler. The multidrug resistance protein 5 functions as an ATP-dependent export pump for cyclic nucleotides. *J Biol Chem* 275: 30069-74, 2000.

14. Kocher, O., N. Comella, K. Tognazzi, and L. F. Brown. Identification and partial characterization of PDZK1: a novel protein containing PDZ interaction domains. *Lab Invest* 78: 117-25, 1998.

15. Kruh, G. D., H. Zeng, P. A. Rea, G. Liu, Z. S. Chen, K. Lee, and M. G. Belinsky. MRP subfamily transporters and resistance to anticancer agents. *J Bioenerg Biomembr* 33: 493-501, 2001.

16. Lai, L., and T. M. Tan. Role of glutathione in the multidrug resistance protein 4 (MRP4/ABCC4)-mediated efflux of cAMP and resistance to purine analogues. *Biochem J* 361: 497-503, 2002.

17. Li, J. Y., R. J. Boado, and W. M. Pardridge. Cloned blood-brain barrier adenosine transporter is identical to the rat concentrative Na⁺ nucleoside cotransporter CNT2. *J Cereb Blood Flow Metab* 21: 929-36, 2001.

18. Lostao, M. P., J. F. Mata, I. M. Larrayoz, S. M. Inzillo, F. J. Casado, and M. Pastor-Anglada. Electrogenic uptake of nucleosides and nucleoside-derived drugs by the

human nucleoside transporter 1 (hCNT1) expressed in *Xenopus laevis* oocytes. *FEBS Lett* 481: 137-40, 2000.

19. Mackay, J. R., S. Y. Yao, K. M. Smith, E. Karpinski, S. A. Baldwin, C. E. Cass, and J. D. Young. Gemcitabine transport in *xenopus* oocytes expressing recombinant plasma membrane mammalian nucleoside transporters. *J Natl Cancer Inst* 91: 1876-81, 1999.

20. Morita, N., H. Kusuhara, T. Sekine, H. Endou, and Y. Sugiyama. Functional characterization of rat organic anion transporter 2 in LLC-PK1 cells. *J Pharmacol Exp Ther* 298: 1179-84, 2001.

21. Pastor-Anglada, M., F. J. Casado, R. Valdes, J. Mata, J. Garcia-Manteiga, M. Molina, A. Felipe, B. del Santo, J. F. Mata, B. Santo, J. Lloberas, and J. Casado. Complex regulation of nucleoside transporter expression in epithelial and immune system cells. *Mol Membr Biol* 18: 81-5, 2001.

22. Ritzel, M. W., S. Y. Yao, M. Y. Huang, J. F. Elliott, C. E. Cass, and J. D. Young. Molecular cloning and functional expression of cDNAs encoding a human Na⁺-nucleoside cotransporter (hCNT1). *Am J Physiol* 272: C707-14, 1997.

23. Sampath, J., M. Adachi, S. Hatse, L. Naesens, J. Balzarini, R. M. Flatley, L. H. Matherly, and J. D. Schuetz. Role of MRP4 and MRP5 in Biology and Chemotherapy. *AAPS PharmSci* 4, 2002.

24. Schaner, M. E., J. Wang, S. Zevin, K. M. Gerstin, and K. M. Giacomini. Transient expression of a purine-selective nucleoside transporter (SPNTint) in a human cell line (HeLa). *Pharm Res* 14: 1316-21, 1997.
25. Schaner, M. E., J. Wang, L. Zhang, S. F. Su, K. M. Gerstin, and K. M. Giacomini. Functional characterization of a human purine-selective, Na⁺-dependent nucleoside transporter (hSPNT1) in a mammalian expression system. *J Pharmacol Exp Ther* 289: 1487-91, 1999.
26. Soler, C., A. Felipe, J. F. Mata, F. J. Casado, A. Celada, and M. Pastor-Anglada. Regulation of nucleoside transport by lipopolysaccharid, phorbol esters, and tumor necrosis factor-alpha in human B-lymphocytes. *273 41: 26939-45.*, 1998.
27. Takeda, M., S. Khamdang, S. Narikawa, H. Kimura, Y. Kobayashi, T. Yamamoto, S. H. Cha, T. Sekine, and H. Endou. Human organic anion transporters and human organic cation transporters mediate renal antiviral transport. *J Pharmacol Exp Ther* 300: 918-24., 2002.
28. Valdes, R., M. A. Ortega, F. J. Casado, A. Felipe, A. Gil, A. Sanchez-Pozo, and M. Pastor-Anglada. Nutritional regulation of nucleoside transporter expression in rat small intestine. *Gastroenterology* 119: 1623-30., 2000.
29. Wada, S., M. Tsuda, T. Sekine, S. H. Cha, M. Kimura, Y. Kanai, and H. Endou. Rat multispecific organic anion transporter 1 (rOAT1) transports zidovudine, acyclovir, and other antiviral nucleoside analogs. *J Pharmacol Exp Ther* 294: 844-9., 2000.

30. Wang, J., S. F. Su, M. J. Dresser, M. E. Schaner, C. B. Washington, and K. M. Giacomini. Na(+)-dependent purine nucleoside transporter from human kidney: cloning and functional characterization. *Am J Physiol* 273: F1058-65, 1997.
31. Wang, S., H. Yue, R. B. Derin, W. B. Guggino, and M. Li. Accessory protein facilitated CFTR-CFTR interaction, a molecular mechanism to potential the chloride channel activity. *Cell* 103: 169-79, 2000.
32. Yao, S. Y., A. M. Ng, W. R. Muzyka, M. Griffiths, C. E. Cass, S. A. Baldwin, and J. D. Young. Molecular cloning and functional characterization of nitrobenzylthioinosine (NBMPR)-sensitive (es) and NBMPR-insensitive (ei) equilibrative nucleoside transporter proteins (rENT1 and rENT2) from rat tissues. *J Biol Chem* 272: 28423-30., 1997.
33. Yao, S. Y., A. M. Ng, M. F. Vickers, M. Sundaram, C. E. Cass, S. A. Baldwin, and J. D. Young. Functional and molecular characterization of nucleobase transport by recombinant human and rat equilibrative nucleoside transporters 1 and 2. Chimeric constructs reveal a role for the ENT2 helix 5-6 region in nucleobase translocation. *J Biol Chem* 277: 24938-48., 2002.



For reference

Not to be taken from the room.



